# EXPLAINING SPATIAL VARIATION IN CORAL SIZE STRUCTURE IN AMERICAN SAMOA

A THESIS SUBMITTED TO THE GRADUATE DIVISION OF THE UNIVERSITY OF HAWAI'I AT MĀNOA IN PARTIAL FULFILLMENT OF THE REQUIREMENTS FOR THE DEGREE OF

MASTER OF SCIENCE

IN

OCEANOGRAPHY

NOVEMBER 2017

By
Marie H. Ferguson

Thesis Committee:

Anna B. Neuheimer, Chairperson
Mark Merrifield
Tom Oliver
Dione W. Swanson

**ACKNOWLEDGEMENTS**

I would like to sincerely thank my advisor, Anna Neuheimer, and committee members, Tom Oliver, Mark Merrifield, and Dione Swanson, for their guidance and support throughout this process. Tom Oliver's passion and enthusiasm for science was contagious and his exceptional ability to think outside of the box helped to instill these same qualities in myself and helped me reach beyond my own limitations in scientific knowledge. Dione Swanson's depth of knowledge of coral populations, population ecology, and sampling design was invaluable in my understanding of coral populations and size structure dynamics and her hard work and dedication to quality science has enabled me to become a better scientist. Mark Merrifield's expertise in physical oceanography, analytic capabilities and, most importantly, his kindness, patience, and ability to effectively teach was essential in guiding my comprehension and application of physical oceanographic dynamics throughout this research. And to my advisor, Anna Neuheimer, I would like to extend my deepest gratitude and appreciation. Throughout my graduate education, Anna has been a mentor in the truest sense of the word. An effective mentor is able to share their life experiences and wisdom as well as their scientific knowledge and expertise and is a good listener, good observer, and good problem-solver. Ultimately, they demonstrate honesty, integrity, and both respect for and responsibility for stewardship as well as establish an environment that enables the student's accomplishments. Anna has demonstrated all of these qualities and, in addition to her role as a mentor, her kindness, patience, hard work, and dedication has been instrumental in my success in my graduate studies and in becoming a better person and scientist. My experiences as a graduate student under Anna have left a positive imprint in my life and I will strive to maintain and pass on these admirable qualities, characteristics, and experiences in my future mentorship and scientific roles.

I additionally would like to thank: Rusty Brainard and Jenni Samson at NOAA's Pacific Islands Fisheries Science Center (PIFSC), Environmental Sciences Division (ESD), the Joint Institute for Marine and Atmospheric Research (JIMAR), and NOAA's Coral Reef Conservation Program for the financial support I received in pursuing graduates throughout my employment at NOAA/PIFSC/ESD; to all of my co-workers at NOAA/PIFSC/ESD who work long, hard hours to collect some of the data used in this research; and to my fellow graduate students for their support and camaraderie. And, last but not least, I would like to thank my family for their support and to my parents who exposed me to the natural wonders of the world and instilled in me both a passion for the outdoors and nature and in protecting the environment.

## ABSTRACT

Coral size structure distributions (i.e. the distribution of individual colony sizes within a population) have been shown to vary between and among populations exposed to different environmental regimes and disturbance histories. Subsequently, assessing size structure spatio-temporal variability in relation to biogeophysical factors can provide insight into underlying mechanisms driving spatial patterns observed in coral populations. A total of 22 species of coral are now listed as threatened under the U.S. Endangered Species Act (ESA); however species level data on demographic processes and responses of corals to threats needed for effective management is deficient. This includes: 1) quantitative assessments of population status, and 2) identification of potential environmental drivers that influence the status of a given species. Here, analysis of a rare ESA-listed species, *Isopora crateriformis* (*Isopora spp.* used as a proxy), and an abundant species, *Montastrea curta*, from a 2015 NOAA Ecosystem Sciences Division (ESD) survey across five islands in American Samoa (within 0 – 30m depth range) was used to determine spatial variation in population size structure patterns across two spatial scales (site- and strata-level resolution). Using co-located data available, a range of environmental (e.g. benthic geomorphology), oceanographic (e.g. temperature, wave energy), biological (e.g. benthic cover), and anthropogenic impact covariates were collated and synthesized at comparable spatial scales to the coral population data. Generalized modeling and multi-model inference were used to evaluate the strength and magnitude of the relationship between biogeophysical/anthropogenic covariates (explanatory covariates) and size distribution parameter estimates (response variable) for each coral species. Due to its versatility and effectiveness, the Weibull distribution was used to characterize the observed size spectra and the distribution shape parameter, $k$, was used as the size spectra response metric in statistical modeling. Analyses reveal that i) size structure spatially

varied among and between species and ii) modeled biogeophysical relationships varied significantly between species. Mean net carbonate accretion rate and net carbonate accretion rate variability (i.e. net carbonate accretion rate coefficient of variation), in addition to geomorphological slope and slope variability, accounted for a large proportion of spatial variation in the *Isopora spp.* site-level size spectra ($R^2$ = 58%). For *Isopora spp.* strata-level analysis, wave energy and mean accretion rate explained a large proportion of spatial variation ($R^2$ = 46%). In contrast, for *Montastrea curta* site-level analysis, irradiance (photosynthetically active radiation), percent coral cover, wave energy, mean depth, *M. curta* juvenile abundance, and SST explained a large proportion of spatial variation in the size spectra ($R^2$ = 45%). For *M. curta* strata-level analysis, irradiance, mean accretion rate, SST, and wave energy explained a large proportion of spatial variation ($R^2$ = 57%). Our results suggest that the Weibull shape parameter, *k*, is a reliable metric that captures variability in the coral size distribution and that species-specific biogeophysical factors explain coral size structure variability across space.

## TABLE OF CONTENTS

## LIST OF TABLES

## LIST OF FIGURES

# 1. INTRODUCTION

Within the marine environment, coral reefs are among the most threatened global ecosystems, and among the most vital (Costanza et al. 1997, Bryant et al. 1998, Reaser et al. 2000, Wilkinson 2000). Reefs are of critical global importance, especially in developing countries, as they provide subsistence food for a large portion of populations, serve as primary structures for coastal protection for many tropical islands, and contribute major income and foreign exchange from tourism (Costanza et al. 1997, Wells et al. 2001, Salm et al. 2001). The value of biological resources (e.g. fisheries) and services (e.g. tourism earnings and coastal protection) provided by coral reefs has been estimated at ~ $375 billion annually (Costanza et al. 1997). Coral reefs also provide habitat for some of the greatest biodiversity globally (Ray 1988).

Crustose coralline algae and scleractinian corals are the foundational benthos which deposit calcium carbonate, acting to consolidate reef substrate and enable coral reef development and persistence (e.g. Littler and Littler 1984). Both physical and biological processes naturally structure coral reef communities over various spatial and temporal scales (Brown 1997, Done 1999). Environmental processes influence coral reef ecosystem functioning including coral growth rates, extent, abundance, morphology, and diversity (Brown 1997). Thus, in studies or assessments of the state of coral reefs, it is important to consider both spatial (e.g. depth, location) and temporal variations in environmental conditions (Anthony & Larcombe 2002).

Coral cover has commonly been used as a composite metric to measure stony coral abundance in coral reef community structure and theoretically represents the net outcome of population dynamic rate processes (i.e. recruitment, growth, and survivorship; Smith et al. 2011). However, studies of total coral cover alone may not accurately determine changes in reef composition and species dominance (Franklin et al. 2013), and do not directly represent the

population dynamic processes themselves (Smith et al. 2011) or possibly reef health. Instead, colony size is an important characteristic for scleractinian corals as many life history processes, such as growth, reproduction and mortality, are strongly related to size (Connell 1973, Hughes and Jackson 1980, Hall and Hughes 1996). An organism's body size reflects its energetic requirements, resource utilization, and its potential in competition (Werner and Gilliam 1984). Within populations and between species, variation in body size is a significant way to avoid overlap in resource use (Schoener 1974) and can act as a driving mechanism in structuring community composition (Brooks and Dodson 1965, Hall et al. 1976). A collapse or disruption in the size structure distribution (i.e. numbers at size) of a population can limit the population's capacity for population replenishment and leave it vulnerable to environmental disturbances, ultimately altering the population's resilience (Haedrich and Barnes 1997). For clonal organisms, such as corals, biological processes are more closely tied to size than age (Connell 1973, Loya 1976, Hughes & Connell 1987, Szmant 1991, Soong 1993). This stems from corals exhibiting fragmentation, fission, fusion, and partial mortality throughout their life cycle (Bak 1975, Highsmith et al. 1980, Hughes & Jackson 1980, 1985, Meesters et al. 1996, 1997), which contributes to the decoupling of size and age (i.e. individuals of the same size may be a different age). Thus, size is a better representation of population structure and dynamics (Meesters et al. 2001).

Coral reef community structure and composition are likely to be determined by the interaction of multiple forcing functions operating on a variety of scales (Murdoch and Aronson 1999). The size structure of coral populations may vary with different management regimes and fishing pressure (McClanahan et al. 2008) and within-species size structure may vary among populations exposed to different environmental conditions and disturbance histories (Meesters et

al. 2001, Bauman et al. 2013b). Subsequently, assessing size structure dynamics enables comparison of key population demographics (differences among individuals and species, growth, mortality, and reproduction) to evaluate effects from ecological processes and environmental conditions over a range of spatial and temporal scales (Bak and Meesters 1998, 1999, Meesters et al. 2001).

Several spatial and environmental variables have been noted as influencing coral species size structure, distribution, growth and community structure. Most notably, and recognized in early studies of global coral reef distribution, limiting environmental variables include light, temperature, salinity, sedimentation, and hydrodynamic factors (Glynn 1976, Achituv and Dubinsky 1990, Brown 1997, Kleypas et al. 1999, Lirman et al. 2003, Done, 2011). Collectively, these factors can affect coral reef growth rate, extent, form and reproduction, ultimately affecting the overall abundance, composition and diversity of reef communities (Brown 1997, Kleypas et al. 1999, Done 2011).

Coral community growth and tolerance limitations have long been synonymous with ocean temperature variability. The sensitivity of corals and their symbiotic zooxanthellae to elevated ocean temperatures has been documented extensively (e.g. Hoegh-Guldberg 1999). Thermal stress can cause coral bleaching where partial and total mortality from bleaching events has resulted in large-scale loss of coral cover, change in coral community structure, and declines in reef health (Baker et al. 2008). Slower coral growth rates have been linked to higher sea surface temperatures and an increase in the frequency of mass bleaching events (Bauman 2013b) and size-dependent responses to bleaching include a higher likelihood of survival for recruits and small/juvenile coral colonies versus larger colonies (Mumby 1999, Loya et al. 2001, Shenkar et al. 2005). Under projected changing global conditions and rates of ocean warming, thermal

tolerance limits of reef building corals could be exceeded altering physiological and genetic adaptability in coral populations (Glynn 1993).

Light attenuation affects the growth and survival of coral communities as coral reefs have minimum light requirements. Variability in light attenuation explains reduced reef calcification with depth (Kleypas et al. 1999) and seasonally low light penetration at higher latitudes could limit reef calcification and growth to shallower depths than observed in the tropics (Grigg 1982). Reduced aragonite saturation and light penetration, both of which co-vary with temperature, are thought to be a limiting factor in reef development (Kleypas et al. 1999) as carbonate saturation is most likely a significant factor in controlling reef calcification and photosynthesis (Buddemeier 1994).

Wave energy and exposure have also been significant contributors to coral reef community spatial distribution and structure (Dollar 1982, Done 1982, van Woesik and Done 1997, Franklin et al. 2013). Disturbance caused by wave energy and storm frequency were found to be the primary driver structuring coral reefs in the Hawaiian Islands (Dollar 1982, Grigg 1983, Engels et al. 2004, Jokiel et al. 2004, Storlazzi et al. 2005) and storm severity can alter coral size structure distributions, increasing probability for dislodgement in larger size classes (Done and Potts 1992). Wave energy and exposure in conjunction with benthic geomorphology can also alter coral population size structure distributions. Higher proportions of small coral colonies at shallower depths has been attributed to decreasing hydrodynamic pressure with increasing depth which inhibits development of large colonies due to strong water motion (Adjeroud et al. 2015).

Declines in coral reefs have been recurrently tied to human rather than natural causes. Fishing pressure may affect coral size structure and reduce coral growth by negatively impacting herbivorous fish populations and subsequently altering competitive interactions with algae

(McCook et al. 2001). Poor water quality has been found to lower the radiation tolerance of scleractinian corals (Wooldridge 2009) and has been linked to a reduction in coral recruitment and the abundance of small colonies yielding populations with fewer small colonies, lower variance, and overly centralized size distributions (Meesters et al. 2001). While eutrophic conditions have typically been associated with anthropogenic activities, recent evidence suggests that natural enhanced levels of chlorophyll-a may positively influence coral reef ecosystems (Gove et al. 2013) through an increase in availability of nutrients important for the growth and development of some benthic organisms, such as corals (e.g. Sebens et al. 1996, Leichter and Genovese 2006). Hence the influences of chlorophyll-a on coral reef ecosystems may be geographically specific (Gove et al. 2013) and covary with anthropogenic influence.

Much of this research has indicated the significance in understanding the responses of coral populations to environmental variation, especially in a changing climate, however little work has been done to identify environmental variables associated with coral size distributions (but see: Adjeroud et al. 2015, Bauman et al. 2013a, 2013b, Crabbe 2009). Additionally, using coral size structure distributions in relation to environmental variables has presented challenges due to the absence of a single robust metric to quantitatively describe the shape of coral size structure distributions. With increasing changes in the global climate, consequential instabilities in a range of environmental variables are predicted to affect the growth rate, growth form, and reproductive capacity of corals (Brown 1997, Kleypas et al. 1999). Additionally, changing global conditions are projected to affect the size structure of coral populations, primarily affecting recruits and smaller size classes, which would shift distributions towards larger size classes with lower variance and more centralized distributions (Bak and Meesters 1999). Thus, investigating the size structure of coral populations at various spatial and temporal scales with a single, robust

size structure metric can provide important insight into how populations have been affected by local environmental conditions and/or recent disturbance events (Bak and Meesters 1999, Meester et al. 2001).

In this context, the purpose of this research was to investigate biophysical relationships by identifying variation in coral population size structure distribution metrics that can be explained by environmental and anthropogenic variables. Two coral species with contrasting spatial size structure and abundance patterns were examined across five American Samoa island/atoll coral reef systems with varying environmental, biological, and anthropogenic gradients. Using a statistical modeling framework, I examine coral size distribution parameters in relation to a range of factors – temperature, irradiance, primary productivity, wave energy, benthic community cover, calcification accretion rates, coral juvenile abundance, slope, human population density – to identify and assess the underlying mechanisms driving coral population size structure patterns and spatial distributions.

Size distribution parameter estimates at both site- and stratum-level spatial resolutions were used to examine biophysical relationships. In contrast to site-specific estimates, stratum-level population estimates are converted from site-level estimates, using robust statistical survey designs (Smith et al. 2011, Swanson 2011), and allow for assessment of coral populations at the ecosystem scale. Stratum-level analysis, hereafter referred to as 'Habitat Use Analysis' (HUA), can potentially provide more relevant and robust estimates of size structure variability and, hence, was used in addition to site-level analysis.

This thesis will address a number of research questions including:

1) How does coral population size structure vary?
2) What are the potential biophysical factors influencing coral population size structure

variability (inter-regional and intra-island) in the American Samoa island complex?

3) How do relevant factors vary across species?

Research questions will be addressed by testing the following hypothesis:

**Variation in coral population size structure can be explained by variability in biophysical factors (oceanographic, geomorphological and biological factors, and species-specific characteristics).** (Null hypothesis: there is no relationship between coral population size-structure and biophysical factors.)

## 2. METHODS

To examine spatial variability in the size structure of each coral species in relation to environmental, biological, and anthropogenic factors, it is necessary to i) establish a robust metric that is able to capture variability among size spectra and ii) estimate the biophysical factors that influence coral population structure on relevant time and space scales. To obtain a size spectra metric, various size structure distribution fits were statistically assessed and a relevant parameter was selected based on these results (see section *2.2 Coral size structure characterization, subsection 'Coral size structure metric'*). In the interest of investigating coral populations at both site- and ecosystem-scales, size distribution parameters were estimated for each spatial resolution (see section *2.2 Coral size structure characterization, subsection 'Coral size structure spatial resolution'*). Descriptive statistics for each size distribution, median size and skewness, were also generated to examine how variability in the chosen size spectrum parameter corresponded with variability in median size and skewness. Using co-located data available, a range of environmental, biological, and anthropogenic covariates were collated and synthesized at comparable spatial scales to the coral population data (see section *2.3 Biophysical characterization*). Finally, generalized modeling and multi-model inference is used to evaluate the strength and magnitude of the relationship between the environmental, biological, and anthropogenic covariates (explanatory covariates) and the size distribution parameters (response variable) for each coral species and at each spatial resolution (see section *2.4 Biophysical statistical analyses*).

### *2.1 Study location*

Coral size spectra variability is examined across American Samoa which consists of four main volcanic islands, one low-lying island, and one atoll situated in the central tropical South

Pacific at approximately 14° S and 170° W (Figure 1). The four volcanic islands are part of a hotspot chain, which includes the islands of independent Samoa and several seamounts to the west as well as ridges extending to the southeast of two American Samoa islands and an active underwater volcano to the east. Swains Island and Rose Atoll are much older than the volcanic islands and are not geologically related (Fenner et al. 2008). In addition to Rose and Swains, the islands of Tutuila and the Manu'as (Ofu, Olosega, Ta'u) will be used in this study, together comprising the "American Samoa island complex". Tutuila is the largest and most populated island (~ 66,900 in 2007) followed by Ta'u, and Ofu/Olosega (human populations ~ 790 and 353 respectively; Fenner et al. 2008). Swains Island is small, about 1.5 miles long, and exhibits a transient human population of about 17. Rose Atoll is uninhabited with 20 acres of land and is protected as part of the Pacific Remote Islands National Wildlife Refuge Complex (http://www.fws.gov/refuge/rose_atoll/). A National Park is distributed across American Samoa's three main islands, consisting of approximately 4,448 acres of coral reef area (http://www.nps.gov/npsa/index.htm).

American Samoa lies within the westward-flowing Pacific South Equatorial Current (SEC), characterized by warm (28-30°C), oligotrophic surface waters with a deep mixed layer, and is seasonally impacted by episodic long period swells originating from both hemispheres (Fenner et al. 2008). The islands exhibit narrow reef flats with shallow water environments (0-30 m) consisting mainly of fringing coral reefs, with spur and groove formations common on the reef slopes of Tutuila and the Manu'as. Rose Atoll has a large (1,600 acres) central lagoon enclosed by a fringing reef with a steep forereef slope, with a single channel connecting the lagoon to the deep ocean.

The coral reef communities in American Samoa are relatively diverse with approximately 288 reef-building coral species (Birkeland et al. 2007). Coral communities appear to maintain resilience from acute disturbances and appear to be in good condition, despite being historically severely affected by large-scale disturbances including predation by outbreaks of crown-of-thorn starfish (*Acanthaster planci*), hurricanes, and warming-induced coral bleaching (Birkeland et al. 2007). Human activity has contributed to declines in reef health at the sub-island scale including chronic sedimentation from high-island watershed run-off and fishing pressure (Birkeland et al. 2007, Fenner et al. 2008). Over the past few years, coral reef communities on Tutuila have been impacted by crown-of-thorn outbreaks, which have propagated to some of the other islands. In 2014, NOAA listed 20 new coral species as threatened under the Endangered Species Act (ESA), including 15 species in the Indo-Pacific (http://www.nmfs.noaa.gov/stories/2014/08/corals_listing.html). Eight of these species are thought to occur in American Samoa.

### *2.2 Coral size structure characterization*

#### *Coral survey data and species*

Coral population data from ESD's (Ecosystem Sciences Division) benthic REA (Rapid Ecological Assessment) surveys from Reef Assessment and Monitoring Program (RAMP) cruises (2002-2015) (http://www.pifsc.noaa.gov/cred/pacific_ramp.php) is used to examine size structure across the American Samoa island complex. Benthic REA surveys of corals are conducted on shallow-water coral reefs, from 0 to 30 m depth, and focus on the distribution, abundance, population structure, and condition of corals. Data collected include individual colony identification, life-stage (juvenile, fragment, adult), morphology, size (maximum diameter), partial morality, and condition. For coral colony size, because maximum diameter is

highly correlated with total surface area, only one size metric (maximum diameter) is obtained during surveys. For this research, the maximum diameter for individual coral colonies is used to characterize individual coral size.

Two coral species of contrasting abundance, *Isopora crateriformis* (Figure 2) and *Montastrea curta* (Figure 3), are used in this study. In 2014, *I. crateriformis* was listed as threatened under the ESA and was the most abundant and widespread ESA-listed species observed during ESD's 2015 survey effort in American Samoa. As *I. crateriformis* was not consistently identified at the species-level across all surveys (due to the similarity to *I. cuneata* when both exhibit an encrusting morphology), quantitative assessment of the genus *Isopora* is used as a proxy, which can provide relevant demographic information about *I. crateriformis*. Complementary assessment of an abundant coral species, *Montastrea curta,* can further yield relevant comparable estimates with *Isopora spp.*

Within the past 4 years, NOAA's ESD has incorporated a probabilistic survey design for corals, employing a two-stage stratified random sampling design with a stratification scheme that includes reef zone, depth, and habitat structure. The purpose of this design is to provide a robust framework for estimating population-level metrics, to obtain high precision estimates at low sample sizes, and to avoid potential bias by randomly selecting sample locations (Smith et al. 2011). ESD has also incorporated habitat-use analysis (see details in '*Coral size structure spatial resolution'* subsection below), following Swanson 2011, which functions as the quantitative foundation to integrate both environmental and biological data to investigate relationships across space and time. Due to this change in sampling methodology and data constraints prior to 2015 in American Samoa, only coral population data from the 2015 RAMP cruise is used. As such, my research focuses on assessment of coral populations in space (versus time) and provides a

snap shot in time. In spite of this limitation, the analyses proposed in this research have the potential to establish a quantitative pathway for future use, investigating biophysical relationships using coral size distributions, and will be critical in determining the essential habitats and respective environmental drivers for coral populations.

***Coral size structure metric***

The size distribution is used to quantify coral population structure and describes the frequency of occurrence of different coral size classes. Various analytic distributions (power law, lognormal, exponential, gamma, and Weibull distributions) and parameters that characterize the size distribution (e.g. mean, maximum, minimum and median size, standard deviation, skewness, kurtosis) were tested. Candidate distributions and their parameter estimates were fit using maximum likelihood estimation and distributions were assessed and compared with goodness-of-fit tests (Cramer-von Mises, Kolmogorov-Smirnov and Anderson-Darling statistics, D'Agostino and Stephens 1986; Akaike and Bayesian information criteria) using the *fitdistrplus* package (Delignette-Muller and Dutang 2015) in R v3.2.3 (R Development Core Team, 2015).

The Weibull distribution was the best-fit distribution and is a comprehensive metric that captures other size characteristics such as median size and skewness (see below), and thus selected to quantify coral size structure. The Weibull distribution has been widely used in survival analysis (e.g. Mudholkar et al. 1996) to model the lifetime of an object and reliability engineering (e.g. Jiang and Murthy 2011) due to its versatility and flexibility as a frequency distribution. Weibull distributions have also been used to quantitatively describe size structure distributions and life data in ecology such as tree diameter frequency distributions (e.g. Muller-Landau et al. 2006, Zhang et al. 2003) and survivorship of individual plants and animals in natural populations (Pinder III et al. 1978).

Coral size data for individual coral colonies was fit to a Weibull distribution with probability density function

$$f(x) = (k/\lambda)\ (x/\lambda)^{k-1}\ \ e\ \wedge\ (-(x/\lambda)^{k})$$

$$x \geq 0\ ;\ k > 0, \lambda > 0$$

where $k$ is the shape parameter and $\lambda$ is the scale parameter. Because variability in the shape parameter, $k$, (also known as the Weibull slope) can have a strong effect on the behavior and shape of the distribution and more effectively captures variability in the distribution shape (compared to the scale parameter, $\lambda$), this parameter was chosen as the representative coral size structure metric and used as the response variable in the statistical model. Prior to generating the shape parameter metric for each distribution, size data was log-transformed to increase resolution amongst the smaller size classes and emphasize variability in the response at the low end of the size-frequency distribution (sensu Bak and Meesters 1998, 1999).

In most empirical analyses of coral population size distributions, the parameters mean and median size, standard deviation, kurtosis, and skewness have typically been used to quantify and assess distribution variability amongst populations, between species, and in space (e.g. Bak and Meesters 1998, 1999, Meesters et al. 2001, Adjeroud et al. 2015). Variability in mean size within species has been shown to vary significantly spatially indicating that colony size is mostly influenced by differences in the environment (e.g. Meesters et al. 2001, Bauman et al. 2013b). With respect to skewness (asymmetry around the mean of a frequency distribution), the size structure of coral populations has been shown to be positively skewed (e.g Soong 1993, Oigman-Pszczol and Creed 2004) where distributions consist primarily of smaller colonies and relatively few large ones. In contrast, negatively skewed distributions exhibit a high frequency of larger colonies and relatively few smaller/juvenile colonies, which may indicate a lack of successful

recruitment and implies a risk of population decline (Meesters et al. 2001, Guzner et al. 2007, Alvarado-Chacon and Acosta 2009). Here, median size and skewness parameters were generated to examine how variability in the size spectra shape parameter corresponds with variability in median size and skewness. These comparisons were used to further characterize spatial variability in the size distribution for each coral species.

Only adult coral size structure distributions (≥ 5 cm maximum diameter) will be assessed in this study. Spatio-temporal variation in adult and juvenile coral populations infers variability in growth and survival between these two life-stages and, subsequently, the abundance and size structure of both life-stages should be examined separately (Swanson 2011). To examine the effects of juvenile influx and survival on adult coral size structure distributions, juvenile abundance will be used as an explanatory covariate in statistical modeling (see section *2.3.3 Biological Data* for details).

***Coral size structure spatial resolution***

Coral size structure, density, and abundance estimates were made for *Isopora spp.* and *Montastrea curta* in the American Samoa island complex. *Isopora spp.* (n = 813 colonies) was present only on the islands of Tutuila, Ofu and Olosega, and Tau whereas *Montastrea curta* (n = 1,526 colonies) was present at all islands and Rose Atoll. Weibull shape parameter metrics were estimated for each coral population at two intra-island spatial scales (Table 1): shape parameter estimates at the raw site-level scale (Figure 4.1) and shape parameter estimates at the stratum-level (based on spatial strata designations via Habitat Use Analysis (HUA)) (Figure 4.2). Because a minimum of five data values is required to generate Weibull distribution parameter estimates, strata with a sample size less than five were excluded from analysis (*Isopora spp.*, n = 1 of 14 strata; *M. curta*, n = 2 of 32 strata) and sites with a sample size less than five were either

pooled or excluded from analysis (*Isopora spp.*, n = 27 of 48 sites; *M. curta*, n = 40 of 132 sites). To minimize elimination of samples from site-level analysis, sites with insufficient samples (< 5 data values) were either pooled with each other or were pooled with another site that had a sufficient sample size. Sites were only pooled if they were adjacent to each other and had the same depth range or adjacent depths (i.e. shallow and mid-depth sites were combined, or mid- and deep-depth sites were combined). A total of 18 sites for *Isopora spp*. (out of 48 sites) and 27 sites for *M. curta* (out of 132 sites) were pooled in this manner. Sites that were not pooled were excluded from analysis (*Isopora spp.*, n = 9 of 48 sites; *M. curta*, n = 13 of 132). Additionally, due to a lack of remote sensing data for the Rose Atoll backreef/lagoon environment, sites and strata that overlaid this area were excluded from analysis (*Isopora spp.*: n = 0 of 48 sites, n = 0 of 14 strata; *M. curta*: n = 3 of 132 sites, n = 1 of 32 strata). See Table 1 for final sizes of samples used in statistical modeling.

Coral size structure, density, and abundance estimates for strata were provided by Dr. Dione Swanson (NOAA/PIFSC/ESD). HUA uses procedures established by Manly et al. 1993 and demonstrated by Swanson (2011) to convert site-level surveys to population level estimates and includes a quantitative evaluation of individual coral populations to determine spatial variation in abundance and size structure. This is done using existing benthic habitat maps and GIS applications to partition the reef by geomorphologic characterizations and habitat strata (e.g. depth zone, habitat type, reef zone, reef complexity). Habitat strata layers were spatially represented as polygon shapefiles in ArcGIS at each island/atoll in American Samoa and were merged where appropriate based on each species' respective abundance (density and total) and size structure distributions. Because of the differences in each species' abundance and density signature, habitat strata layers vary for each species.

HUA analyses result in stratum-specific estimates of size-structure that may represent more meaningful (less noisy) measures of size structure dynamics (vs. site-specific estimates of size structure). The resulting size distribution patterns potentially infer spatial variation in growth and survival of coral populations which ultimately tells us how a population is selecting and utilizing resource(s) as well as how other population dynamics may vary over space (Manly et al. 1993). HUA results show distinct size distribution patterns that correspond to habitat use of individual species and identifies areas where individual coral species have relatively low, moderate, or high abundance estimates (negative, neutral, or positive habitat use respectively, inferring variation in coral growth and survival from size distribution patterns; Swanson 2011). See Figure 5 for a spatial overview and size structure histograms of *Montastrea curta* HUA results for Tutuila.

***2.3 Biophysical characterization***

A suite of oceanographic, geomorphological, biological, and anthropogenic factors was identified and characterized to evaluate biophysical relationships at the intra-island scale along the American Samoa island complex. Factors include: chlorophyll-a, sea surface temperature, irradiance, wave energy, net accretion rates, benthic cover, coral juvenile abundance, mean depth, geomorphological slope metrics, and human population density (see Table 2 for list of final variable metrics and details). These variables were selected as they are theorized to be primary and fundamental biophysical factors in structuring coral communities. To evaluate biophysical relationships, variables were used as explanatory covariates in statistical modeling. While there were a wide range of candidate biophysical predictors identified, not all variables were included in statistical modeling (see section *2.4 Biophysical modeling* for details on predictor selection).

Satellite-derived chlorophyll-a, sea surface temperature, and irradiance data was provided by Dr. Jamison Gove (NOAA/PIFSC/ESD) and Dr. Melanie Abecassis (NOAA/PIFSC/ESD) and model-derived wave energy flux (hereafter referred to as wave energy) was provided by S. Jeanette Clark (NOAA/PIFSC/ESD).

Benthic cover, net accretion rates, coral juvenile abundance, mean depth, and geomorphological slope metrics were obtained from ESD's American Samoa RAMP cruises. Benthic photoquadrat surveys were conducted at both benthic and fish REA sites in 2015 and serve as the basis of estimating benthic cover and composition. Rates of net calcium carbonate accretion were quantified from calcification accretion units (CAUs) collected in 2015 (deployed in 2012), which are used as recruitment and colonization instruments for primary calcifying organisms, crustose coralline algae and scleractinian corals (details below). Coral juvenile abundance and mean depth estimates were obtained from 2015 RAMP benthic REA surveys. Benthic habitat mapping products (from ESD RAMP and provided by the Pacific Islands Benthic Habitat Mapping Center, http://www.soest.hawaii.edu/pibhm) provide comprehensive bathymetric data in order to derive geomorphological metrics.

In order to link the coral size structure distributions to each explanatory covariate for statistical modeling, all oceanographic, geomorphological, biological, and anthropogenic data were spatially associated with each site and strata via ArcGIS spatial joining techniques. For strata, all explanatory covariates were initially obtained at each site. Sites and the linked covariates retained within their respective strata were then pooled and averaged to give covariate estimates for each stratum.

### *2.3.1 Oceanographic Data*

***Remote Sensing Data***

Monthly averaged composites for AVHRR sea surface temperature (SST, units: °C) data covered months spanning from January 2002 to April 2016. Monthly averaged composites for MODIS chlorophyll-a (chl-*a*, units: mg $m^{-3}$) and irradiance/photosynthetically active radiation (PAR, units: Einstein $m^{-2}$ $d^{-1}$) covered months spanning from July 2002 to July 2016. In order to obtain comparable spatial resolutions, chl-*a* and PAR (native spatial resolution of 0.04º) and SST (native spatial resolution of 0.1º) data sets were each regridded to 0.05º. This resolution is necessary to accurately evaluate biophysical relationships at the island/atoll scale, as exemplified by Gove et al. (2013). When integrating remotely sensed data, Gove et al. (2013) decreased the synthesized resolution to 0.0439° (4 km) which captured considerable spatial heterogeneity among each studied island/atoll. Due to contamination by land and increased reflectance in shallow water areas, remote sensing data in pixels in nearshore environments (< 30-m depth contour zone around each island) was removed from analysis (sensu Gove et al. 2013, Boss and Zaneveld 2003). Gap filling for missing or poor quality temporal data was achieved via linear interpolation or was excluded. The filtered dataset was used to generate climatological long-term mean values for chl-*a* and PAR (mean of monthly time series from July 2002 to July 2016) and SST (mean of monthly time series from January 2002 to April 2016) for each pixel around each island.

***Nearshore remote sensing extrapolation***

As a result of data elimination by spatial filtering within nearshore pixels, data holes were created in nearshore pixels that coincide with coral sampling sites. In order to obtain estimates for these blank pixels, a combination of both nearest neighbor spatial joining and extrapolation via statistically significant nearshore-offshore gradients in sectors of each island, were obtained to attach values to the blank pixels (sensu Tempera and Bates 2009; dataflow scheme outlined in

Figure 6). Nearest neighbor spatial joining was first used to attach long term mean chl-*a*, PAR, and SST values to all blank nearshore pixels (Figure 7-10). To more accurately capture spatial heterogeneity and the distribution of chl-*a*, PAR, and SST, nearshore-offshore gradients were extracted to different sectors of each island. Empirical Orthogonal Function (EOF) analysis of climatological seasonal means around each island was used to describe spatial modes or patterns of variability and how they change with time (Figure 11). EOF methodology decomposes time series data into representative dominant modes and enables analysis of data with complex spatial and temporal structures (Kaihatu et al. 1998). Mode 1 values were used for spatial pattern diagnostics as Mode 1 from the EOF analysis captured a majority of the variance for all remote sensing variables.. Additionally, seasonal means were used for spatial diagnostics (versus monthly means) as this metric better reflects spatial variability as it is subject to lower levels of high-frequency noise (Tempera and Bates 2009). Once spatial patterns were identified, cluster analysis was conducted around each island using Mode 1 values from EOF analysis. K-means cluster analysis was performed using base functions in R v3.2.3 (R Development Core Team, 2015) and is a multivariate analysis approach that forms groups or "clusters" of observations that are similar to each other but differ among groups, using the Hartigan-Wong algorithm (1979). Sectors were created based off the optimal number of clusters identified and subsequent heterogenous groups formed around each island. Regression analysis was then run with the range of values found in each sectors and used as estimators of the nearshore-offshore gradients. In island sectors where statistically significant gradients were identified, nearest neighbor values were not used and, instead, each blank pixel was given predicted values based off the relative distance to shore. A total of six datasets were produced including three nearest neighbor datasets (SST, chl-*a*, PAR; hereafter referred to as 'nearest neighbor' variables) and three nearest

neighbor plus corrected nearshore-offshore gradient datasets (SST, chl-*a*, PAR; hereafter referred to as 'gradient' variables), which were subsequently used as predictors in statistical modeling. GIS was further used to relate the coral data and remote sensing products using a spatial joining technique (Figure 12a-c, 13a-c, and 14a-c).

***Wave Energy Data***

In the absence of numerical wave model and wave forcing observational site-level data at the desired spatial resolution, a wave exposure proxy was used to examine coral size structure distributions. Wave energy is represented as the cumulative wave power a site is exposed to over the course of one year (units: MW $hr^{-1}$ $m^{-1}$). Annual integrated mean estimates cover years spanning from 2002 to 2012 with a spatial resolution of 0.01º.

Developed by S. Jeanette Clark to examine Pacific Island nearshore ecological communities in relation to wave exposure, wave energy estimates were derived utilizing Wave Watch III (WW3) global wave model data and coastline analysis of wave exposure. This is achieved by: 1) Determining the incident wave swath for a specific site at an island using a 360º radial plot and degree-bin elimination based on a swath's intersection with land or relevant bathymetric contour. 2) Selecting the closest WW3 pixel and extracting the time-series for significant wave height, peak period, and peak direction. 3) Calculating wave power (units: kW $hr^{-1}$ $m^{-1}$) with significant wave height and peak period using the following equation:

$$E_f = \rho g / 64\pi \ * H_s^2 * T_p /1000$$

where ρ is the density of seawater (1024 kg $m^{-3}$), $g$ is the acceleration of gravity (9.8 m $s^{-2}$), $H_s$ is the offshore significant wave height, and $T_p$ is the dominant wave period (1/wavelength). 4) Lastly, annual wave energy data is filtered and organized into respective degree bins based on peak direction and summed to give a wave energy estimate at each site.

Climatological long-term means for annual wave energy were calculated for each 0.01º pixel and estimates were spatially coupled with each coral REA site and strata via ArcGIS spatial joining techniques (Figure 15a-c). Wave energy data was available for pixels in the nearshore environment (<30 m depth contour zone) and did not require extrapolation methods used for the remote sensing data. For coral sites with unavailable wave energy data (n=55 sites), nearest neighbor methodology was performed to extrapolate values to sites. Because the wave energy metric calculated here is based on offshore wave height and does not account for variation with depth, an interaction term between depth and wave energy was included in all starting models to capture variation in wave effects when they are extrapolated inshore.

### *2.3.2 Geomorphological Data*

Multibeam bathymetric data for the American Samoa island complex was collected during the 2004 and 2006 NOAA Reef Assessment and Monitoring Program (RAMP) surveys and combined with 2001-2002 multibeam data collected by Dr. Dawn Wright at Oregon State University and Dr. Dave Naar of University of South Florida. Data was post-processed and bathymetric products (spatial resolution of 5 m) were provided by the Pacific Islands Benthic Habitat Mapping Center (PIBHMC, www.soest.hawaii.edu/pibhmc). Multibeam data was incomplete for the 0-25 m depth nearshore environments. In order to provide complete bathymetric coverage of nearshore reef environments around the American Samoa island complex, bathymetric gaps for the 0-25 m depth zone were filled in with "estimated depths" using IKONOS satellite imagery (Lyzenga 1985).

For the island of Tutuila, NOAA Coastal Digital Elevation Model (DEM) bathymetry (spatial resolution of 10 m) was used (https://www.ngdc.noaa.gov/mgg/inundation/nthmp/nthmp.html). NOAA's National

Geophysical Data Center (NGDC) builds integrated bathymetric-topographic DEMs which are used to support tsunami forecasting and modeling efforts and provides high-resolution and more accurate, seamless bathymetry. NOAA Coastal DEM products were unavailable for other American Samoa islands.

Four measures of benthic geomorphology were derived from the native bathymetry data layers: slope, mean slope, slope range, and slope coefficient of variation (hereafter referred to as 'slope variability'). Slope, measured in degrees, is the maximum change in elevation (0º to 90º) between a depth grid cell and its 8 neighbors and was derived using the slope function in the ArcGIS v10.4.1 Spatial Analyst toolbox. Mean slope and slope range, measured in degrees, were derived from the slope layer product using the Focal Statistics function in the ArcGIS v10.4.1 Spatial Analyst toolbox. Mean slope is the average slope value and slope range is the difference between the maximum and minimum slope values of the grid cells in the specified surrounding neighborhood. Slope variability is the amount of variation around the mean slope and was calculated by dividing the standard deviation by the mean slope.

In order to synthesize slope metrics (mean, range, variability) at the same spatial scale as coral REA site-level data (50 $m^2$), neighborhood settings were set to quantify 50 $m^2$ rectangular planar areas surrounding each site. Geomorphological metrics were spatially coupled with each coral site and strata via ArcGIS spatial joining techniques.

Average depth was also used as a geomorphological covariate. For site-level data, average depth estimates were obtained directly at each benthic REA site. For each strata, depth estimates were averaged for all site-level data that fell within a given strata to give a strata mean depth.

### *2.3.3 Biological Data*

Benthic cover and composition data were collected via benthic photoquadrat surveys in the American Samoa island complex in 2015. Photoquadrat surveys were conducted along two 25 m transects at both benthic and fish REA sites in which photographs were obtained at 1 m intervals (30 photographs per site). Benthic photographs were analyzed for percent cover of five benthic functional groups (coral, crustose coralline algae (CCA), macroalgae, turf algae, and soft coral) using Coral Point Count with Excel Extensions (Kohler and Gill 2006). For site-level coral size structure distributions, benthic percent cover estimates were obtained directly at each benthic REA site. For each strata, benthic percent cover estimates were averaged for all benthic and fish REA sites that fell within a given strata to give a strata mean percent cover of each benthic group.

Net carbonate accretion rate (hereafter referred to as accretion rate) data was measured via calcification accretion units (CAUs) collected in the American Samoa island complex in 2015. CAUs are used for the recruitment and colonization of primary reef calcifiers (CCA and hard corals) and measurements of net accretion provide information on how much calcium carbonate is deposited on a coral reef over a given time frame (i.e. spatio-temporal variability in accretion rates). CAUs collected in 2015 in American Samoa were deployed in 2012 (3-year soak time) and total net accretion was calculated by measuring the change in weight of each CAU at each site deployed over the given time period (units: g $CaCO_3$ $m^{-2}$ $yr^{-1}$). A CAU site has on average 4 CAU units and thus the metrics i) mean net carbonate accretion rate (average of all CAU units at each site) and the ii) net carbonate accretion rate coefficient of variation (standard deviation divided by the mean rate; hereafter referred to as 'accretion rate variability') were calculated for each CAU site and used in these analyses. Because benthic REA and CAU sites did not overlap, a nearest neighbor approach was used to obtain accretion rate estimates at

benthic REA sites. For strata, all CAU sites that fell within a given stratum were used and accretion rate estimates were calculated using CAU units to obtain a stratum-level mean accretion rate and accretion rate variability estimates.

As coral-recruit settlement patterns and post-settlement survivorship to adulthood (Done 1982) are important causal factors in the distribution and structure of coral communities, juvenile coral abundance was also used as an explanatory covariate. Juvenile abundance is a proxy for larval supply, settlement, and growth and survival to adulthood (Swanson 2011) and juvenile corals are defined as individuals ≤ 4 cm maximum diameter. Juvenile coral demographic data is collected at benthic REA sites where site-level abundance metrics are estimated for each site. For strata, Dr. Swanson provided strata-weighted juvenile abundance estimates.

### *2.3.4 Anthropogenic Data*

It is suggested that, when considering predictors of coral community structure and condition, environmental variables should include anthropogenic activity. Multiple studies have tied declines in coral reefs to human rather than natural causes. The American Samoa island complex exhibits a range of human impact sites, from high human-impact to almost no human-impact. As a proxy for potential human impact, human population density estimates scaled per unit reef area were used in this research. Human population density estimates are expressed as number of people (2010 US census; http://www.census.gov/2010census/) within a 10 km and 20 km buffer divided by the forereef area (sensu Williams et al. 2015b). Estimates were obtained for each benthic REA site and thus used directly in correlation with site-level coral size structure distributions. Site-level estimates within the respective strata were averaged to give human population density estimates for each stratum.

## *2.4 Biophysical statistical analyses*

Prior to developing statistical models, potential (multi)collinearity among explanatory covariates was examined using Pearson correlations, unconstrained ordination (e.g. PCA), and variance inflation factors (VIF). PCA biplots were initially used to assess which covariates were moving together and potentially exhibiting collinearity. Pearson's correlation values were used next to remove covariates with a threshold correlation of 0.75 (exclusion if $r > 0.75$). The following variables were strongly correlated: percent cover of soft coral and macroalgae ($r = 0.86$); chl-a gradient and nearest neighbor ($r = 0.86$); mean slope and slope range ($r = 0.81$); human population density within a 10-km radius and chl-a nearest neighbor ($r = 0.89$) and chl-a gradient ($r = 0.81$). Percent soft coral cover was the only covariate removed using Pearson's correlation values. Percent macroalgae cover, chl-a gradient and nearest neighbor, human population density, mean slope, and slope range were of mechanistic interest in testing the hypothesis and were not removed. These covariates were further assessed using VIF calculations (see below) and were removed based off these results.

With the remaining covariates, VIFs were calculated and evaluated using 3 as a threshold (Zuur et al. 2010). Covariates with the highest VIF were dropped, then recalculated and sequentially dropped until all VIFs were less than 3. Covariates were tested for multi-collinearity and removed as needed for both site-level and strata-level datasets. Nineteen in total environmental, biological, and anthropogenic variables were used as explanatory covariates in statistical modeling (see Table 2 for final list of predictors; see section *3. Results* for final predictors used in each model). To account for differences in sampling effort at each site, the total area surveyed at each site ($m^2$) was used as a predictor in site-level analysis. Because the survey design and analysis used to generate coral population-level metrics for strata inherently

accounts for variation in sampling effort, it was not necessary to use total area surveyed as a predictor in strata analysis.

For each coral species and spatial resolution (site and strata), the Weibull shape parameter, *k*, of log transformed data was used as the response variable to examine relationships between coral size structure distributions and variations in the predictors. Initial examination of the response versus predictors showed no evidence of major non-linearity. Generalized Linear Models (GLM) were initially fit with a gamma distribution using the inverse link function and the assumptions of linearity and the error distribution were tested. Due to a small sample size, only main predictor effects were initially tested in all models and two-way interactions were later tested based on initial top candidate model selection (see interactions below).

Model selection and model-averaging procedures were conducted using the *dredge* function in the *MuMIn* R package (Bartoń 2016) and models were ranked according to Akaike's Information Criterion corrected (AICc) for small sample sizes. As an additional measure of model performance, likelihood-ratio based $R^2$ values were calculated. All models were retained based on $\Delta AICc \leq 2$. For candidate models with $\Delta AICc \leq 2$, importance of each predictor was assessed to assist with best model selection. Predictor importance calculates the sum of the Akaike weights (based on normalized, relative model likelihoods) over all models (models with $\Delta AICc \leq 2$) where the predictor variable occurs. Top candidate main effects GLMs were selected based on a combination of $\Delta AICc \leq 2$ criteria, likelihood-ratio based $R^2$ values, and predictor variable importance.

On the basis of results for main effects GLMs, interaction models were fit and tested with combinations of all top candidate model main effects and all two-way interactions. Model selection and model-averaging procedures were performed on interaction models and models

were ranked and retained based on ΔAICc ≤ 2. If interaction terms were significant, the top candidate interaction GLM(s) was compared to the top candidate main-effects GLM(s) and ranked based on ΔAICc ≤ 2. Top candidate models were chosen based on ΔAICc ≤ 2.

To account for spatial autocorrelation, a Generalized Additive Model (GAM) using the *mgcv* package in R (Wood 2011) was fit which included a 2D smoother on 'site' and 'strata' location, i.e. s(latitude, longitude). GAM models were compared to their equivalent GLM and/or interaction GLM based on ΔAICc ≤ 2. Models were compared based on ΔAICc ≤ 2 criteria.

Finally, the top candidate main effects and interaction GLMs were refit as a GAM in order to test the assumption of linearity. Given a small sample size in all models, the number of knots for the smoothing terms was reduced to three to prevent overfitting. GAM models were compared to both main effect GLMs and interaction GLMs based on ΔAICc ≤ 2. A final best-fit model(s) was selected based off these results (see Results section for all main effect GLM, interaction GLM, and GAM results).

Model diagnostics were assessed by examining residual diagnostic plots. Significant or influential outliers (criteria of Cook distance > 1; Fox 2002) were identified. If influential outliers were present, they were removed from the dataset and models were re-run and reexamined using residual diagnostic plots. Influential outliers were removed permanently only if this greatly improved residual behavior in model diagnostics. Additionally, models were refit with alternate link functions (e.g. 'log') and model diagnostics were reassessed to determine the most relevant link function needed.

For final best-fit models, the relative importance of each predictor in explaining the total variance was determined by hierarchical partitioning using the *hier.part* package in R (Walsh and MacNally 2013). Hierarchical partitioning examines the effect of removing each predictor

from the whole model hierarchy using all combinations of variables and subsequently provides the average contribution of each variable of the total explained variance.

All computations and statistical modeling was carried out using R v3.2.3 (R Development Core Team, 2015). EOF analysis was carried out in MATLAB R2014a.

# 3. RESULTS

## *3.1 Site-level results*

### *3.1.1 Isopora spp. site-level data*

*Isopora spp*. size structure varied significantly across sites and islands, with shape parameters, k, ranging from 3.89 to 14.06. Variability in size structure shape parameters was also highly correlated with variability in median coral colony size and skewness but deviated from the observed patterns for shape parameters > 10 (Figure 17a, 18a, 19a). When compared to median size, there was a significant positive linear relationship with the size structure shape parameter (shape parameter < 10; analysis of deviance type II test, p = 7.13e-04) where sites with the higher shape parameters also had larger median coral colony size (Figure 17a). In relation to skewness, there was a significant negative linear relationship (shape parameter < 10; analysis of deviance type II test, p = 1.76e-03) where sites with lower shape parameters were more positively skewed (higher frequency of smaller colonies and relatively few large colonies) and sites with higher shape parameters were more negatively skewed (high frequency of larger colonies and relatively few small colonies; Figure 18a). Sites with positively skewed distributions had an average size structure shape parameter of 5.43 (ranging from 3.89 to 10.30) whereas negatively skewed distributions had, on average, a slightly larger size structure shape parameter of 6.91 (ranging from 4.83 to 14.06). Median size and skewness exhibited a strong

negative linear relationship (shape parameter < 10; analysis of deviance type II test, p = 7.42e-05) where an increase in positive skewness correlated with smaller median size and an increase in negative skewness correlated with larger median size (Figure 19a). The relationship between median size and skewness appeared to deviate from the observed pattern for shape parameters > 10.

*Isopora spp*. size structure spatial variability in relation to intra-island biophysical variability was modeled using GLMs. Initial steps included testing for multi-collinearity among predictors, in which the following covariates were removed from the starting model: percent turf alga and coral cover, and chl-a (gradient and nearest neighbor), SST and PAR (gradient), mean slope, and slope variability. Remaining predictors were total area surveyed at each site, mean depth, human population density within a 10-km radius, PAR and SST (nearest neighbor), wave energy, *Isopora* juvenile abundance, 2015 mean accretion rate and accretion rate variability, percent CCA cover, slope, and slope variability. In all candidate models, influential outliers were assessed in model diagnostics however no outliers were removed.

A GLM fit with a gamma distribution using the inverse link and only main effects were initially tested due to a low sample size (n = 48 sites; see interactions below). Two candidate models were chosen based on $\Delta AICc \leq 2$. Based on these results, candidate models were re-run with all 2-way interactions included and three models were chosen based on $\Delta AICc \leq 2$ (Table 3). The top ranked models included 2015 mean accretion rate and accretion rate variability, slope, and slope variability. The additional predictor, *Isopora* juvenile abundance, was included in the third best model ($\Delta AICc = 1.84$) however this covariate did not significantly improve model explanatory power (analysis of deviance type II test, p = 0.152).

The model with the highest AICc weight included the interaction between slope and slope variability, which had a significant effect on the response (analysis of deviance type II test, $p = 0.05$) and increased the overall explained deviance of the model from 48 to 58%. The selected best model was:

(1) shape_log ~ 2015 mean accretion rate + 2015 accretion rate variability + slope + slope variability + slope : slope variability

To account for spatial autocorrelation, a GAM was fit and included a 2D smoother on 'site':

(2) shape_log ~ 2015 mean accretion rate + 2015 accretion rate variability + slope + slope variability + slope : slope variability + s(latitude, longitude)

Based on $\Delta AICc \leq 2$ criteria, model 1 (without 2D smoothed term; $\Delta AICc = 0$) was significantly better than model 2 (with the 2D smoothed term; $\Delta AICc = 7.96$) and model 1 was chosen. The assumption of linearity was then tested by refitting model 1 as a GAM:

(3) shape_log ~ s(2015 mean accretion rate) + s(2015 accretion rate variability) + s(slope) + s(slope variability)

The GLM (model 1) was the best model, however there was not a significant difference between the GLM (model 1; $\Delta AICc = 0$) and the GAM (model 3; $\Delta AICc = 0.77$). Because the GLM is a simpler and "less expensive" model, the GLM (model 1) was selected as the final best-fit model. Model diagnostics were run on the resulting best model and residuals were uniformly distributed with no significant outliers. Residuals did not differ significantly from a normal distribution (Shapiro-Wilks test, $p = 0.11$). The best-fit model was refit with alternate link functions (e.g. 'log'), however the 'inverse' link function yielded better model diagnostic results based on inspection of the residuals.

Modeled biological and geomorphological variables explained a large proportion of spatial variation in site-specific *Isopora spp*. size spectra (overall deviance explained, $R^2$ = 58%) and varied significantly across sites and islands (Figure 20). Accretion rates ranged from a low of 0.045 (southeast side of Tutuila) to a high of 0.092 g $CaCO_3$ $m^{-2}$ $yr^{-1}$ (southeast side of Ofu/Olosega), accretion rate variability ranged from 0.10 (southwest side of Tutuila) to 0.504 g $CaCO_3$ $m^{-2}$ $yr^{-1}$ (southeast side of Ofu/Olosega), slope ranged from 1.274 degrees (southwest side of Tutuila) to 21.252 (southeast side of Tutuila), and slope variability from 0.285 degrees (east side of Tutuila) to 1.019 degrees (southeast side of Tutuila). Results from hierarchical partitioning indicated that accretion rate variability, mean accretion rate, slope, and slope variability explained 14, 12, 12, and 10% of the overall deviance, respectively. These predictors explained 48% of the overall variance and the interaction term, slope and slope variability, increased the overall deviance to 58%. All covariates had strong effects on size spectra. Size spectra shape parameters decreased linearly with increasing mean accretion rates (analysis of deviance type II test, p = 0.05), accretion rate variability (analysis of deviance type II test, p = 0.001), and slope variability (analysis of deviance type II test, p = 0.03). Size spectra shape parameters increased linearly with increasing slope (analysis of deviance type II test, p = 0.014) (Figure 20). The significant interaction between slope and slope variability (analysis of deviance type II test, p = 0.05) indicated that at low to moderate slope values, the shape parameter does not change significantly with increasing slope variability, however along steeper slopes (higher values) the shape parameter decreases significantly with increasing slope variability, especially when slope variability is low (Figure 20).

### *3.1.2 Montastrea curta site-level data*

*M. curta* size structure varied significantly across sites and islands, with shape parameters, k, ranging from 3.13 to 17.33. Variability in size structure shape parameters was also highly correlated with variability in median coral colony size and skewness but deviated from the observed pattern with median size for shape parameters > 13 (Figure 17b, 18b, 19b). When compared to median coral colony size, there was a significant positive linear relationship with the size structure shape parameter (shape parameter < 13; analysis of deviance type II test, p = 0.02) where sites with higher shape parameters also had larger median coral colony size (Figure 17b). In relation to skewness, there was a significant negative linear relationship (analysis of deviance type II test, p = 2.89e-11) where sites with lower shape parameters were more positively skewed (higher frequency of smaller colonies and relatively fewer large colonies) and sites with higher shape parameters were more negatively skewed (high frequency of larger colonies and relatively fewer small colonies; Figure 18b). Sites with positively skewed distributions had an average size structure shape parameter of 5.72 (ranging from 3.13 to 9.16) whereas negatively skewed distributions had a larger average size structure shape parameter of 8.36 (ranging from 5.99 to 17.33). Median size and skewness exhibited a strong negative linear relationship where an increase in positive skewness correlated with smaller median size and an increase in negative skewness correlated with larger median colony size (analysis of deviance type II test, p = 1.58e-04; Figure 19b).

*M. curta* size structure spatial variability in relation to intra-island biophysical variability was modeled and explained using GLMs. Initial steps included testing for multicollinearity among predictors, in which the following covariates were removed from the starting model: percent turf alga cover, chl-a (nearest neighbor), SST and PAR (gradient), 2015 accretion rate variability, mean slope, and slope variability. Remaining predictors were total area surveyed at

each site, mean depth, human population density within a 10-km radius, chl-a (gradient), PAR and SST (nearest neighbor), wave energy, *M. curta* juvenile abundance, 2015 mean accretion rate, percent CCA and coral cover, slope, and slope range.

A GLM fit with a gamma distribution using the inverse link and only main effects was initially tested due to low sample size (n = 132 sites; see interactions below). Three influential outliers were identified in initial model runs. Model tests were performed in which these three outliers were removed, models were rerun, and reexamined using residual diagnostic plots. Two outliers were removed permanently as this greatly improved residuals in model diagnostics and increased the overall deviance explained from 29% to 43%. The third outlier was not permanently removed as removal did not improve model performance and the site (Swains pooled sites) was of interest mechanistically in testing the research hypothesis.

One candidate model was chosen based on a combination of $\Delta AICc \leq 2$ criteria, ranking in model dredge, likelihood-ratio based $R^2$ values, and predictor variable importance (threshold > 0.20). Based on these results, candidate models were re-run with all 2-way interactions included and two models were chosen based on $\Delta AICc \leq 2$ (Table 3). The top ranked models included the main effects PAR, percent coral cover, mean depth, *M. curta* juvenile abundance, SST, wave energy, and the interaction between SST and *M. curta* juvenile abundance.

The two top ranked models performed similarly ($\Delta AICc = 0.41$). The model with the highest AICc weight included two additional interaction predictors however these covariates did not significantly improve model explanatory power: mean depth and wave energy (p=0.11); *M. curta* juvenile abundance and wave energy (p=0.07). Thus, the simpler model was chosen. The selected best model was:

(1) shape_log ~ mean depth + *M. curta* juvenile abundance + % coral cover + PAR + SST + wave energy + SST : *M. curta* juvenile abundance

To account for spatial autocorrelation, a GAM was fit and included a 2D smoother on 'site':

(2) shape_log ~ mean depth + *M. curta* juvenile abundance + % coral cover + PAR + SST + wave energy + SST : *M. curta* juvenile abundance + s(latitude, longitude)

Based on $\Delta AICc \leq 2$ criteria, model 1 (without 2D smoothed term; $\Delta AICc = 0$) was significantly better than model 2 (with the 2D smoothed term; $\Delta AICc = 3.81$) and model 1 was chosen. The assumption of linearity was then tested by refitting model 1 as a GAM:

(3) shape_log ~ s(mean depth) + s(*M. curta* juvenile abundance) + s(% coral cover) + s(PAR) + s(SST) + s(wave energy) + SST : *M. curta* juvenile abundance

Based on $\Delta AICc \leq 2$ criteria there was not a significant difference between the GAM (model 3; $\Delta AICc = 0$) and the GLM (model 1; $\Delta AICc = 0.36$). Because the GLM is a simpler and "less expensive" model, the GLM (model 1) was selected as the final best-fit model.

Model diagnostics were run on the resulting best model and residuals were uniformly distributed with no significant outliers. Residuals did not differ significantly from a normal distribution (Shapiro-Wilks test, $p = 0.19$). The best-fit model was refit with alternate link functions (e.g. 'log'), however the 'inverse' link function yielded better model diagnostic results based on inspection of the residuals.

Modeled biological and geomorphological variables explained a large proportion of spatial variation in site-specific *M. curta* size spectra (overall deviance explained, $R^2 = 45\%$) and varied significantly across sites and islands (Figure 21). Mean depth ranged from 4.75 to 23 m, *M. curta* juvenile abundance ranged from 0 (west Ofu/Olosega) to 16 colonies (southern offshore bank on Tutuila), percent coral cover ranged from 0.34 (southern offshore bank on Tutuila) to

70.24% (north Tutuila), PAR ranged from 42.41 (northwest Tutuila) to 44.0 E $m^{-2}$ $d^{-1}$ (northeast Ofu/Olosega), wave energy ranged from 28.73 (north Tutuila) to 158.33 MW $hr^{-1}$ $m^{-1}$ (south Rose Atoll), and SST ranged from 28.73 (south Rose Atoll) to 29.3 °C (Swains). Results from hierarchical partitioning indicated that PAR, coral cover, wave energy, mean depth, juvenile abundance, and SST explained 16, 11, 8, 5, and <1% of the overall deviance, respectively. These predictors explained 43% of the overall variance and the interaction term, juvenile abundance and SST, increased the overall deviance to 45%. All covariates had strong effects on size spectra except for the main effect, SST. Size spectra shape parameters decreased linearly with increasing PAR (analysis of deviance type II test, p = 1.54e-05), juvenile abundance (analysis of deviance type II test, p = 0.04), and SST (analysis of deviance type II test, p = 0.14). In contrast, size spectra shape parameters increased linearly with increasing mean depth (analysis of deviance type II test, p = 4.0e-04) and coral cover (analysis of deviance type II test, p = 4.0e-03; Figure 21). The significant interaction between juvenile abundance and SST (analysis of deviance type II test, p = 0.03) indicated that at higher SST values, the shape parameter did not change with increasing juvenile abundance (however variance is high at high juvenile abundance) while, at lower-moderate SST, the shape parameter decreased with increasing juvenile abundance, especially at low SST values (Figure 21).

During initial model runs with the three strongest outliers removed, all main effects predictors were the same with the exception of model human population density within a 10-km radius, which did not have a significant effect on size structure shape parameter variability (analysis of deviance type II test, p = 0.21).

### *3.2 Strata-level results*

#### *3.2.1 Isopora spp. strata-level data*

*Isopora spp*. size structure varied across strata and islands, with shape parameters, *k*, ranging from 4.6 (Ofu/Olosega southeast shallow- and mid-depth stratum) to 8.09 (Tau northwest mid-depth stratum). Variability in size structure shape parameters was also correlated with variability in skewness but was not correlated with median coral colony size (Figure 17a, 18a, 19a). When compared to median size, the relationship with the size structure shape parameter was insignificant and variable across strata (analysis of deviance type II test, $p = 0.99$; Figure 17a). Skewness and the size structure parameter displayed a negative, but weak, linear relationship (analysis of deviance type II test, $p = 0.06$) where strata with lower shape parameters were positively skewed (higher frequency of smaller colonies and fewer larger colonies) and strata with higher shape parameters were negatively skewed (higher frequency of larger colonies and fewer smaller colonies; Figure 18a). Strata with positively skewed distributions had an average size structure shape parameter of 5.24 (ranging from 4.59 to 5.98) whereas negatively skewed distributions had an average size structure shape parameter of 6.08 (ranging from 4.77 to 8.09). Median size and skewness exhibited a strong negative linear relationship (analysis of deviance type II test, $p = 3.30e\text{-}03$) where an increase in positive skewness correlated with smaller median size and an increase in negative skewness correlated with larger median size (Figure 19a).

*Isopora spp*. size structure spatial variability in relation to intra-island biophysical variability was modeled using GLMs. Initial steps included testing for multi-collinearity among predictors, in which the following covariates were removed from the starting model: percent turf alga, CCA and coral cover, chl-a (gradient and nearest neighbor), SST and PAR (gradient), human population density within a 10-km radius, 2015 accretion rate variability, mean slope, slope, slope range. Remaining predictors were mean depth, PAR and SST (nearest neighbor),

wave energy, *Isopora* juvenile abundance, 2015 mean accretion rate, and slope variability. The covariates 2015 mean accretion rate and wave energy both had VIFs above 3 (4.15 and 4.10, respectively) and were negatively correlated when assessed via Pearson's correlation ($r = 0.61$). Because these covariates were potentially mechanistically important, they were not removed from initial model runs. In all candidate models, influential outliers were assessed in model diagnostics however no outliers were removed.

A GLM fit with a gamma distribution using the inverse link and only main effects were initially tested due to a low sample size ($n = 14$ strata; see interactions below). One candidate model was chosen based on $\Delta AICc \leq 2$. Based on these results, the candidate model was re-run with all 2-way interactions included. No interactions were included in the best models ($\Delta AICc \leq 2$ criteria) and the results did not differ (Table 3). Thus, the candidate model was selected as the best model:

(1) shape_log ~ 2015 mean accretion rate + wave energy

To account for spatial autocorrelation, a GAM was fit and included a 2D smoother on 'stratum':

(2) shape_log ~ 2015 mean accretion rate + wave energy + s(latitude, longitude)

Based on $\Delta AICc \leq 2$ criteria, model 1 (without 2D smoothed term; $\Delta AICc = 0$) was significantly better than model 2 (with the 2D smoothed term; $\Delta AICc = 12.33$) and model 1 was chosen. The assumption of linearity was then tested by refitting model 1 as a GAM:

(3) shape_log ~ s(2015 mean accretion rate) + s(wave energy)

The GLM (model 1) was the best model, however there was not a significant difference between the GLM (model 1; $\Delta AICc = 0$) and the GAM (model 3; $\Delta AICc = 0.35$). Because the GLM is a simpler and "less expensive" model, the GLM (model 1) was selected as the final best-fit model.

Model diagnostics were run on the resulting best model with no significant outliers. Residuals were not uniform due to a small sample size (n = 14), but did not differ significantly from a normal distribution (Shapiro-Wilks test, p = 0.47). The best-fit model was refit with alternate link functions (e.g. 'log'), however the 'inverse' link function yielded better model diagnostic results based on inspection of the residuals.

Modeled biological and geomorphological variables explained a large proportion of spatial variation in stratum-level *Isopora spp*. size spectra (overall deviance explained, $R^2$ = 46%) and varied significantly across strata and islands (Figure 22). Mean accretion rates ranged from 0.05 (Aunu'u Island stratum on southeast Tutuila, all depths) to 0.08 g $CaCO_3$ $m^{-2}$ $yr^{-1}$ (Ofu/Olosega southeast shallow- and mid-depth stratum) and wave energy ranged from 43.33 (Ofu/Olosega northwest mid-depth stratum) to 120.20 MW $hr^{-1}$ $m^{-1}$ (Aunu'u Island stratum on southeast Tutuila, all depths). Results from hierarchical partitioning indicated that wave energy and mean accretion rate explained 40 and 6% of the overall deviance, respectively. Size spectra shape parameters decreased linearly with increasing mean accretion rate (analysis of deviance type II test, p = 0.16; Figure 22) and wave energy where the effect of wave energy on the response was significant (analysis of deviance type II test, p = 0.005; Figure 22).

***3.4 Montastrea curta strata-level data***

*M. curta* size structure varied significantly across strata and islands, with shape parameters, *k*, ranging from 2.73 (Swains southeast deep-depth stratum) to 12.74 (Tutuila southwest shallow/mid-depth stratum). Variability in size structure shape parameters was also highly correlated with variability in skewness and median coral colony size (Figure 17b, 18b, 19b). When compared to median size, there was a strong positive linear relationship with the size structure shape parameter (analysis of deviance type II test, p = 6.55e-03; Figure 17b) where

sites with higher shape parameters also had larger median coral colony size (Figure 9b). Skewness and the size structure parameter displayed a strong negative linear relationship (analysis of deviance type II test, p = 6.57e-03) where strata with lower shape parameters were more positively skewed (higher frequency of smaller colonies and fewer larger colonies) and strata with higher shape parameters were more negatively skewed (higher frequency of larger colonies and fewer smaller colonies; Figure 18b). Strata with positively skewed distributions had an average size structure shape parameter of 6.13 (ranging from 2.73 to 12.74) whereas negatively skewed distributions had a larger average size structure shape parameter of 8.28 (ranging from 6.28 to 11.05). Median size and skewness exhibited a strong negative linear relationship (analysis of deviance type II test, p = 3.44e-03) where an increase in positive skewness correlated with smaller median size and an increase in negative skewness correlated with larger median size (Figure 19b).

*M. curta* size structure spatial variability in relation to intra-island biophysical variability was modeled and explained using GLMs. Initial steps included testing for multi-collinearity among predictors, in which the following covariates were removed from the starting model: percent turf alga and CCA cover, chl-a (nearest neighbor and gradient), SST and PAR (gradient), 2015 mean accretion rate variability, mean slope, and slope range. Remaining predictors were mean depth, human population density within a 10-km radius, PAR and SST (nearest neighbor), wave energy, *M. curta* juvenile abundance, 2015 mean accretion rate, percent coral cover, slope, and slope variability.

A GLM fit with a gamma distribution using the inverse link and only main effects were initially tested due to a low sample size (n = 25 strata; see interactions below). One influential outlier was identified in initial model runs (data point for Swains). In order to test the research

hypothesis and examine inter-island variability, this outlier was not removed permanently. One candidate model was chosen based on a combination of $\Delta AICc \leq 2$ criteria, likelihood-ratio based $R^2$ values, and predictor variable importance (threshold > 0.20). Based on these results, the candidate model was re-run with all 2-way interactions however model results did not change and did not include any interaction terms (Table 3). The second ranked model included all covariates and had the highest $R^2$ value ($R^2 = 57\%$) and was thus selected as the best model:

(1) shape_log ~ 2015 mean accretion rate + PAR + SST + wave energy

To account for spatial autocorrelation, a GAM was fit and included a 2D smoother on 'stratum':

(2) shape_log ~ 2015 mean accretion rate + PAR + SST + wave energy + s(latitude, longitude)

Based on $\Delta AICc \leq 2$ criteria, model 1 (without 2D smoothed term; $\Delta AICc = 0$) was significantly better than model 2 (with the 2D smoothed term; $\Delta AICc = 4.72$) and model 1 was chosen. The assumption of linearity was then tested by refitting model 1 as a GAM:

(3) shape_log ~ s(2015 mean accretion rate) + s(PAR) + s(SST) + s(wave energy)

The GAM (model 3) was the second best model, however there was not a significant difference between the GAM (model 3; $\Delta AICc = 0.6$) and the GLM (model 1; $\Delta AICc = 0$). Because the GLM is a simpler and "less expensive" model, the GLM (model 1) was selected as the final best-fit model.

Model diagnostics were run on the resulting best model. Residuals were not uniform due to the outlier (data point for Swains), but did not differ significantly from a normal distribution (Shapiro-Wilks test, $p = 0.38$). The best-fit model was refit with alternate link functions (e.g. 'log'), however the 'inverse' link function yielded better model diagnostic results based on inspection of the residuals.

Modeled biological and geomorphological variables explained a large proportion of spatial variation in stratum-level *M. curta* size spectra (overall deviance explained, $R^2$ = 57%) and varied significantly across strata and islands (Figure 23). Mean accretion rates ranged from 0.05 (Aunu'u Island shallow-depth stratum on southeast Tutuila) to 0.16 (Rose Atoll forereef stratum), PAR ranged from 42.41 (Tutuila northwest mid-depth stratum) to 43.81 E $m^{-2}$ $d^{-1}$ (Swains southeast deep-depth stratum), wave energy ranged from 22.87 (Tutuila northwest deep-depth stratum) to 128.79 MW $hr^{-1}$ $m^{-1}$ (Tutuila southeast deep-depth stratum), and SST ranged from 28.75 (Rose Atoll forereef stratum) to 29.3 °C (Swains southeast deep-depth stratum). Results from hierarchical partitioning indicated that PAR, mean accretion rate, wave energy, and SST explained 29, 15, 7, and 7% of the overall deviance, respectively. These predictors explained 57% of the overall variance. PAR and SST had strong effects on size spectra where size spectra shape parameters significantly decreased linearly with increasing PAR (analysis of deviance type II test, p = 0.004) and SST (analysis of deviance type II test, p = 0.02). Size spectra shape parameters also decreased linearly with increasing mean accretion rate (analysis of deviance type II test, p = 0.05) and wave energy (analysis of deviance type II test, p = 0.13) however the effect was not strong (Figure 23).

# 4. DISCUSSION

## 4.1 Coral size structure metric

In general, coral size structure distributions have been shown to be positively skewed where populations consist primarily of smaller colonies and relatively few large ones (e.g. Soong 1993). Additionally, "healthy" coral population size structure distributions typically consist of a wide range of size classes, with few missing size classes and overall higher densities (Bak and

Meesters 1998, Meesters et al. 2001). The degree of skewness varies among species where some populations can be negatively skewed; however, highly negatively skewed distributions may indicate a lack of successful recruitment (Guzner et al. 2007, Alvarado- Chacòn and Acosta 2009) and implies a risk of population decline (Meesters et al. 2001).

For both *Isopora* and *M. curta*, we find that shape parameter estimates scale well with skewness and median size estimates, implying that the Weibull shape parameter metric is a comprehensive metric that captures other important coral size structure characteristics. Additionally, shape parameter estimates can be used to assess the status and health of each coral population across space. Based off the assumption that "healthy" populations exhibit distributions close to zero skewness (on a log scale) with a higher frequency of smaller colonies and fewer large ones, *Isopora* site-level shape parameters that exhibit an average of 5.53, median size of 18.37 cm, and skewness of -0.07 appeared to resemble "healthy" subsets of the population. Strata-level estimates had similar results with a "healthy" shape parameter average of 5.52, median size of 22.02 cm, and skewness of 0.05. Shape parameter site- and strata-level estimates that deviated from this pattern had either enhanced positive or negative skewness as well as lower or higher median sizes, depending on the direction that the shape parameter deviated from the "healthy" estimate (see Figure 26 for example of *Isopora spp.* size structure distributions with low, moderate, and high shape parameter estimates).

*M. curta* site-level shape parameters in proximity of an average of 6.37, median size of 11.39 cm, and skewness of 0.28 appeared to resemble "healthy" subsets of the population. Strata-level estimates had similar results with a "healthy" shape parameter average of 6.09, median size of 12.48 cm, and skewness of 0.41. As with *Isopora*, *M. curta* shape parameter site- and strata-level estimates that deviated from this pattern had either enhanced positive or negative skewness

as well as lower or higher median sizes, depending on the direction that the shape parameter deviated from the "healthy" estimate.

Overall shape parameter averages reveal differences between *Isopora* and *M. curta* size structure distributions. *Isopora* exhibited a lower average shape parameter (site = 6.23, strata = 5.76), higher median sizes (site = 18.57, strata = 21.23), and negative skewness (site = -0.06, strata = -0.12) versus *M. curta* ($k$ = 6.64 and 6.61; median size = 11.25 and 13.06; skewness = 0.30 and 0.40, for site and strata resolution, respectively). These dissimilarities most likely reflect differences in their underlying life-history traits (e.g. fecundity, growth, mortality, morphology; Meesters et al. 2001, Guzner et al. 2007). These findings highlight variability in demographic processes between coral species as well as support the evidence that demographic processes are strongly dependent on size in coral populations (Connell 1973, Hughes and Jackson 1980, Hall and Hughes 1996).

### 4.2 *Isopora spp.* and *Montastrea curta* spatial variability

When assessing spatial variability in size structure, *Isopora* and *Montastrea curta* size structure distributions varied at both the inter- and intra-island scale (see Figure 27a-b and 28a-b for spatial overview of site-level and strata-level shape parameter estimates across islands) and inter-island shape parameter estimates scaled relative to each other across spatial resolutions. For both *Isopora* spatial resolutions, Tau Island had the highest average shape parameter estimates (site, $k$ = 7.59; strata, $k$ = 7.13); however, the lowest *Isopora* shape parameter averages across islands differed for each spatial resolution (site - Ofu and Olosega, $k$ = 5.27; strata – Tutuila, $k$ = 5.41). At the intra-island scale, each spatial resolution identified the Ofu and Olosega southeast reef as having the lowest shape parameter averages (site, $k$ = 4.69; strata, $k$ = 4.59) and the Tau northwest reef as having the highest shape parameter averages (site, $k$ = 7.59; strata, $k$ = 7.13). At

both the intra-island and inter-island scale, *M. curta* shape parameters appeared to vary more between spatial resolutions (especially at the intra-island scale) but were, in general, similar to each other. Across islands, analysis for each spatial resolution indicated that Swains Island had the lowest shape parameter averages (site = 3.25, strata = 2.73) but differed with respect to the highest shape parameter averages (site - Tau, $k = 7.40$; strata – Tutuila, $k = 7.26$).

The strong differences observed at the intra-island scale between site- and strata-level resolutions could be an artifact of the inherent differences in how shape parameter estimates were derived for each resolution. For strata, sites are pooled together and abundance estimates are weighted using the strata area, thus resulting in weighted size-frequency distributions for each stratum. In contrast, shape parameters are generated at the rawest form with minimal pooling of sites for site-level analysis. These intrinsic differences may not allow one to adequately compare shape parameter estimates between spatial resolutions. For a more accurate comparison between spatial resolutions, a testable method may be to pool site-level data prior to generating shape parameter estimates (at the same resolution as strata) and, thus, make comparisons across strata.

### 4.3 *Isopora spp.* and *Montastrea curta* HUA results

In survey design theory, biological population metrics (i.e. means, proportions, totals) are designed to generate estimates within a finite spatial domain (quantified habitat area; Cochran 1977, Swanson 2011). HUA analysis incorporates this design and domain mean estimates are used to identify habitat areas (to combine or separate adjacent strata) where subsets of the coral population have low, moderate, or high densities (i.e. strata densities that are below, at, or above the domain mean, respectively). Subsequently, strata abundance values are compared to the percent habitat area and resulting strata represent where the population is using habitat space

negatively, neutrally, or positively, respectively, assuming homogeneous distribution in space (Swanson 2011).

For *Isopora* strata, the domain shape parameter was estimated at 5.31 with a median size of 21.14 cm and skewness of 0.07. HUA analysis revealed three positive HUA habitats (Ofu and Olosega northwest shallow reef, Tutuila east shallow reef, and Tutuila southwest shallow reef) with strata-level shape parameters close to the domain mean (5.08, 5.08, and 6.08, respectively). Three areas were identified as negative strata (Tau northwest shallow and moderate-depth reefs, and Tutuila Aunu'u island reef) with shape parameter estimates far above the domain mean (6.17, 8.09, and 5.98, respectively). All other strata were identified as neutral habitats with an average shape parameter ($k$ = 5.48) just above the domain mean (see Figure 24 and Table 5a for HUA results).

For *M. curta* strata, the domain shape parameter was estimated at 5.23 with a median size of 13.06 cm and skewness of 0.40. HUA analysis revealed six positive, eleven neutral, and nine HUA habitats (see Table 5b). While much higher than the domain mean, positive strata shape parameter estimates (average $k$ = 6.25) were closest to the domain mean with neutral and negative shape parameter estimates (average $k$ = 6.63 and 6.63, respectively) deviating more significantly from the domain mean (see Figure 24 and Table 5b for HUA results).

Overall, shape parameter estimates scaled relative to HUA results, where lower shape parameter estimates were correlated with positive strata (i.e. higher density), moderate shape parameter estimates were correlated with moderate strata (i.e. moderate density), and high shape parameter estimates were correlated with negative strata (i.e. lower density); however this relationship was not as strong for *M. curta*. Shape parameter estimates for each strata were not strongly tied to domain level estimates and HUA outcome (positive, neutral, negative). This

weak relationship between shape parameter estimates and strata density (expressed as low, moderate, and high) may, in part, be due to the fact that the Weibull shape parameter metric does not strongly reflect patterns in overall density.

The Weibull shape parameter serves as a useful metric in characterizing coral size structure distributions but does exhibit limitations. For one, this metric does not adequately capture missing size classes in the size distribution. Coral size distributions with many missing size classes can indicate an "unhealthy" population due to low survivorship at different life stages (Bak and Meesters 1998, Meesters et al. 2001). Second, while a general trend is observed in shape parameter variability (i.e. higher shape parameters exhibit a higher frequency of larger individuals and less small ones versus lower shape parameters exhibit a higher frequency of smaller individuals and relatively few large ones), these shape parameter estimates appear to deviate from this trend at anomalously high and low estimates. Bailey and Dell (1973) observed that as $k$ increases towards infinity above a certain threshold, the distribution approaches a spike over a single point. This pattern was observed for each coral species and spatial resolution where the relationship between the shape parameter, median size and skewness deviated from the observed trend at anomalous values (Figures 17,18, and 19). Caution should thus be taken with atypical shape parameter estimates and these distributions potentially should be examined separately.

**4.2 Biogeophysical Relationships**

For biological communities across environmental gradients, adult survivorship and community composition are often strongly coupled with and reflective of their ambient environment (Margalef 1975, Sousa 1984). With respect to coral communities, structure and composition are likely to be determined by the interaction of multiple forcing functions operating

on a variety of scales (Murdoch and Aronson 1999). Nearshore marine systems are biogeochemically and physically dynamic environments characterized by high spatial and temporal variability, subsequently resulting in complex and diverse habitats (Alin et al. 2015).

The onset of ocean acidification (OA) threatens coral reefs and will inevitably affect marine organisms especially those dependent on the accretion and accumulation of $CaCO_3$ (Andersson and Gledhill 2013). As a consequence of increasing atmospheric $CO_2$ concentrations and OA, the rate of $CaCO_3$ production on reefs may significantly decrease (e.g. Gattuso et al. 1999), however ecological consequences of OA on coral reefs are largely unknown due to a lack of data available at relevant spatial and temporal resolutions in the natural environment. While causality for the biogeophysical spatial patterns and relationships cannot be rectified here, this study offers an opportunity to evaluate coral size structure distribution dynamics and relevant biogeophysical relationships at finer spatial scales.

***Isopora spp. biogeophysical relationships***

Seawater chemistry dynamics in coral reef ecosystems are driven by co-varying processes, including biological activity and physical forcing, over different temporal and spatial scales (Price et al. 2012). Small spatial-scale physiochemical differences in microhabitats have also been found to strongly influence accretion-erosion patterns on coral reefs in which carbonate chemistry dynamics was more significant in explaining spatial patterns of reef accretion and erosion when compared to other environmental variables (resource availability, temperature, depth, and distance to shore; Silbiger et al. 2014).

In this study, ambient variability in both mean net carbonate accretion rates and net carbonate accretion rate variability was substantial between American Samoa islands and also within islands. Variability in *Isopora spp.* coral size structure distributions at the site-level spatial

resolution was positively correlated with both net carbonate accretion rate variability and mean net carbonate accretion rates despite a number of other biological (e.g. benthic cover), physical oceanographic (e.g. irradiance, SST, chl-*a*, wave energy), and anthropogenic (e.g. human population density) drivers. For strata-level patterns, mean net carbonate accretion rates were also positively related to *Isopora spp*. size structure variability.

***Mean net carbonate accretion rate and accretion rate variability***

Within the *Isopora spp.* spatial distribution range (Tutuila and the Manu'as islands), sites along the eastern section of the island of Ofu and Olosega (OFU-694, OFU-722, OFU-751) experienced both the highest net carbonate accretion rate variability (average of 0.50 g $CaCO_3$ $m^{-2}$ $yr^{-1}$) as well as some of the highest mean net carbonate accretion rates (average of 0.08 g $CaCO_3$ $m^{-2}$ $yr^{-1}$) observed across sites and islands (Figure 25a-e). These sites collectively also had the lowest shape parameter estimates (average of 4.42) compared to all other sites across all islands and also had the lowest median size averages (average of 11 cm) and exhibited positive skewness (average of 0.60).

This pattern of dominance by smaller-sized *Isopora* individuals at locations experiencing high accretion rate variability (i.e. accretion rate coefficient of variation) and high mean accretion rates may be correlated with positive *Isopora* settlement and post-settlement survival and may be indicative of co-varying biological and physical processes as well as size-selective environmental suitability. Sites experiencing these gradients in carbonate accretion rates are located on the windward shores of Ofu and Olosega with high wave energy exposure, averaged at 96.85 MW $hr^{-1}$ $m^{-1}$. Changes in community structure have been explained by hydrodynamic variability in which enhancement of carbonate production (due to the transport of nutrients and removal of biologic metabolic waste) has been associated with lower wave energy (Hearn et al.

2001; Veron 2011). At higher wave energy levels, community composition transitions to one that favors more stress-tolerant species, such as encrusting and massive corals, and calcifying algae, due to mechanical forcing (Massel 2005), and overall community carbonate production decreases due to stress-tolerant organisms calcifying at lower rates (Hamylton et al. 2013). Additionally, seawater carbonate chemistry can locally vary depending on community composition, due to variations in metabolic rates and ratios of net community calcification (NCC) to net community organic carbon production (NCP) between reef benthic functional groups (Anthony et al. 2013, Page et al. 2016), which has implications for the biology exposed to these highly dynamic habitats.

Consequences to coral size structure distributions exposed to gradients in both carbonate production and hydrodynamic forcings may be two-fold: high wave energy environments may be unfavorable to larger colonies due to co-varying mechanical forcing and small-scale carbonate chemistry dynamics and these environments may also be favorable habitats for both the growth and survival of smaller colonies as well as for facilitating recruitment. As both accretion rate variability and mean accretion rates were highly correlated with *Isopora* size structure distributions (shape parameter decreased with increasing covariates), these variables may have collectively created a favorable environment for smaller *Isopora* colonies and, at the same time, created a less favorable environment for larger sized individuals which may have created space for smaller individuals to grow. In this study, accretion rates were measured at fine spatial scales (tens of meters) where microhabitats exhibit an additional layer of biogeochemical complexity, owing to metabolic processes and remineralization that contribute to varying rates of precipitation and dissolution of $CaCO_3$ (Andersson and Gledhill 2013). Coral populations exposed to co-varying extreme wave energy and highly variable net carbonate accretion rate

regimes, such as *Isopora* sub-populations on eastern shores of Ofu and Olosega, can have energetic costs on corals, affecting both photosynthesis and respiration (Porter et al. 1999), ultimately leading to reduced growth and/or survivorship to larger-sized size colonies (Jokiel et al. 2014). Results from strata-level analysis of *Isopora* indicated that wave energy was, in fact, the strongest predictor in explaining spatial variation in size structure where the shape parameter decreased with increasing wave energy, supporting the claim that *Isopora* sub-populations exposed to high wave energy shift size structure distributions towards dominance by smaller size classes.

Additionally, these sites also exhibited high mean net carbonate accretion rates. The additive effects of both high mean net accretion rates and high accretion rate variability may have enabled these sites to be dominated by crustose coralline algae (CCA), a pattern that has been observed elsewhere. For example, Price et al. 2012 found that spatial variability in net carbonate accretion was positively correlated to the temporal magnitude and duration of pH above background climatological lows which was also linked to a dominance of organisms precipitating high Mg calcite (e.g. CCA and bryozoans). CCA is a key settlement substrate that enables coral recruitment (Hoegh-Guldberg et al. 2007) and is both strongly positively associated with accretion rates (Vargas-Ángel et al. 2015) and higher wave energy regimes (Massel 2005). These sites located on the windward shores of Ofu and Olosega also exhibited some of the highest CCA coverage across the *Isopora* spatial range, which may have acted as both a facilitator for recruitment and enabled the growth and survival of smaller *Isopora* colonies as well as led to competitive inhibition of larger corals (Babcock and Mundy 1996, Ruiz-Zarate et al. 2000).

In contrast, sites on the far southwest corner of Tutuila (TUT-2106, TUT-2116), the north side of Tau Island (TAU-637, TAU-692, TAU-668), the northwest side of Ofu and Olosega (OFU-710, OFU-765, OFU-789), and the southern end of Tutuila by Pago Pago Harbor (TUT-1878, TUT-1936, TUT-2095) had the lowest net carbonate accretion rate variability (total average of 0.15 g $CaCO_3$ $m^{-2}$ $yr^{-1}$) with high mean net carbonate accretion rates (total average of 0.07 g $CaCO_3$ $m^{-2}$ $yr^{-1}$; Figure 25a-e). These sites also had some of the highest shape parameter estimates (Tutuila south sites - average of 7.49; Tutuila southwest sites - average of 7.20; Tau sites – average of 7.59; Ofu/Olosega sites – average of 6.90) and high median size averages (Tutuila south sites - average of 39 cm; Tutuila southwest sites - average of 31.08 cm; Tau sites – average of 20 cm; Ofu/Olosega sites – average of 14.33 cm) with varying skewness (total average of -0.05).

This pattern of dominance by larger-sized *Isopora* individuals at locations experiencing low accretion rate variability and high mean accretion rates most likely reflect the same co-varying processes as those influencing distributions with a preponderance of small-sized individuals. These are located on the leeward shores of each with low wave energy exposure (averaged at 82.78 MW $hr^{-1}$ $m^{-1}$), which is associated with the enhancement of carbonate production and community composition representative of low wave energy environments (Hearn et al. 2001; Veron 2011). These sites exhibited communities with relatively low CCA cover (average of 24.74%) in comparison to high coral cover (40.16%). A reduction in accretion rates of CCA has been associated with a shift towards communities dominated by competitive calcitic (i.e. scleractinian corals), aragonitic, and non-calcifying species (Price et al. 2012). High mean accretion rates and low accretion rate variability (possible in conjunction with low wave energy environments) may reflect a shift in reef community composition, where the community begins

to consist of more adult corals of varying species, which may have ultimately set the stage for both competitive inhibition of *Isopora* recruitment/settlement (Vermeij and Sandin 2008) as well as for *Isopora* sub-population size distributions to be dominant in larger-sized classes.

***Slope and slope variability***

Spatial variability in both seabed slope and slope variability (slope coefficient of variation; proxy for topographic habitat complexity), with respect to *Isopora* size structure distributions, was substantial across sites and islands with no distinct homogenous spatial patterns observed. Overall, the trend observed and verified by generalized linear models revealed that lower shape parameters ($k < 5$) were associated with habitats that had shallower slopes (average = 5.12 degrees) and higher measures of complexity (average of 0.58). In contrast, higher shape parameters ($k > 6$) were associated with habitats that had steep slopes (average = 10.02 degrees) and lower measures of complexity (average of 0.44). As would be expected, moderate shape parameters ($5 \leq k \geq 6$) fell in the middle and were associated with habitats that had both moderate slopes (average = 7.07 degrees) and moderate measures of complexity (average = 0.42).

Habitat heterogeneity has been shown to be important in medium to large coral reef areas as these areas typically comprise several habitat types as well as transition zones between habitats, overall contributing to reef complexity (Cornell and Karlson 2000), which likely contributed to the spatial variability observed in *Isopora* size distributions. Seabed slope and seafloor rugosity have been responsible for marine benthic community spatial distribution and composition (e.g. Tempera et al. 2011) and are considered direct variables (i.e. aspects of the environment that are sought out by species) in explaining the occurrence of biological populations in specific locations (Harris 2011). Habitat-specific substratum preferences for coral

larvae have been widely reported for various species (e.g. Baird, Babcock, and Mundy 2003) and coral settlement spatial patterns have, in part, been attributed to the structural makeup of a reef (Lillis et al. 2016). The data presented here identify habitats with high topographic complexity, especially along steeper slopes, as an important control on *Isopora* distributions dominated by smaller size classes. Overall, lower shape parameters ($k < 5$) were associated with habitats that had shallower slopes (average = 5.12 degrees) and higher measures of complexity (average of 0.58). Sessile intertidal invertebrates have been shown to employ tactile cues to find rugose surfaces during settlement stages to reduce exposure to predation (Petraitis 1990; Raimondi 1990); and spatial differences in settlement have been found to reflect differences in habitat type where settlement density was highest on substrate with higher complexity (Raimondi 1990). If the assumption is that competition, mortality, resources, etc. vary at the same spatial scale as habitat preference, then selectivity of high complexity habitat by small *Isopora* individuals may enhance individual performance (Price 2010) and specific habitats may act as a refuge for smaller individuals.

Variability in slope was also a significant predictor for *Isopora* size structure, in which higher shape parameters ($k > 6$) were associated with habitats that had steep slopes (average = 10.02 degrees) and lower measures of complexity (average of 0.44). Coral reef studies have shown that dramatic changes in environmental variability can occur over short distances due to dynamic shorelines and geomorphic features along with steep physical and chemical gradients across different depths (Guadayol et al. 2014, Silbiger et al. 2014). For instance, Guadayol et al. 2014 examined the high frequency temporal variability and spatial distribution of ambient carbonate chemistry from sites distributed along a 32- meter transect at different depths (reef flat to reef slope) on a coral reef. Results revealed extreme variation in the temporal fluctuation

spectrum (i.e. diurnal versus weekly frequencies) of each environmental parameter over a scale of meters. In other words, ecological communities on the reef flat experienced a highly variable environment whereas those further down on the reef slope experienced a relatively stable one, highlighting the importance of environmental variance at small scales. Just as high complexity habitats may have acted as a refuge for small *Isopora* individuals, habitats with steeper slopes may have acted as a refuge for large *Isopora* individuals, sheltering them from environmental extremes on and near the reef flats.

***Montastrea curta biogeophysical relationships***

***PAR***

Variability in *Montastrea curta* coral size structure distributions at both the site-level and strata-level spatial resolution were primarily explained by the covariate PAR (i.e. irradiance). While the gradient in PAR levels was not significant across islands (minimum = 42.41 E $m^{-2}$ $d^{-1}$; maximum = 44.00 E $m^{-2}$ $d^{-1}$), the spatial distribution of *Montastrea curta* coral size structure distributions varied greatly with gradients in PAR estimates. Across islands, PAR long-term mean estimates were highest along the northern reefs of Ofu and Olosega (average = 43.91 E $m^{-2}$ $d^{-1}$), Rose Atoll forereef (average = 43.91 E $m^{-2}$ $d^{-1}$), Swains forereef (average = 43.81 E $m^{-2}$ $d^{-1}$), and northwestern reef of Tau (average = 43.74 E $m^{-2}$ $d^{-1}$). In contrast, northwest-west Tutuila, west Tau, and southeast Ofu and Olosega, had the lowest PAR long-term mean estimates (average = 42.47, 42.64, and 43.00 E $m^{-2}$ $d^{-1}$, respectively). Across islands, *M. curta* size structure distributions scaled negatively with PAR where reefs with highest PAR estimates had lower shape parameters (average = 6.21) and reefs with the lowest PAR estimates had higher shape parameters (average = 8.63). This pattern held at the intra-island scale except for Rose Atoll where shape parameters did not vary with gradients in PAR.

Coral communities have minimum light requirements in which light attenuation influences calcification physiology, metabolism, and overall survivorship, affecting the overall growth and survival of corals (Falkowski et al. 1984). Over large spatial scales, light relevant to marine biological communities is heavily influenced by latitude and depth and, at local scales, is attenuated by particulate matter and dissolved organics in the water column (Marubini et al. 2001). Interestingly, when PAR and chl-*a* were examined at the island-scale, using Pearson correlations, Tutuila, the Manuas (Ofu and Olosega, Tau), and Rose Atoll all exhibited high negative correlations ($R^2$ = 56, 88, and 63 %, respectively) where PAR decreased with increasing chl-*a*. As chl-*a* is a proxy for ocean photosynthetic productivity (Gove et al. 2013), spatial variability in chl-a is typically indicative of eutrophic conditions, with elevated levels of dissolved organics and nutrients in the water column, which can influence post-settlement processes (Tremblay 2014). In low light environments, adult coral populations can acclimate by reducing energetic requirements through decreasing respiration rates, tissue biomass and skeleton thickness, as well as growth (Anthony and Hoegh-Guldberg 2003), resulting in the hindrance of precipitation of $CaCO_3$ skeletons in corals (Falkowski et al. 1990). Thus a reduction in light attenuation due to eutrophic conditions likely impacted coral physiological processes in smaller individuals, hindering post-settlement survivorship (Tremblay 2014), which ultimately resulted in a shift towards *M. curta* size distributions dominated by smaller colonies with increasing levels of irradiance.

***Mean net carbonate accretion rates***

In addition to PAR, mean net carbonate accretion rates explained a significant amount of variability observed in *M. curta* coral size structure distributions at the strata-level spatial resolution, in which higher accretion rates were associated with distributions with smaller size

individuals. Mean accretion rates were highest along the forereef of Rose Atoll (average = 0.17 g $CaCO_3$ $m^{-2}$ $yr^{-1}$; maximum = 0.26 g $CaCO_3$ $m^{-2}$ $yr^{-1}$) followed by the south-southwest forereef of Ofu and Olosega (average = 0.11 g $CaCO_3$ $m^{-2}$ $yr^{-1}$; maximum = 0.12 g $CaCO_3$ $m^{-2}$ $yr^{-1}$), which was correlated with lower shape parameters (average = 5.81). Mean accretion rates were lowest along northeast-east and northwest Tutuila (average = 0.05 g $CaCO_3$ $m^{-2}$ $yr^{-1}$; minimum = 0.04 g $CaCO_3$ $m^{-2}$ $yr^{-1}$) northwest Tau (average = 0.04 g $CaCO_3$ $m^{-2}$ $yr^{-1}$; minimum = 0.04 g $CaCO_3$ $m^{-2}$ $yr^{-1}$), which was correlated with higher shape parameters (average = 6.79). Across islands, mean accretion rate spatial patterns corresponded well with spatial patterns in PAR and chl-*a* where higher accretion rates were spatially correlated with higher levels of PAR and lower levels of chl-*a*, although the relationships were not highly correlated ($R^2 \leq 35\%$; except for Ofu and Olosega, mean accretion rates and PAR, $R^2 = 56\%$, and chl-*a*, $R^2 = 58\%$; for Rose Atoll, mean accretion rates and PAR, $R^2 = 42\%$). We also find a positive correlation with percent turf algae cover and lower accretion rates and PAR and higher chl-*a*, suggesting a shift in community composition in these environmental conditions, which can reduce the settlement and survivorship success of coral recruits (Vermeij et al. 2008). Research on various reefs in the Pacific, including American Samoa, found a statistically significant negative correlation between net carbonate accretion rates and chl-*a*, attributing a reduction in accretion rates to artifacts of elevated chl-a such as human-induced degraded water quality, increased runoff, and overgrowth of competitors such as turf algae (Vargas-Ángel et al. 2015). Here, the results provide additional evidence that covarying light attenuation and eutrophic conditions can either dampen or enhance coral calcification, altering physiological and growth processes in corals (Falkowski et al. 1990, Anthony and Hoegh-Guldberg 2003), as well as hinder coral settlement and survivorship (Vermeij et al. 2008). Reduced calcification and competitive overgrowth of turf algae, as a result

of low light and eutrophic conditions, likely negatively impacted recruitment and post-settlement survivorship processes in *M. curta*, which contributed to a lack of smaller sized individuals in these environments around American Samoa.

***Coral cover and wave energy***

For site-level resolution data, percent coral cover was secondary in explaining the most deviance in *M. curta* coral size structure distributions, in which higher percent coral cover was associated with higher shape parameters (i.e. distributions dominated by higher size classes). Across islands, coral cover estimates were highest along leeward shores of each island (average = 50.04 %) with highest coverage (> 50 %) along Tutuila northeast and northwest reefs, Ofu and Olosega northeast reefs, and Tau northeast reefs. In contrast, windward shores of each island had the lowest estimates (average = 7.87 %) with lowest coverage (< 5%) on Tutuila's exposed south-southeast reefs and on Tau's exposed southern reefs. *M. curta* size structure distributions scaled positively with coral cover where reefs with highest coral cover estimates had higher shape parameters (average = 8.00) and reefs with the lowest coral cover estimates had lower shape parameters (average = 5.45). Incidentally, wave energy was also found to be a significant covariate in explaining the spatial variation in *M. curta* size structure, where we see a shift to distributions with smaller size classes with increasing wave energy. As would be expected, both higher percent coral cover and higher shape parameters were correlated with low wave energy (average = 78.16 MW $hr^{-1}$ $m^{-1}$) and lower percent coral cover and lower shape parameters were correlated with high wave energy (average = 111.05 MW $hr^{-1}$ $m^{-1}$). Water motion, wave energy, and exposure are significant contributors to coral reef community spatial distribution and structure (Dollar 1982, Done 1982, van Woesik and Done 1997, Franklin et al. 2013) and storm severity can alter coral size structure distributions, increasing probability for dislodgement in

larger size classes (Done and Potts 1992). Higher proportions of small coral colonies at shallower depths have been attributed to decreasing hydrodynamic pressure with increasing depth, which inhibits development of large colonies due to strong water motion (Adjeroud et al. 2015). The data presented here reveals the same pattern where higher wave energy may put a limit on larger *M. curta* colonies, which is reflected in the gradients observed in spatial coral cover patterns.

Just as we see a shift in size structure towards distributions with higher size classes and, thus higher coral cover, in response to low wave energy, we also see the opposing effect in distributions dominated by smaller size classes; in response to high wave energy, we see a shift in size structure towards distributions with lower size classes, which is also reflected in lower estimates of coral cover. Settlement rates and post-settlement survivorship have been shown to decrease with increasing adult coral cover (with settlement rates saturating at a maximum of 10% adult coral cover), which indicates structuring density-dependent effects in coral settlement and survival (Vermeij and Sandin 2008). These density-dependent effects are artifacts of the local environment including amassing predators (Anderson 2001) and resource competition such as competition for space (Roughgarden et al. 1985, Carlon 2001). The data presented here identify high wave energy as an important control on larger *M. curta* size classes and density dependent effects could act to limit settlement of recruits and survivorship of smaller colonies at high densities of larger individuals (Vermeij and Sandin 2008).

***SST***

While SST was found to partially explain the variability observed in *M. curta* coral size structure distributions for both site- and strata-level resolution, this relationship was primarily driven by gradients in SST across islands as opposed to variability at the intra-island scale.

Swains, the northern-most location (latitude approximately 11° S), exhibited the highest temperatures at 29.30 °C and Rose Atoll, the southern-most location (latitude approximately 14.5° S), exhibited the lowest temperatures at 28.73 °C. Shape parameters scaled negatively with SST where highest shape parameters (Tau, average = 8.74) were correlated with lower SST estimates (average = 28.84 °C) and higher shape parameters (Swains, average = 3.25) were correlated with higher SST estimates (average = 29.30 °C). This relationship did not hold true for Rose Atoll, which had the lowest SST estimates and had the second lowest island-scale shape parameter estimates (average = 5.31). Higher sea surface temperatures have been linked to slower coral growth rates (Bauman 2013b) and have been shown to have a positive effect on coral larval settlement (Nozawa and Harrison 2007), which could have contributed to the size structure distribution patterns observed along SST gradients.

***Depth***

Depth additionally explained a portion of the total deviance observed ($R^2$ = 5%) in *M. curta* coral size structure distributions at the site-level resolution. With increasing depth, distributions exhibited a shift towards ones with a prevalence of larger colonies and relatively fewer small ones. Shape parameter gradients were observed across depth zones with an average shape of 6.03 in shallower depths (average = 6.38 m), 6.64 in moderate depths (average = 12.97 m), and 7.04 in deeper depths (average = 19.93 m). While this pattern can't be assigned to a particular covariate(s) due to a lack of high spatio-temporal resolution data, this pattern can most likely be attributed to gradients in exposure to environmental extremes as a result of multiple interacting variables (Cornell and Karlson 2000). As exemplified in this study, wave energy plays a role in the spatial distribution of population size structure. In American Samoa, shallower forereef areas typically experience higher levels of tidal flux and wave energy generated from the

predominant southeast tradewinds and backreefs are characterized by high thermal and biogeochemical variability controlled by tidal modulation of wave-driven flow (Birkeland et al. 2007, Koweek et al. 2015). These extreme environmental gradients experienced by shallower reef areas may be tolerated by smaller *M. curta* colonies but may act as stress-inducing environments for larger *M. curta* colonies, in which habitat along deeper slopes may be more stable regimes (Guadayol et al. 2014) and act as refuge from these predominant conditions.

***Juvenile abundance***

Because sampling effort for juveniles was not consistent across sites, results regarding juvenile abundance as an explanatory covariate should be interpreted with caution. In this study, *M. curta* juvenile abundance explained an insignificant portion of the total deviance observed ($R^2$ = 2%) in *M. curta* coral size structure distributions at the site-level resolution; however, the effect of this predictor on the response was significant. With increasing juvenile abundance, distributions exhibited a shift towards ones with a prevalence of smaller colonies and relatively fewer small ones. While most sites had zero or very few juveniles (≤ 1), the highest juvenile abundances (total = 34) were found on Tutuila's southern-southeastern reefs, which collectively had the lowest average shape parameter, 5.60. Reefs along the Tau northwestern and southern coast, Tutuila Aunu'u island MPAs, and Ofu and Olosega northwest coast also exhibited relatively high juvenile abundances (17, 16, and 15, respectively) and also had lower shape parameters (6.45, 6.04, and 6.09 respectively). A coral population's resilience can, in part, consist of good connectivity to larval sources as well as essential habitat that promotes larval settlement and survivorship (Crabbe 2009). While the mechanisms (i.e. recruitment rate and/or juvenile mortality rate variability, competitive inhibition, etc.) underlying *M. curta* juvenile abundance spatial variability patterns can't be assigned, it is clear that larval supply and

successful settlement as well as recruit and juvenile survivorship can contribute to the success and health of a coral population (Hughes et al. 2000, Meesters et al. 2001).

Ultimately there are many other causal factors, in addition to the ones mentioned in this section that contribute to coral community structure and distribution. These may be environmental in nature (e.g. hydrodynamic processes such as currents and storm frequency) and/or biological (e.g. coral-recruit settlement patterns and post-settlement survival, Done 1982;, disease, competition, e.g. Connell et al. 2004). Additional data, however, is either currently unavailable or unavailable at the necessary resolution and/or scale to explore these mechanisms.

## 5. CONCLUSION

In this study, size structure distributions for both *Isopora* and *M. curta* varied both between species and across space. While the Weibull shape parameter metric has some limitations in describing coral size structure distributions, overall, this metric adequately characterized distributions as well as effectively captured spatial heterogeneity observed for each coral species. Additionally, this study exemplifies the utility of a single size distribution metric to quantify coral size distributions versus previous coral size structure studies which use multiple descriptive statistics of the distribution shape to explain spatial variability observed in populations. While these studies have laid the groundwork in effectively characterizing coral size spectra and examining spatio-temporal variability, the use of multiple size metrics inhibits adequate assessment of coral size structure in relation to biogeophysical factors. Additionally, our findings emphasize coral size as an important characteristic for scleractinian corals, which accurately reflects population dynamics processes. Risk assessments and protection efforts have typically been predicated on measures of a species' abundance, which may be inappropriate for

some sessile marine invertebrates, such as corals, where abundance does not accurately describe population dynamics and processes (Birkeland et al. 2013). A given species may be abundant and dominant but this may not protect a species from huge declines or extinction due to disease (Vollmer and Palumbi 2007) or threats from increasing $CO_2$ (Birkeland et al. 2013).

While direct mechanisms regarding biogeophysical relationships and size structure distributions cannot be assigned, it is clear that both *Isopora* and *M. curta* coral populations experienced highly dynamic oceanographic, biological, and geomorphological regimes, which corresponded to key spatial differences in coral size structure distributions. Dominant biogeophysical relationships with size also differed between coral species where oceanographic, biological, and geomorphological variables were significant influential drivers in explaining *M. curta* size structure. In contrast, ocean carbonate chemistry, wave energy and geomorphological variables were significant influential drivers in explaining *Isopora* size structure, which emphasizes the species-specific differences in environmental factors driving observed spatial patterns. Finally, model results show carbonate accretion rates and variability as important controls on *Isopora* size structure, suggesting that the onset of ocean acidification will likely compromise *Isopora* demographic processes. These findings can inform managers of the threats and status of coral populations and greatly assist managers in monitoring efforts, especially with ESA-listed species.

Given the spatial heterogeneity observed in coral size structure distributions between spatial resolutions examined here (i.e. site versus strata), future studies should consider spatial resolution in examining coral size structure, especially in relation to biogeophysical relationships. Site-level analysis has the ability to capture size structure variability at a higher spatial resolution (especially with larger sample sizes), which, in turn, captures the highly

dynamic biogeophysical processes at finer spatial scales. However, at small sample sizes, site-level analysis has its limitations and can lead to higher variance. Strata-level assessments yield higher sample sizes, thus improving statistical power; however, assessing biogeophysical relationships at a coarser spatial scale may mask highly dynamic and potentially important environmental processes. Both site- and strata-level assessments are valuable and future coral size structure studies incorporating biogeophysical relationships should take into consideration the environmental variable spatial scales. Additionally, while remote sensing data has proven to be valuable in assessing biogeophysical relationships in the absence of site-level data, higher resolution data should be used to assess patterns at small spatial scales when available. Future work on the coral size spectra and biogeophysical relationships should also examine various climatological metrics (i.e. anomalous highs and lows, minimums, maximums, etc.) for oceanographic variables. Because biological communities, including coral populations, respond to variation in environmental regime, dynamic variability should be considered when assessing the status and trends of populations and communities, especially in a changing climate.

## RESEARCH CITED


1. Achituv Y and Dubinsky Z. 1990. Evolution and zoogeography of coral reefs. In: Z. Dubinsky (ed.), Ecosystems of the world 25. Coral Reefs, Chapter 1, pp. 1-9. Elsevier, Amsterdam.
2. Adjeroud M, Mauguit Q, Penin L. 2015. The size-structure of corals with contrasting life-histories: A multi- scale analysis across environmental conditions. Marine Environmental Research 112: 131-139.
3. Aeby GS, Kenyon JC, Maragos JE and Potts DC. 2003. First Record of Mass Coral Bleaching in the Northwestern Hawaiian Islands Coral Reefs. 22:3, p256.
4. Alvarado-Chacon, E.M., Acosta, A., 2009. Population size-structure of the reef-coral Montastraea annularis in two contrasting reefs of a marine protected area in the Southern Caribbean Sea. Bull. Mar. Sci. 85, 61-76.
5. Anderson TW. 2001. Predator responses, prey refuges, and density-dependent mortality of a marine fish. Ecology 82: 245–257.
6. Anderson KD, Pratchett MS. 2014. Variation in size-frequency distribution of branching corals between a tropical versus sub-tropical reef. Mar. Ecol. Prog. Ser. 502, 117-128.
7. Andersson AJ and Mackenzie FT. 2012. Revisiting four scientific debates in ocean acidification research. *Biogeosciences* 9, 893–905. doi: 10.5194/bg-9-893-2012
8. Andersson A and Gledhill D. 2013. Ocean acidification and coral reefs: Effects on breakdown, dissolution, and net ecosystem calcification. Annual Review of Marine Science, 5: 321-48.
9. Anthony KRN and Hoegh-Guldberg O. 2003. Variation in coral photosynthesis, respiration and growth characteristics in contrasting light microhabitats: an analogue to plants in forest gaps and understoreys? *Funct. Ecol.* 17, 246–259. doi: 10.2307/3599181
10. Anthony KRN, Diaz-Pulido G, Verlinden N, Tilbrook B, and Andersson AJ. 2013. Benthic buffers and boosters of ocean acidification on coral reefs, Biogeosciences, 10, 4897-4909, https://doi.org/10.5194/bg-10-4897-2013.
11. Anthony KRN, Larcombe P. 2002. Coral reefs in turbid waters: sediment- induced stresses in corals and likely mechanisms of adaptation. Proceedings of the Ninth International Coral Reef Symposium Bali 1, 239-244
12. Anthony KRN, Ridd PV, Orpin AR, Larcombe P, Lough J. 2004. Temporal variation of light availability in coastal benthic habitats: effects of clouds, turbidity and tides. Limnology and Oceanography 49: 2201–2211.
13. Babcock R and Mundy C. 1996. Coral recruitment: consequences of settlement choice for early growth and survivorship in two scleractinians. Journal of Experimental Marine Biology and Ecology. 206: 179-201.
14. Bahr KD, Jokiel PL, Rodgers KS. 2016. Relative sensitivity of five Hawaiian coral species to high temperature under high-$pCO_2$ conditions. *Coral Reefs.* 35, 729–738. doi: 10.1007/s00338-016-1405-4
15. Bailey RL and Dell TR. 1973. Quantifying diameter distributions with the Weibull function. Forest Sci. 19:97-104.
16. Baird A, Babcock R, Mundy C. 2003. Habitat selection by larvae influences the depth distribution of six common coral species. Marine Ecology Progress Series 252:289–293 DOI 10.3354/meps252289.
17. Baird AH, Marshall PA. 2002. Mortality, growth and reproduction in scleractinian corals

following bleaching on the Great Barrier Reef. Marine Ecology progress Series 237: 133–141.
18. Bak RPM. 1975. Ecological aspects of the distribution of reef corals in the Netherlands Antilles. Contr Zool 45:181–190
19. Bak RPM, Meesters EH. 1997. Coral diversity, populations and ecosystem functioning. In: Den Hartog JC (ed) Proceedings 6th International Conference Coelentarate Biology. National Museum Natural History, Leiden, p 27–38
20. Bak RPM, Meesters EH. 1998. Coral population structure: the hidden information of colony size-frequency distributions. Mar Ecol Prog Ser 162:301–306
21. Bak RPM, Meesters EH. 1999. Population structure as a response of coral communities to global change. Am Zool 39:56–65
22. Baker AC, Glynn PW, Riegl B. 2008. Climate change and coral reef bleaching: an ecological assessment of long-term impacts, recovery trends and future outlook. Estuarine, Coastal and Shelf Science 80, 435-471
23. Bartoń K. 2016. MuMIn: Multi-Model Inference. R package version 1.15.6. https://CRAN.R-project.org/package=MuMIn
24. Bauman AG, Feary DA, Heron SF, Pratchett MS, Burt JA. 2013a. Multiple environmental factors influence the spatial distribution and structure of reef communities in the northeastern Arabian Peninsula. *Marine Pollution Bulletin*, *72*(2), 302–312. doi:10.1016/j.marpolbul.2012.10.013
25. Bauman AG, Pratchett MS, Baird AH, Riegl B, Heron SF, Feary DA. 2013b. Variation in the size structure of corals is related to environmental extremes in the Persian Gulf. *Marine Environmental Research*, *84*, 43–50. doi:10.1016/j.marenvres.2012.11.007
26. Birkeland C, Craig P, Fenner D, Smith L, Kiene W, Riegl B. 2007. Geologic setting and ecological functioning of coral reefs in American Samoa. Chap. 20. In: Riegl B., R. Dodge, (Eds). Coral reefs of the USA. Springer Publishers.
27. Birkeland C, Miller MW, Piniak GA, Eakin CM, Weijerman M, Elhany PM, Dunlap M, Brainard RE. 2013. Safety in Numbers? Abundance May Not Safeguard Corals from Increasing Carbon Dioxide: GCU Library Resources - Sciences, *63*(12), 967–974. doi:10.1525/bio.2013.63.12.9
28. Boss E and Zaneveld JR. 2003. The effect of bottom substrate on inherent optical properties: Evidence of biogeochemical processes. - Limnol. Oceanogr. 48: 346–354.
29. Brainard RE, Birkeland C, Eakin CM, McElhany P, Miller MW, Patterson M, Piniak GA. 2011. Status review report of 82 candidate coral species petitioned under the U.S. Endangered Species Act, (September), 530. Retrieved from: http://www.pifsc.noaa.gov/library/pubs/tech/NOAA_Tech_Memo_PIFSC_27.pdf
30. Brooks JL, Dodson SI. 1965. Predation, body size, and composition of plankton. Science 150:28-35.
31. Brown BR. 1997. Adaptations of reef corals to physical environmental stress. Adv. Mar. Biol. 31, 221–299.
32. Brown BE, Dunne RP, Goodson MS, Douglas AE. 2002. Experience shapes the susceptibility of a reef coral to bleaching. Coral Reefs 21: 119–126.
33. Bryant D, Burke L, McManus J, Spalding M. 1998. Reefs at risk: a map-based indicator of threats to the world's coral reefs. World Resources Institute, Washington, D.C.
34. Buddemeier RW. 1994. Symbiosis, calcification, and environmental interactions. Bulletin de l'Institut océanographique, Monaco, n° special 13:119-131.

35. Burke L, Reytar K, Spalding M, Perry A. 2011. Reefs at Risk Revisited. World Resources Institute.
36. Carlon DB. 2001. Depth-related patterns of coral recruitment and cryptic suspension-feeding invertebrates on Guana Island, British Virgin Islands. Bulletin of Marine Science 68:525–541.
37. Carpenter KE, Abrar M, Aeby G, Aronson RB and others. 2008. One-third of reef-building corals face elevated extinction risk from climate change and local impacts. Science 321: 560−563
38. Carreiro-Silva M, McClanahan TR, Kiene WE. 2009. Effects of inorganic nutrients and organic matter on microbial euendolithic community composition and microbioerosion rates. Marine Ecology Progress Series 392: 1–15.
39. Cleary DFR, Suharsono, Hoeksema BW. 2006. Coral diversity across a disturbance gradient in the Pulau Seribu reef complex off Jakarta, Indonesia. *Biodiversity and Conservation* 15:3653-3674.
40. Cochran WG. 1977. Sampling techniques, 3rd ed. Wiley, New York Connell
41. Connell JH. 1973. Population ecology of reef-building corals. In: Jones, O.A., Endean, R. (Eds.), Biology and Geology of Coral Reefs. Academic Press, London, pp. 271-324.
42. Connell JH, Hughes TP, Wallace CC. 1997. A 30-year study of coral abundance, recruitment, and disturbance at several scales in space and time. Ecol. Monogr.67:461-488.
43. Connell JH, Hughes TP, Wallace CC, Tanner JE, Harms KE, Kerr AM. 2004. A long-term study of competition and diversity of corals. Ecological Monographs, 74(2) pp. 179-210.
44. Connor EF, McCoy ED. 1979. The statistics and biology of the species-area relationship. Am Nat 113:791-833.
45. Cornell HV, Karlson RH. 1996. Species richness of reef-building corals determined by local and regional processes. J Anim Ecol 65:233-241.
46. Cornell HV, Karlson RH. 2000. Coral species richness: ecological versus biogeographical influences. Coral Reefs 19:37–49
47. Costanza R. et al. 1997. The value of the world's ecosystem services and natural capital. Nature 387:253–260.
48. Crabbe MJC. 2009. Scleractinian coral population size structures and growth rates indicate coral resilience on the fringing reefs of North Jamaica. *Marine Environmental Research*, *67*(4-5), 189–198. doi:10.1016/j.marenvres.2009.01.003
49. Curran LM et al. 2004. Lowland forest loss in protected areas of Indonesian Borneo. – Science 303: 1000–1003.
50. D'Agostino RB, Stephens MA (1986). Goodness-of-Fit Techniques. 1st edition. Dekker.
51. De'ath G and Fabricius KE. 2000. Classification and Regression Trees: a powerful yet simple technique for ecological data analysis. *Ecology* 81:3178-3192.
52. Delignette-Muller ML, Dutang C. 2015. fitdistrplus: An R Package for Fitting Distributions. Journal of Statistical Software, 64(4), 1-34. URLhttp://www.jstatsoft.org/v64/i04/.
53. Dollar SJ. 1982. Wave stress and coral community structure in Hawaii. *Coral Reefs* 1:71-81.
54. Done TJ. 1982. Patterns in the distribution of coral communities across the Central Great Barrier Reef. *Coral Reefs* 1:95-107.

55. Done TJ, Potts DC. 1992. Influences of habitat and natural disturbances on contributions of massive Porites corals to reef communities. Mar. Biol. 114, 479-493.
56. Done TJ. 1999. Coral community adaptability to environmental change at the scales of regions, reefs and reef zones. American Zoologist 39: 66-79.
57. Done T. 2011. Corals: environmental controls on growth. In: Hopley, D. (Ed.), Encyclopedia of Modern Coral Reefs: Structure, Form and Process, Encyclopedia of Earth Science Series. Springer-Verlag, London, pp. 281–282.
58. Dunne RP, Brown BE. 1996. Penetration of solar UVB radiation in shallow tropical waters and its potential biological effects on coral reefs; results from the central Indian Ocean and Andaman Sea. Marine Ecology progress Series 144: 109–118.
59. Eakin CM, Lough JM, Heron SF. 2009. Climate variability and change: Monitoring data and evidence for increased coral bleaching stress. Ecological Studies 205: 41–67.
60. Elith J, Leathwick JR, Hastie T. 2008. A working guide to boosted regression trees. Journal of Animal Ecology, 77, 802-813.
61. Engels MS, Fletcher CH, Field ME, Storlazzi CD and others. 2004. Holocene reef accretion: southwest Molokai, Hawaii, USA. J Sed Res 74:255−269.
62. Fabricius KE. 2005. Effects of terrestrial runoff on the ecology of corals and coral reefs: review and synthesis. Marine Pollution Bulletin 50: 125–146.
63. Falkowski PG, Dubinsky Z, Muscatine L, Porter JW. 1984. Light and the bioenergetics of a symbiotic coral. Bioscience 34, 705–709.
64. Falkowski PG, Jokiel PL, Kinzie RA. 1990. Irradiance and corals. In: Dubinsky Z (ed) Ecosystems of the world 25: coral reefs. Elsevier, Amsterdam, p 89–107
65. Fenner D, Speicher M, Gulick S. Contributing authors: Aeby G, Cooper Aletto S, Anderson P, Carroll B, DiDonato E, DiDonato G, Farmer V, Fenner D, Gove J, Gulick S, Houk P, Lundblad E, Nadon M, Riolo F, Sabater M, Schroeder R, Smith E, Speicher M, Tuitele C, Tagarino A, Vaitautolu S, Vaoli E, Vargas-Angel B, Vroom P. 2008. The State of Coral Reef Ecosystems of American Samoa. pp. 307-352. In: J.E. Waddell and A.M. Clarke (eds.), The State of Coral Reef Ecosystems of the United States and Pacific Freely Associated States: 2008. NOAA Technical Memorandum NOS NCCOS 73. NOAA/NCCOS Center for Coastal Monitoring and Assessment's Biogeography Team. Silver Spring, MD. 569 pp.
66. Folke C et al. 2011. Reconnecting to the biosphere. – Ambio 40: 719–738.
67. Fox J, 2002. An R and S-Plus companion to applied Regression. Sage publications, Thousand Oaks, CA
68. Franklin EC, Jokiel PL, Donahue MJ. 2013. Predictive modeling of coral distributions and abundance in the Hawaiian Islands. Mar Ecol Prog Ser. Vol. 481: 121-132.
69. Glynn PW. 1976. Some physical and biological determinants of coral community structure in the eastern Pacific. *Ecological Monographs* 46:431-456.
70. Glynn PW. 1993. Coral reef bleaching: ecological perspectives. Coral Reefs. Vol. 12, issue 1, pp 1-17.
71. Gove JM, Williams GJ, McManus MA, Heron SF, Sandin SA, Vetter OJ, Foley DG. 2013. Quantifying climatological ranges and anomalies for Pacific coral reef ecosystems. PLoS ONE 8(4): e61974. DOI: 10.1371/journal.pone.0061974.
72. Grigg RW. 1982. Darwin point: A threshold for atoll formation. Coral Reefs 1:29- 34.
73. Grigg RW. 1983. Community structure, succession, and development of coral reefs in Hawaii. Mar Ecol Prog Ser 11:1−14.

74. Grigg RW. 2006. Depth limit for reef building corals in the Au'au Channel, S.E. Hawaii. Coral Reefs 25:77–84
75. Guadayol O`, Silbiger NJ, Donahue MJ, Thomas FIM. 2014. Patterns in Temporal Variability of Temperature, Oxygen and pH along an Environmental Gradient in a Coral Reef. PLoS ONE 9(1): e85213. doi:10.1371/journal.pone.0085213.
76. Gutierrez AP. 1996. Applied population ecology: a supply-demand approach. 300p Wiley, New York
77. Guzner B, Novoplansky A, Chadwick NE. 2007. Population dynamics of the reef-building coral Acropora hemprichii as an indicator of reef condition. Mar. Ecol. Prog. Ser. 333, 143-150.
78. Haedrich RL and Barnes SM. 1997. Changes over time of the size structure in an exploited shelf fish community. Fisheries Research. 31:229-239.
79. Hall DJ, Threlkland ST, Burns CW, Crowley PH. 1976. The size-efficiency hypothesis and the size-structure of zooplankton communities. Ann. Rev. Ecol. Syst. 7:177-208.
80. Hall VR, Hughes TP. 1996. Reproductive strategies of modular organisms: comparative studies of reef-building corals. Ecology 77, 950-963.
81. Harris PT. 2011. Surrogacy, in: Harris PT and Baker EK (Eds.), Seafloor Geomorphology as Benthic Habitat: GeoHab Atlas of Seafloor Geomorphic Features and Benthic Habitats, Elsevier, Amsterdam, 2011 (Chp. 5).
82. Hartigan, JA and Wong, MA. 1979. A K-means clustering algorithm. Applied Statistics 28, 100–108.
83. Hearn CJ, Atkinson MJ, Falter JL. 2001. A physical derivation of nutrient-uptake rates in coral reefs: effects of roughness and waves. Coral Reefs 20:347–356
84. Highsmith RC, Riggs AC, D'Antonio CM. 1980. Survival of hurricane-generated coral fragments and a disturbance model of reef calcification/growth rates. Oecologia 46: 322–329
85. Hoegh-Guldberg O. 1999. Mar. Freshw. Res. 50, 839.
86. Hoeke RK, Gove JM, Wong KB, Brainard RE, Smith E, Fisher-Pool P, Lammers M, Merritt D, Vetter OJ, Young CW. 2009. Coral reef ecosystem integrated observing system: In-situ oceanographic observations at the US Pacific islands and atolls. Journal of Operational Oceanography 2(2): 3-14. http://www.imarest.org/Publications/TechnicalProceedings/JOO.
87. Hofmann GE, Smith JE, Johnson KS, Send U, Levin LA, Micheli F et al. 2011. High-frequency dynamics of ocean pH: a multi-ecosystem comparison. *PLoS ONE* 6:e28983. doi: 10.1371/journal.pone.0028983
88. Hughes TP, Jackson JBC. 1980. Do corals lie about their age? Some demographic consequences of partial mortality, fission and fusion. Science 209, 713-714.
89. Hughes TP, Jackson JBC. 1985. Population dynamics and life histories of foliaceous corals. Ecol Monogr 55:141–166
90. Hughes TP, Connell JH. 1987. Population dynamics based on size or age? A reef coral analysis. Am Nat 129:818–829
91. Hughes TP, Tanner JE. 2000. Recruitment failure, life histories, and long-term decline of Caribbean corals. Ecology, 81:2250−2263
92. Hughes TP, Baird AH, Bellwood DR, Card M, Connolly SR, Folke C, Grosberg R, Hoegh-Guldberg O, Jackson JBC, Kleypas J, Lough JM, Marshall P, Nyström M, Palumbi SR, Pandolfi JM, Rosen B, Roughgarden J. 2003. Climate change, human

impacts, and the resilience of coral reefs. Science 301, 929-933
93. Huston MA. 1985. Patterns of species diversity on coral reefs. Annu Rev Ecol Syst 16:149-177
94. Jiang R, Murthy DNP. 2011. A study of Weibull shape parameter: Properties and significance. Reliability Engineering and System Safety. 96, 1619-1626.
95. Jokiel et al. 2014. Coral-algae metabolism and diurnal changes in the $CO_2$-carbonate system of bulk sea water. PeerJ 2:e378; DOI 10.7717/peerj.378
96. Jokiel PL and Coles SL. 1990. Response of Hawaiian and other Indo-Pacific reef corals to elevated temperature. *Coral Reefs.* 8, 155–162. doi: 10.1007/BF00265006
97. Jokiel PL, Brown EK, Friedlander A, Rodgers SK, Smith WR. 2004. Hawai‘i coral reef assessment and monitoring pro- gram: spatial patterns and temporal dynamics in reef coral communities. Pac Sci 58:159−174.
98. Jolliffe IT. 2002. Principal component analysis. 2nd edn. Springer, New York.
99. Kaihatu JM, Handler RA, Marmorino GO, Shay LK. 1998. Empirical Orthogonal Function analysis of ocean surface currents using complex and real-vector methods. Journal of Atmospheric and Oceanic Technology. Vol. 15. doi:10.1175/1520-0426(1998)015<0927:EOFAOO>2.0.CO;2
100. Kenyon JC, Aeby GS, Brainard RE, Chojnacki JD, Dunlap M and Wilkinson CB. 2004. Mass Coral Bleaching on High-Latitude Reefs in the Hawaiian Archipelago. 10th Int Coral Reef Symp, Okinawa.
101. Kenyon J and Brainard R. 2006. Second Recorded Episode of Mass Coral Bleaching in the Northwestern Hawaiian Islands. Atoll Research Bulletin. 543, pp505-523.
102. Kleypas JA, McManus JW, Meñez LAB. 1999. Environmental limits to coral reef development: where do we draw the line? Am. Zool. 39, 146–159.
103. Kohler KE, Gill SM. 2006. Coral Point Count with Excel extensions (CPCe): A Visual Basic program for the determination of coral and substrate coverage using random point count methodology. Comput Geosci 32: 1259−1269
104. Koweek DA, Dunbar RB, Monismith SG et al. 2015. High-resolution physical and biogeochemical variability from a shallow back reef on Ofu, American Samoa: an end-member perspective. Coral Reefs (2015) 34: 979. https://doi.org/10.1007/s00338-015-1308-9
105. Leichter JJ and Genovese SJ. 2006. Intermittent upwelling and subsidized growth of the scleractinian coral Madracis mirabilis on the deep fore-reef slope of Discovery Bay, Jamaica. Marine Ecology Progress Series 316: 95-103.
106. Lirman D, Orlando B, Maciá S, Manzello D, Kaufman L, Biber P, Jones T. 2003. Coral communities of Biscayne Bay, Florida and adjacent offshore areas: diversity, abundance, distribution, and environmental correlates. *Aquatic Conservation: Marine and Freshwater Ecosystems* 13:121-135.
107. Littler MM and Littler DS. 1984. Models of tropical reef biogenesis. – Phycol. Res. 3: 324–364.
108. Loya Y. 1976. Effects of water turbidity and sedimentation on community structure Puerto Rican corals. Bulletin of Marine Science 26: 450–466.
109. Loya Y, Sakai K, Yamazato K, Nakano Y, Sambali H, van Woesik R. 2001. Coral bleaching: the winners and the losers. Ecol Lett 4:122–131
110. Lyzenga DR. 1985. Shallow-water bathymetry using combined lidar and passive multispectral scanner data. Int J Remote Sens 6:115–125.

111. Maina J, McClanahan TR, Venus V, Ateweberhan M, Madin J. 2011. Global Gradients of Coral Exposure to Environmental Stresses and Implications for Local Management. Plos One 6.
112. Manly BFJ, McDonald LL, Thomas LL. 1993. Resource selection by animals. Chapman and Hall, London
113. Margalef R. 1975. Diversity, stability and maturity in natural eco- systems. – In: Dobben, W. H. and Lowe-McConnell, R. H. (eds), Unifying concepts in ecology. Springer, pp. 151–160.
114. Marubini F, Barnett H, Langdon C, Atkinson MJ. 2001. Dependence of calcification on light and carbonate ion concentration for the hermatypic coral *Porites compressa*. Marine Ecology Progress Series. 220: 153-162.
115. Massel SR. 2005. Ocean surface waves: their physics and prediction. Advanced Series on Ocean Engineering, World Scientific
116. MATLAB 2014a, 8.3.0.532. The MathWorks, Inc. 2014.
117. McClanahan TR, Ateweberhan M, Omukoto J. 2008. Long-term changes in coral colony size distribution on Kenyan reefs under different management regimes and across the 1998 bleaching event. Mar. Biol. 153, 755-768.
118. McCook LJ, Jompa J, Diaz-Pulido G. 2001. Competition between corals and algae on coral reefs: a review of evidence and mechanisms. Coral Reefs 19:400–417
119. Meesters EH, Wesseling I, Bak RPM. 1996. Partial mortality in three species of reef-building corals (Scleractinia) and the relation with colony morphology. Bull Mar Sci 58:838–852
120. Meesters EH, Wesseling I, Bak RPM. 1997. Coral colony tis- sue damage in six species of reef-building corals: partial mortality in relation with depth and surface area. J Sea Res 37:131–144
121. Meesters E, Hilterman M, Kardinaal E, Keetman M, de Vries M, Bak R. 2001. Colony size-frequency distributions of scleractinian coral populations: spatial and interspecific variation. *Marine Ecology Progress Series*, *209*, 43–54. doi:10.3354/meps209043
122. Möllmann C et al. 2009. Reorganization of a large marine ecosystem due to atmospheric and anthropogenic pressure: a discontinuous regime shift in the Central Baltic Sea. – Global Change Biol. 15: 1377–1393.
123. Morris DW. 2003. Toward an ecological synthesis: a case for habitat selection. Oecologia 136: 1-13
124. Mudholkar GS, Srivastava DK, Kollia GD. 1996. A generalization of the Weibull distribution with application to the analysis of survival data. Journal of the American Statistical Association, Vol. 91, No. 436, pp. 1575-1583.
125. Muller-Landau HC et al. 2006. Comparing tropical forest tree size distributions with the predictions of metabolic ecology and equilibrium models. Ecology Letters 9: 589-602. doi: 10.1111/j.1461-0248.2006.00915.x
126. Mumby PJ. 1999. Bleaching and hurricane disturbances to popula- tions of coral recruits in Belize. Mar Ecol Prog Ser 190:27–35
127. Murdoch TJT and Aronson RB. 1999. Scale-dependent spatial variability of coral assemblages along the Florida Reef Tract. *Coral Reefs* 18:341-351.
128. NOAA Coastal Digital Elevation Model for Tutuila. National Geophysical Data Center (NGDC) and National Centers for Environmental Information (NESDIS), NOAA, U.S. Department of Commerce. URL:

https://www.ngdc.noaa.gov/metaview/page?xml=NOAA/NESDIS/NGDC/MGG/DEM/iso/xml/4610.xml&view=getDataView&header=none
129. Nozawa Y and Harrison PL. 2007. Effects of elevated temperature on larval settlement and post-settlement survival in scleractinian corals, *Acropora solitaryensis* and *Favites chinensis*. Mar Biol (2007) 152:1181–1185. DOI 10.1007/s00227-007-0765-2
130. Odum EP. 1969. The strategy of ecosystem development. – Science 164: 262–270.
131. Oigman-Pszczol SS, Creed JC. 2004. Size-structure and spatial distribution of the corals Mussismilia hispida and Siderastrea stellata (Scleractinia) at Armaçao Dos Buzios, Brazil. Bull. Mar. Sci. 74, 433-448.
132. Page HN, Andersson AJ, Jokiel PL, Rodgers KS, Lebrato M, Yeakel K et al. 2016. Differential modification of seawater carbonate chemistry by major coral reef benthic communities. *Coral Reefs*. 35, 1311–1325. doi: 10.1007/s00338-016-1490-4
133. Petraitis PS. 1990. Direct and indirect effects of predation, herbivory and surface rugosity on mussel recruitment. Oecologia 83:405–413
134. Pinder III JE, Wiener JG, Smith MH. 1978. The Weibull distribution: A new method of summarizing survivorship data. Ecology, 59 (1), pp. 175-179.
135. Porter JW, Lewis SK, Porter KG. 1999. The effect of multiple stressors on the Florida Keys coral reef ecosystem: a landscape hypothesis and a physiological test. Limnology and Oceanography 44, 941-949.
136. Price NN, Martz TR, Brainard RE, Smith JE. 2012. Diel Variability in Seawater pH Relates to Calcification and Benthic Community Structure on Coral Reefs. PLoS ONE 7(8): e43843. doi:10.1371/journal.pone.0043843
137. R Core Team (2015). R: A language and environment for statistical computing. R Foundation for Statistical Computing, Vienna, Austria. URL - https://www.R-project.org/.
138. Raimondi PT. 1990. Patterns, mechanisms, consequences of variability in settlement and recruitment of an intertidal barnacle. Ecol Monogr 60:283–309
139. Ray CG. 1988. Ecological diversity in coastal zones and oceans. Pages 36–50 in E. O. Wilson, editor. Biodiversity. National Academy Press, Washington, D.C.
140. Reaser JK, Pomerance R, Thomas PO. 2000. Coral bleaching and global climate change: scientific findings and policy recommendations. Conservation Biology **14:**1500–1511.
141. Roughgarden J, Iwasa Y, and Baxter C. 1985. Demographic theory for an open marine population with space-limited recruitment. Ecology 66:54–57.
142. Ruiz-Zarate MJ, Fragosa JED, and Carricart-Ganivet JP. 2000. Relationships between *Maicina areloata* (Cnidaria: Scleractinia), *Thalassia testudinum* (Anthophyta) and *Neogoniolithon* sp. (Rhodophyta). Marine Ecology Progress Series. 206: 135-146.
143. Salm RV and Coles SL. 2001. Coral bleaching and marine protected areas. Proceedings of the workshop on mitigating coral bleaching impact through MPA design. Asia Pacific Coastal Marine Program Report 0102. The Nature Conservancy, Honolulu. Also available from http://www.conserveonline.org (accessed 18 May 2003).
144. Schoener TW. 1974. Resource partitioning in ecological communities. Science 185:27-39.
145. Sebens KP, Vandersall KS, Savina LA, Graham KR. 1996. Zooplankton capture by two scleractinian corals, *Madracis mirabilis* and *Montastrea cavernosa*, in a field enclosure. Mar Biol 127:303–317
146. Shenkar N, Fine M, Loya Y. 2005. Size matters: bleaching dynamics of the coral

Oculina patagonica. Mar Ecol Prog Ser 294:181– 188
147. Silbiger NJ, Guadayol Ó, Thomas FIM, Donahue MJ. 2014. Reefs shift from net accretion to net erosion along a natural environmental gradient. Mar Ecol Prog Ser, Vol. 515: 33–44. doi: 10.3354/meps10999
148. Smith SG, Swanson DW, Chiappone M, Miller SL, Ault JS. 2011. Probability sampling of stony coral populations in the Florida Keys. Environ Monit Assess. 183:121-138.
149. Soong K. 1993. Colony size as a species character in massive reef corals. Coral Reefs 12:77–83
150. Sousa WP. 1984. The role of disturbance in natural communities. – Annu. Rev. Ecol. Syst. 15: 353–391.
151. Storlazzi CD, Field ME, Dykes JD, Jokiel PL, Brown E. 2002. Wave control on reef morphology and coral distribution: Moloka'i, Hawai'i. Pages 784-793 *in* Proceedings, 4th International Symposium on Waves. American Society of Civil Engineers, Reston, Virginia.
152. Storlazzi CD, Brown EK, Field ME, Rodgers K, Jokiel PL. 2005. A model for wave control on coral breakage and species distribution in the Hawaiian Islands. Coral Reefs 24:43−55
153. Swanson DW and Ault J. 2011. Spatial dynamics of coral populations in the Florida Keys. *Marine Biology and Fisheries*, *Ph.D.*, 323pgs.
154. Szmant A. 1991. Sexual reproduction by the Caribbean reef corals *Montastrea annularis* and *M. cavernosa*. Mar Ecol Prog Ser 74:13–25
155. Tempera F, McKenzie M, Bashmachnikov I, Puotinen M, Santos RS, Bates R. 2011. Predictive modeling of dominant macroalgae abundance on temperate island shelves (Azores, northeast Atlantic), in: Harris PT and Baker EK (Eds.), Seafloor Geomorphology as Benthic Habitat: GeoHab Atlas of Seafloor Geomorphic Features and Benthic Habitats, Elsevier, Amsterdam, 2011 (Chp. 8).
156. Tempera F and Bates RC. 2009. Benthic habitats of the extended Faial Island shelf and their relationship to geologic, oceanographic and infralittoral biologic features. School of Geography and Geosciences, University of St. Andrews, Ph.D., 341pgs.
157. Tremblay P, Grover R, Maguer JF, Hoogenboom M, Ferrier-Pagés C. 2014. Carbon transloction from symbiont to host depends on irradiance and food availability in the tropical coral Stylophora pistillata. Coral Reefs 33 (1), 1–13.
158. Van Hooidonk R, Maynard JA, Planes S. 2013. Temporary refugia for coral reefs in a warming world. Nature Climate Change 3: 508–511.
159. Van Woesik R and Done TJ. 1997. Coral communities and reef growth in the southern Great Barrier Reef. *Coral Reefs* 16:103-115.
160. Vargas-Ángel B, Richards CL, Vroom PS, Price NN, Schils T, Young CW, et al. 2015. Baseline Assessment of Net Calcium Carbonate Accretion Rates on U.S. Pacific Reefs. PLoS ONE 10(12): e0142196. doi:10.1371/journal.pone.0142196
161. Vermeij MJA, Smith JE, Smith CM et al. 2009. Survival and settlement success of coral planulae: independent and synergistic effects of macroalgae and microbes. Oecologia 159: 325. https://doi.org/10.1007/s00442-008-1223-7
162. Vermeij MJA and Sandin SA. 2008. Density-dependent settlement and mortality structure: the earliest life phases of a coral population. Ecology, 89(7), pp. 1994-2004.
163. Vermeij MJA, Bak RPM. 2002. Inferring demographic processes from population size structure in corals. In: Proceedings of the 9th International Coral Reef Symposium 5, pp.

593-598
164. Veron JEN. 2011. Corals: biology, skeletal deposition, and reef- building. In: Hopley D (ed) Encyclopedia of modern coral reefs: Structure form and process. Springer, Berlin, pp 275–281
165. Vollmer SV, Palumbi SR. 2007. Restricted gene flow in the Caribbean staghorn coral *Acropora cervicornis*: Implications for the recovery of endangered reefs. Journal of Heredity 98: 40–50.
166. Walsh C and MacNally R. 2013. hier.part: Hierarchical Partitioning. R package version 1.0-4. https://CRAN.R-project.org/package=hier.part
167. Wells S, West J, Westmacott S, Teleki K. 2001. Management of bleached and severely damaged coral reefs. Pages 73–80 in H. Z. Schuttenberg, editor. Coral bleaching: causes, consequences, and response. Coastal management report 2230. Coastal Resources Center, Narragansett, Rhode Island. Also available from http:// www.crc.uri.edu/comm/asia_pubs.html (accessed 18 May 2003).
168. Werner EE, Gilliam JF. 1984. The ontogenetic niche and species interactions in size-structured populations. Ann Rev Ecol Syst. 15:393-425.
169. Wilkinson C. 2000. Status of coral reefs of the world: 2000. Australian Institute of Marine Science, Cape Ferguson, Queensland.
170. Williams GJ, Gove JM, Eynaud Y, Zgliczynski B, Sandin SA. 2015a. Local human impacts decouple natural biophysical relationships on Pacific coral reefs. Ecography doi:10.1111/ecog.01353
171. Williams ID, Baum JK, Heenan A, Hanson KM, Nadon MO, Brainard RE. 2015b. Human, Oceanographic and Habitat Drivers of Central and Western Pacific Coral Reef Fish Assemblages. PLoS ONE 10(4): e0120516. doi:10.1371/journal. pone.0120516
172. Wood SN. 2011. Fast stable restricted maximum likelihood and marginal likelihood estimation of semiparametric generalized linear models. Journal of the Royal Statistical Society (B) 73(1):3-36. https://cran.r-project.org/package=mgcv
173. Wooldridge SA. 2009. Water quality and coral bleaching thresholds: Formalising the linkage for the inshore reefs of the Great Barrier Reef, Australia. Marine Pollution Bulletin 58: 745–751.
174. Zhang L, Packard KC, Liu C. 2003. A comparison of estimation methods for fitting Weibull and Johnson's SB distributions to mixed spruce-fir stands in northeastern North America. Can. J. For. Res. 33: 1340–1347. doi: 10.1139/X03-054
175. Zuur AF, Ieno EN, Elphick CS. 2010. A protocol for data exploration to avoid common statistical problems. Methods in Ecology and Evolution. 1, 3-14.

# 7. TABLES

**Table 1**: Coral species and number of individuals, N, modeled at 2 intra-island spatial resolutions, 1) Site-level (Figure 4.1), and 2) Strata-level (Figure 4.2) resolution. Site-level and strata sample size, n, is the final sample size resulting from post-pooling and excluding of insufficient sample sizes, N, for each site and excluding of insufficient sample sizes, N, for each strata. See section ***2.2 Coral size structure characterization, 'Coral size structure spatial resolution'*** for details.

| **Coral species** | **N** | **Spatial resolution** | **n** |
|---|---|---|---|
| *Isopora spp.* | 813 | Site | 24 sites |
| | | Strata | 13 strata |
| *Montastrea curta* | 1526 | Site | 85 sites |
| | | Strata | 25 strata |

**Table 2:** Biogeophysical and anthropogenic predictor covariates examined as drivers of coral size structure distributions around American Samoa. Listed covariates are final predictors after being tested for multi-collinearity. Covariates are predictors used in final models for *Isopora* and/or *Montastrea curta* at the site-level and/or strata-level resolution.

| Predictor | Units | Description | Source |
|---|---|---|---|
| Depth | Meters | Average depth from each benthic REA site | NOAA ESD 2015 RAMP data |
| PAR | Einstein $m^{-2}$ $d^{-1}$ | Climatological long term mean derived from 5km, weekly data (gradient and nearest neighbor metric) | See methods |
| SST | °C | Climatological long term mean derived from 5km, weekly data (gradient and nearest neighbor metric) | See methods |
| Chl-*a* | mg $m^{-3}$ | Climatological long term mean derived from 5km, weekly data (gradient and nearest neighbor metric) | See methods |
| Wave energy | MW $hr^{-1}$ $m^{-1}$ | Climatological long term mean derived from 1km, annual integrated mean data | See methods |
| Mean net carbonate accretion rates | g CaCO3 m-2 yr-1 | Mean calcium carbonate deposition rate for each site (derived from 3-year deployment) | NOAA ESD 2015 RAMP data |
| Net carbonate accretion rate variability | (dimensionless) | Amount of variation around the mean calcium carbonate deposition rate for each site (derived from 3-year deployment) | NOAA ESD 2015 RAMP data |
| Coral cover | Percent | Benthic functional group cover derived from image analysis | NOAA ESD 2015 RAMP data |
| CCA cover | Percent | Benthic functional group cover derived from image analysis | NOAA ESD 2015 RAMP data |
| Turf algae cover | Percent | Benthic functional group cover derived from image analysis | NOAA ESD 2015 RAMP data |
| Juvenile coral abundance | Count | Juvenile abundance per site and strata | NOAA ESD 2015 RAMP data |
| Slope | Degrees | Maximum change in elevation | See methods |
| Slope range | Degrees | Difference between min. and max. slope | See methods |
| Slope variability | (dimensionless) | Amount of variation around the mean slope | See methods |
| Total area surveyed | $m^2$ | Area surveyed at each site | NOAA ESD 2015 RAMP data |
| Human population density | # / land area | Population resident on island within 10-km and 20-km radius divided by land area | sensu Williams et al. 2011 |

**Table 3**: Summary of final model results for each coral species and spatial resolution. Best-fit models were selected based off of $\Delta AICc \leq 2$ criteria initially amongst main effects models and subsequently for models with both main effects and all two-way interactions. All model assumptions and spatial autocorrelations were tested in best-fit models (see Results section for detailed approach in determining best-fit models).

| Resolution | Predictors | Log Likelihood | AICc | ΔAICc | $R^2$ |
|---|---|---|---|---|---|
| *Isopora* site-level | Mean net carbonate accretion rates + Net carbonate accretion rate variability + Slope + Slope variability + Slope:Slope variability | -39.020 | 99.0 | 0.00 | 0.58 |
| *Isopora* strata-level | Mean net carbonate accretion rates + Wave energy | -13.978 | 41 | 1.97 | 0.46 |
| *M. curta* site-level | Depth + PAR + SST + Wave energy + Juvenile abundance + Coral cover + SST:Juvenile abundance | -149.519 | 319.5 | 0.76 | 0.45 |
| *M. curta* strata-level | Mean net carbonate accretion rates + PAR + SST + Wave energy | -42.117 | 100.9 | 0.69 | 0.57 |

**Table 4a**: *Isopora spp*. strata names and details

| ***Isopora spp.*** | |
|---|---|
| **Strata** | **Strata details** |
| OFU_NW_M | Ofu and Olosega: Northwest, moderate depth |
| OFU_NW_S | Ofu and Olosega: Northwest, shallow depth |
| OFU_SE_S/M | Ofu and Olosega: Southeast, shallow/moderate depth |
| TAU_NW_M | Tau: Northwest, moderate depth |
| TAU_NW_S | Tau: Northwest, shallow depth |
| TUT_AASU_ALL | Tutuila: Aunu'u – A, all depths |
| TUT_ABSU_D | Tutuila: Aunu'u – B, deep depth |
| TUT_ABSU_M | Tutuila: Aunu'u – B, moderate depth |
| TUT_EAST_M | Tutuila: East, moderate depth |
| TUT_EAST_S | Tutuila: East, shallow depth |
| TUT_SW_D | Tutuila: Southwest, deep depth |
| TUT_SW_M | Tutuila: Southwest, moderate depth |
| TUT_SW_S | Tutuila: Southwest, shallow depth |

**Table 4b**: *Montastrea curta* strata names and details

| ***Montrastrea curta*** | |
|---|---|
| **Strata** | **Strata details** |
| OFU_NW_ALL | Ofu and Olosega: Northwest, all depths |
| OFU_SE_D | Ofu and Olosega: Southeast, deep depths |
| OFU_SE_S_M | Ofu and Olosega: Southeast, shallow/moderate depths |
| ROS_FRF_ALL | Rose Atoll: All forereef, all depths |
| SWA_SE_D | Swains: Southeast, deep depth |
| TAU_OPEN_D | Tau: All forereef, deep depth |
| TAU_OPEN_M | Tau: All forereef, moderate depth |
| TAU_OPEN_S | Tau: All forereef, shallow depth |
| TAU_TMPA_D | Tau: MPA, deep depth |
| TAU_TMPA_S_M | Tau: MPA, shallow/moderate depth |
| TUT_AASU_ABSU_M_D | Tutuila: Aunu'u – A and B, moderate/deep depth |
| TUT_AASU_ABSU_S | Tutuila: Aunu'u – A and B, shallow depth |
| TUT_FBSU_D | Tutuila: Fagatele Bay, deep depth |
| TUT_FBSU_S_M | Tutuila: Fagatele Bay, shallow/moderate depth |
| TUT_FFSU_M_D | Tutuila: Fagalua Bay, moderate/deep depth |
| TUT_FFSU_S | Tutuila: Fagalua Bay, shallow depth |
| TUT_NE_D | Tutuila: Northeast, deep depth |
| TUT_NE_S_M | Tutuila: Northeast, shallow/moderate depth |
| TUT_NW_D | Tutuila: Northwest, deep depth |
| TUT_NW_M | Tutuila: Northwest, moderate depth |
| TUT_SE_D | Tutuila: Southeast, deep depth |
| TUT_SE_M | Tutuila: Southeast, moderate depth |
| TUT_SE_S | Tutuila: Southeast, shallow depth |
| TUT_SW_D | Tutuila: Southwest, deep depth |
| TUT_SW_S_M | Tutuila: Southwest, shallow/moderate depth |

**Table 5a**: *Isopora spp.* strata results and associated shape parameters. Refer to Table 4a for strata details.

| **Strata** | **HUA outcome** | **Shape parameter, *k*** |
|---|---|---|
| OFU_NW_S | positive | 5.08 |
| TUT_EAST_S | positive | 5.08 |
| TUT_SW_S | positive | 6.08 |
| OFU_NW_M | neutral | 7.65 |
| OFU_SE_S/M | neutral | 4.60 |
| TUT_ABSU_D | neutral | 4.94 |
| TUT_ABSU_M | neutral | 5.67 |
| TUT_SW_D | neutral | 5.48 |
| TUT_SW_M | neutral | 4.77 |
| TAU_NW_M | negative | 8.09 |
| TAU_NW_S | negative | 6.17 |
| TUT_AASU_ALL | negative | 5.98 |
| TUT_EAST_M | negative | 5.25 |
| **DOMAIN** | **DOMAIN** | **5.31** |

**Table 5b**: *Montastrea curta* strata results and associated shape parameters. Refer to Table 4b for strata details.

| **Strata** | **HUA outcome** | **Shape parameter, *k*** |
|---|---|---|
| TUT_SE_M | positive | 5.81 |
| TUT_FFSU_M_D | positive | 6.97 |
| TUT_SW_D | positive | 8.46 |
| ROS_FRF_ALL | positive | 4.79 |
| TUT_AASU_ABSU_M_D | positive | 5.72 |
| TAU_TMPA_S_M | positive | 5.73 |
| OFU_SE_D | neutral | 4.39 |
| TUT_SE_D | neutral | 4.46 |
| OFU_NW_ALL | neutral | 4.68 |
| TUT_NE_S_M | neutral | 5.68 |
| TAU_OPEN_M | neutral | 5.94 |
| TAU_OPEN_S | neutral | 6.38 |
| OFU_SE_S_M | neutral | 6.80 |
| TAU_TMPA_D | neutral | 7.34 |
| TAU_OPEN_D | neutral | 7.64 |
| TUT_FBSU_D | neutral | 8.62 |
| TUT_NW_M | neutral | 11.05 |
| SWA_SE_D | negative | 2.73 |
| TUT_FBSU_S_M | negative | 4.72 |
| ROS_ROSU_BRF_ALL | negative | 4.80 |
| TUT_NW_D | negative | 5.69 |
| TUT_NE_D | negative | 6.12 |
| TUT_SE_S | negative | 6.28 |
| TUT_FFSU_S | negative | 7.19 |
| TUT_AASU_ABSU_S | negative | 9.38 |
| TUT_SW_S_M | negative | 12.74 |
| **DOMAIN** | **DOMAIN** | **5.23** |

# 8. FIGURES

**Figure 1**: Detailed map of American Samoa island/atoll complex

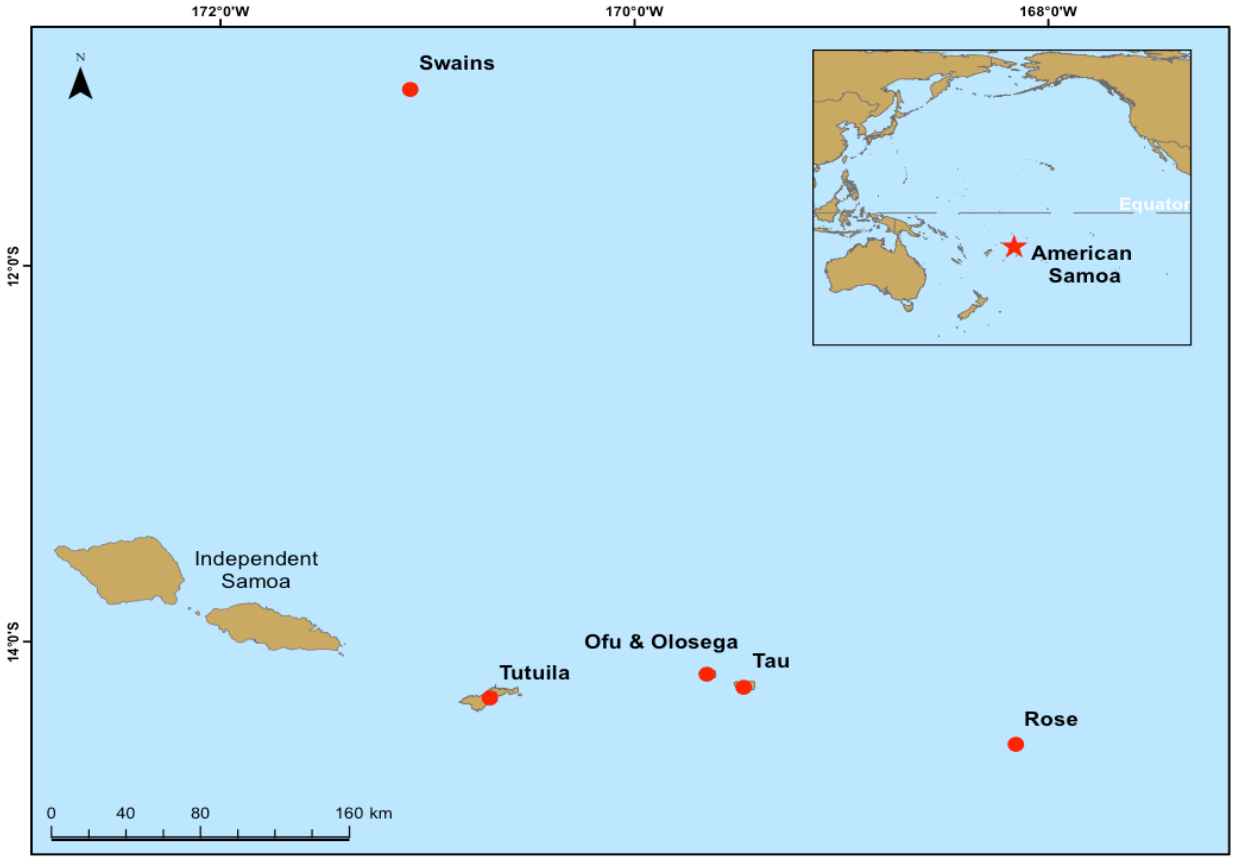

**Figure 2**: *Isopora crateriformis*

**Figure 3**: *Montastrea curta*

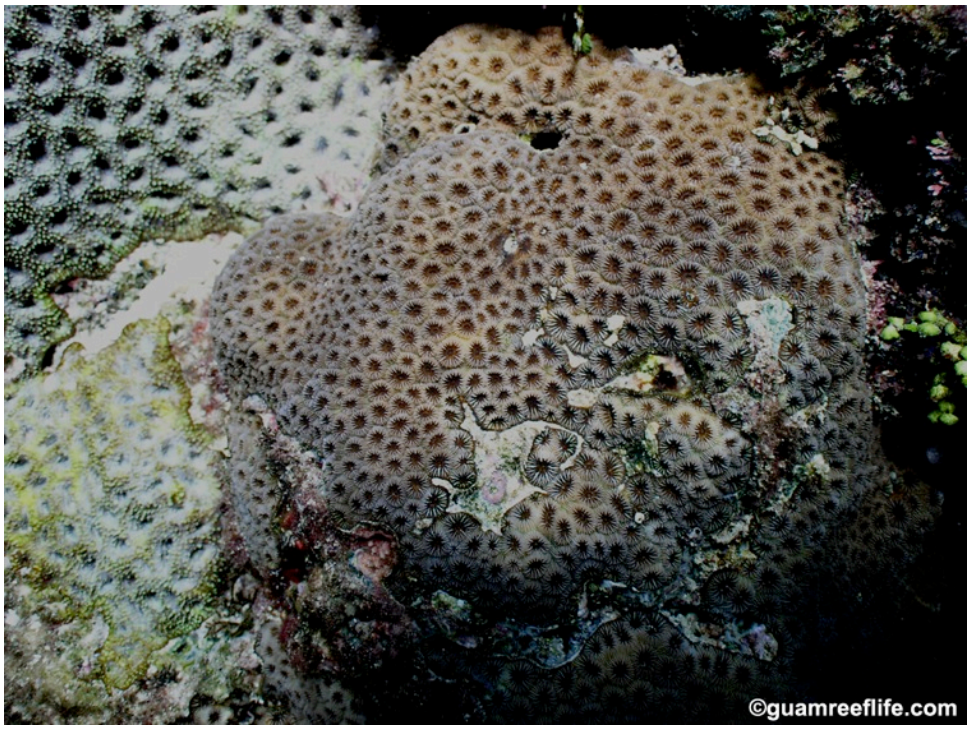

**Figure 4.1**: Example of site –level spatial resolution for Ofu and Olosega

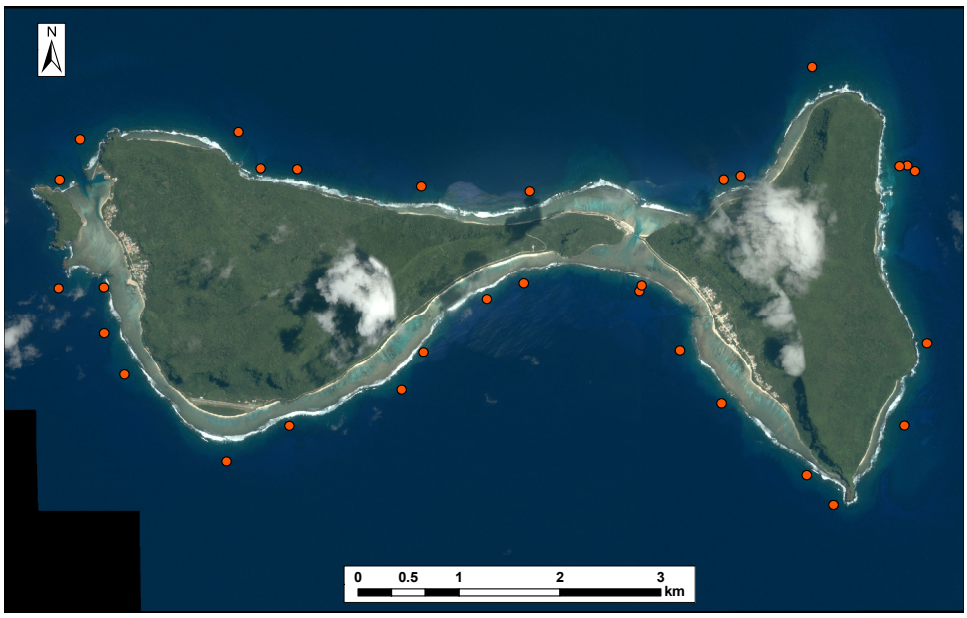


**Figure 4.2**: Example of strata-level spatial resolution for Ofu and Olosega

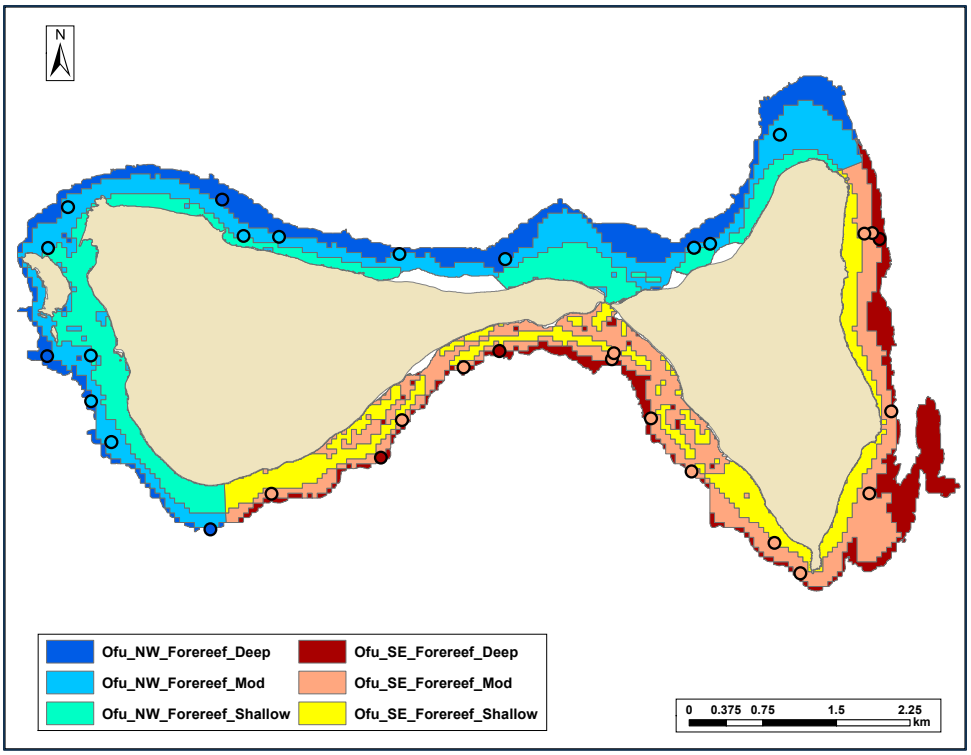

**Figure 5**: Tutuila map displaying strata with respective positive, neutral, and negative habitat use areas for *Montastrea curta*. **A**: Example of *M. curta* size structure histograms yielding positive habitat use (red line: Weibull fit). **B**: Example of *M. curta* density size structure histograms yielding neutral habitat use (red line: Weibull fit). **C**: Example of *M. curta* density size structure histogram yielding negative habitat use (red line: Weibull fit).

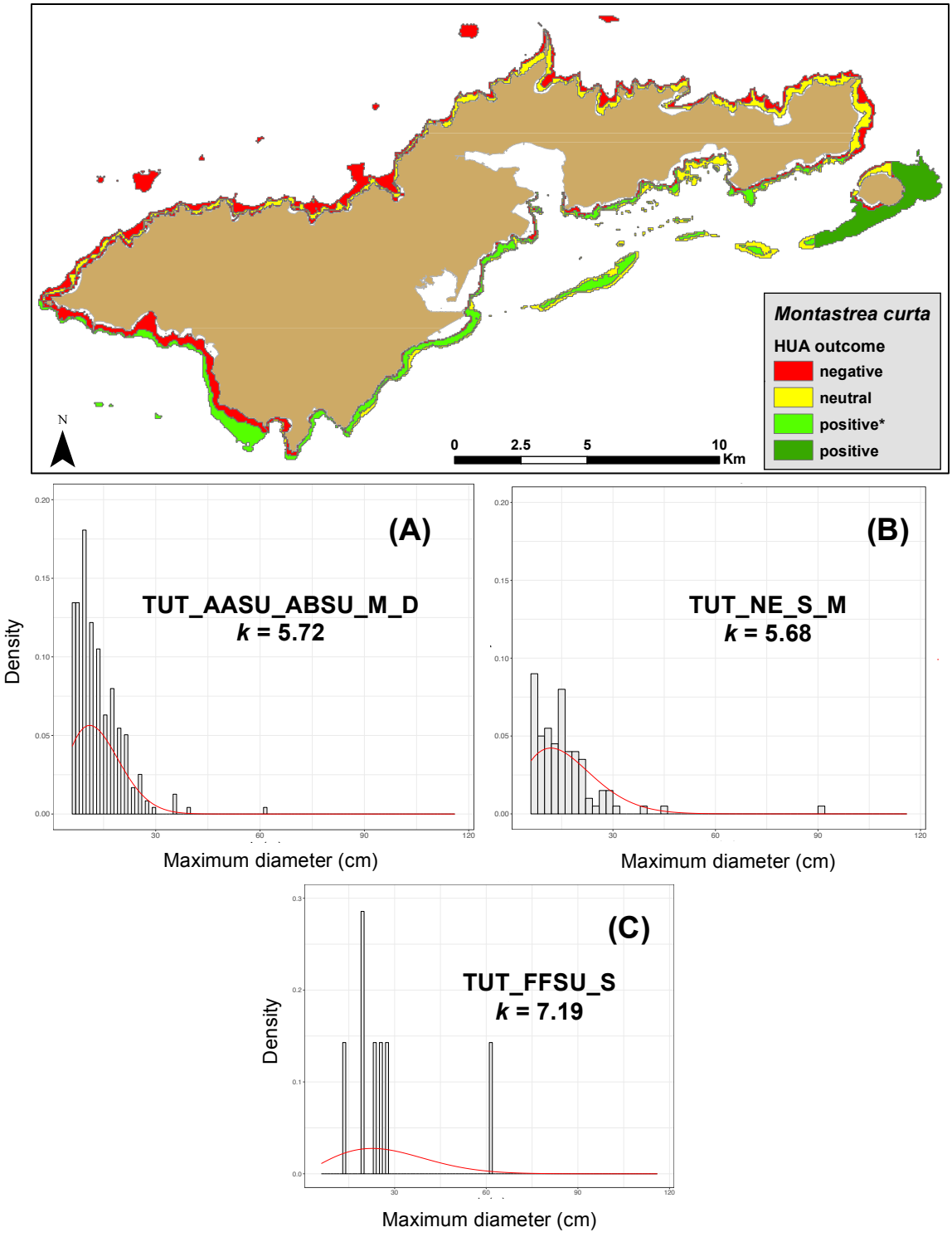

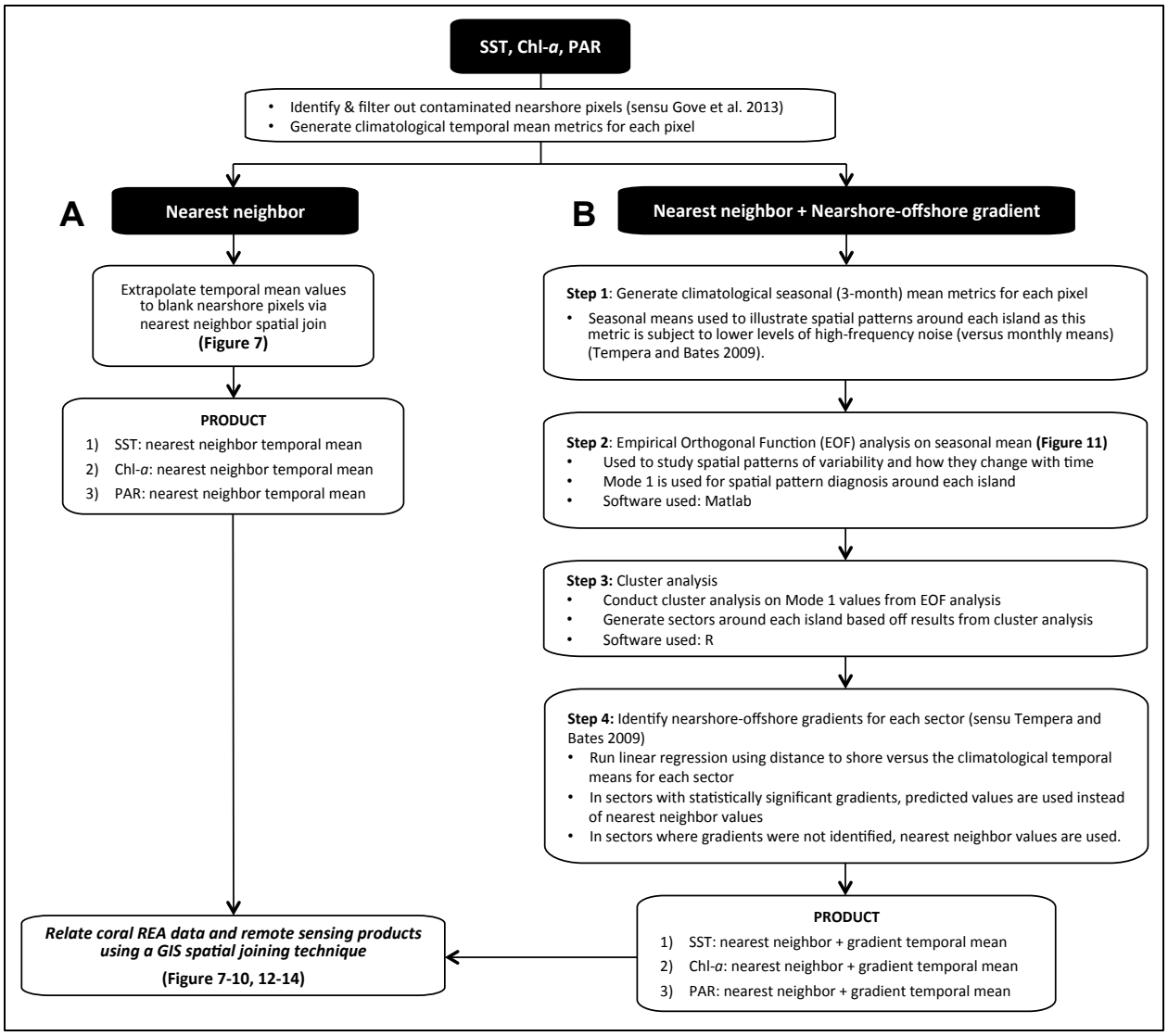


**Figure 6**: Dataflow scheme to extrapolate climatological values to nearshore blank pixels (sensu Tempera and Bates 2009). Extrapolation via: A) nearest neighbor spatial joining or B) combination of statistically significant nearshore-offshore gradients and nearest neighbor spatial joining in sectors of each island.

**Figure 7**: Chl-a remote sensing pixels and associated temporal mean values for each pixel around Tutuila. **A**) Filtered chl-a remote sensing data with contaminated nearshore pixels (white) with no data. **B**) Extrapolated temporal mean values to blank nearshore pixels via nearest neighbor spatial join. **C**) End product showing coral REA sites with spatially joined chl-a temporal mean nearest neighbor values.

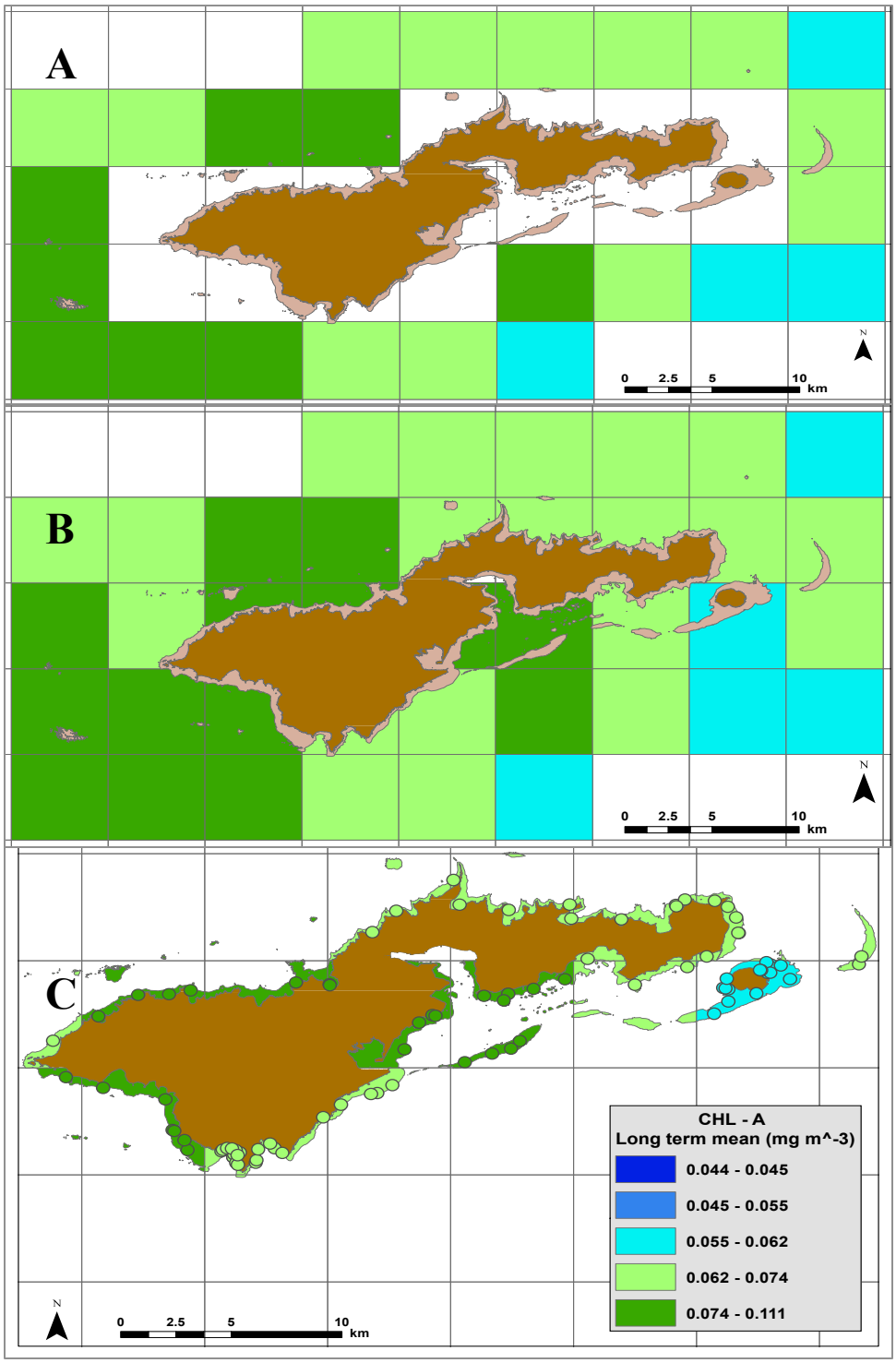

**Figure 8a**: End product showing coral REA sites with spatially joined chl-a temporal mean nearest neighbor values. Ofu and Olosega (top) and Tau Island (bottom)

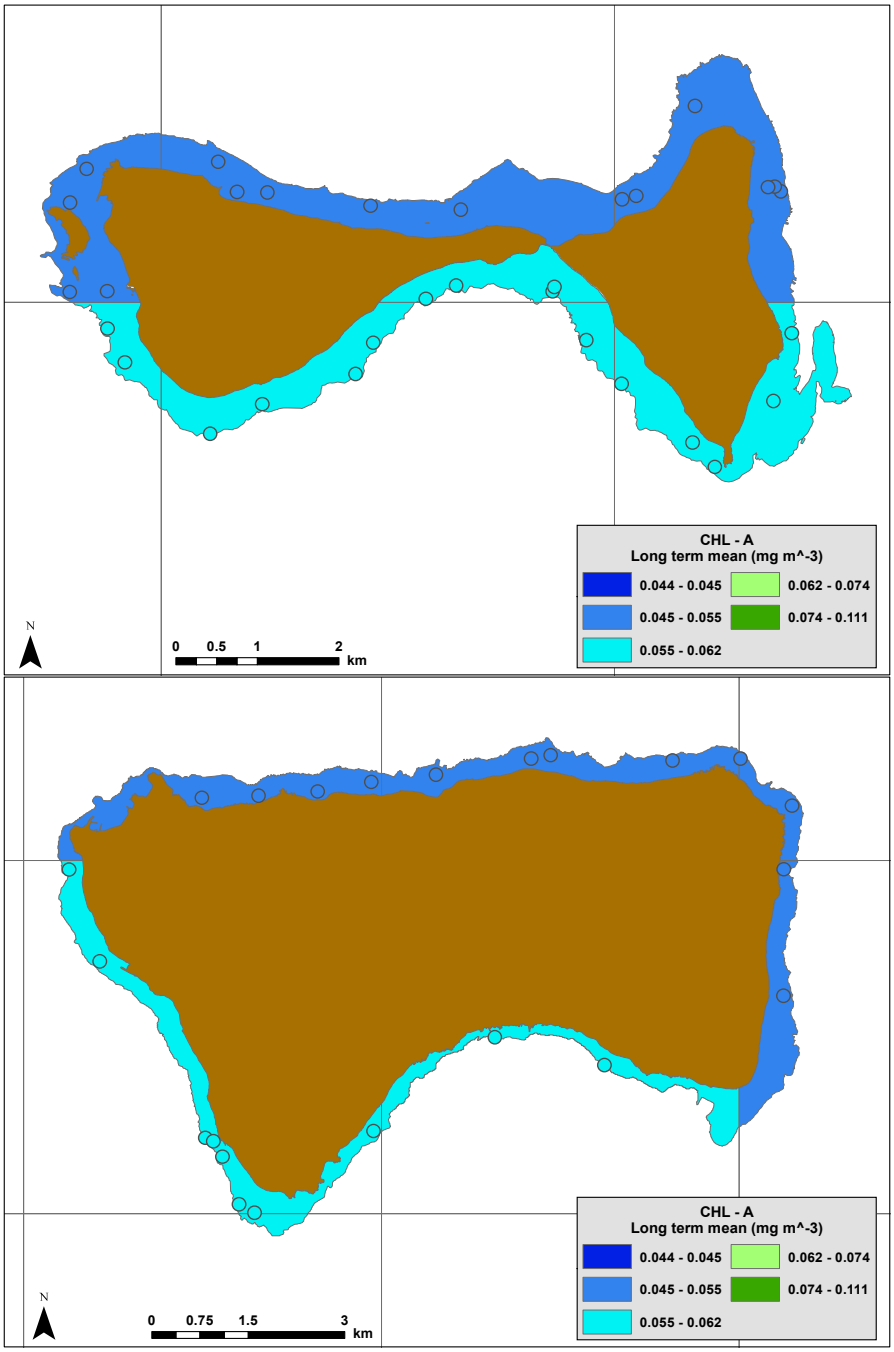

**Figure 8b**: End product showing coral REA sites with spatially joined chl-a temporal mean nearest neighbor values. Rose Atoll (top) and Swains Island (bottom)

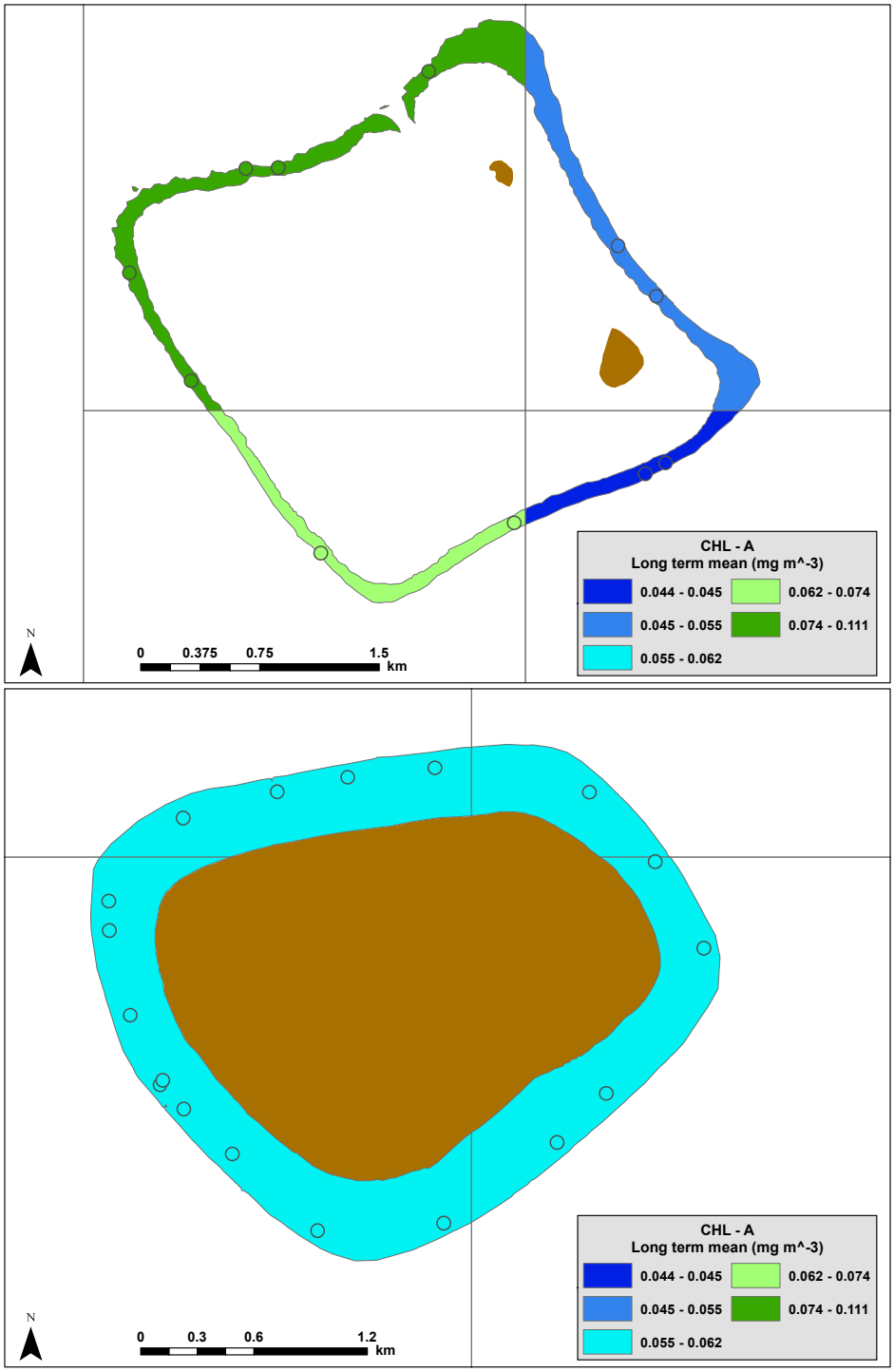

**Figure 9a**: End product showing coral REA sites with spatially joined PAR temporal mean nearest neighbor values on Tutuila.

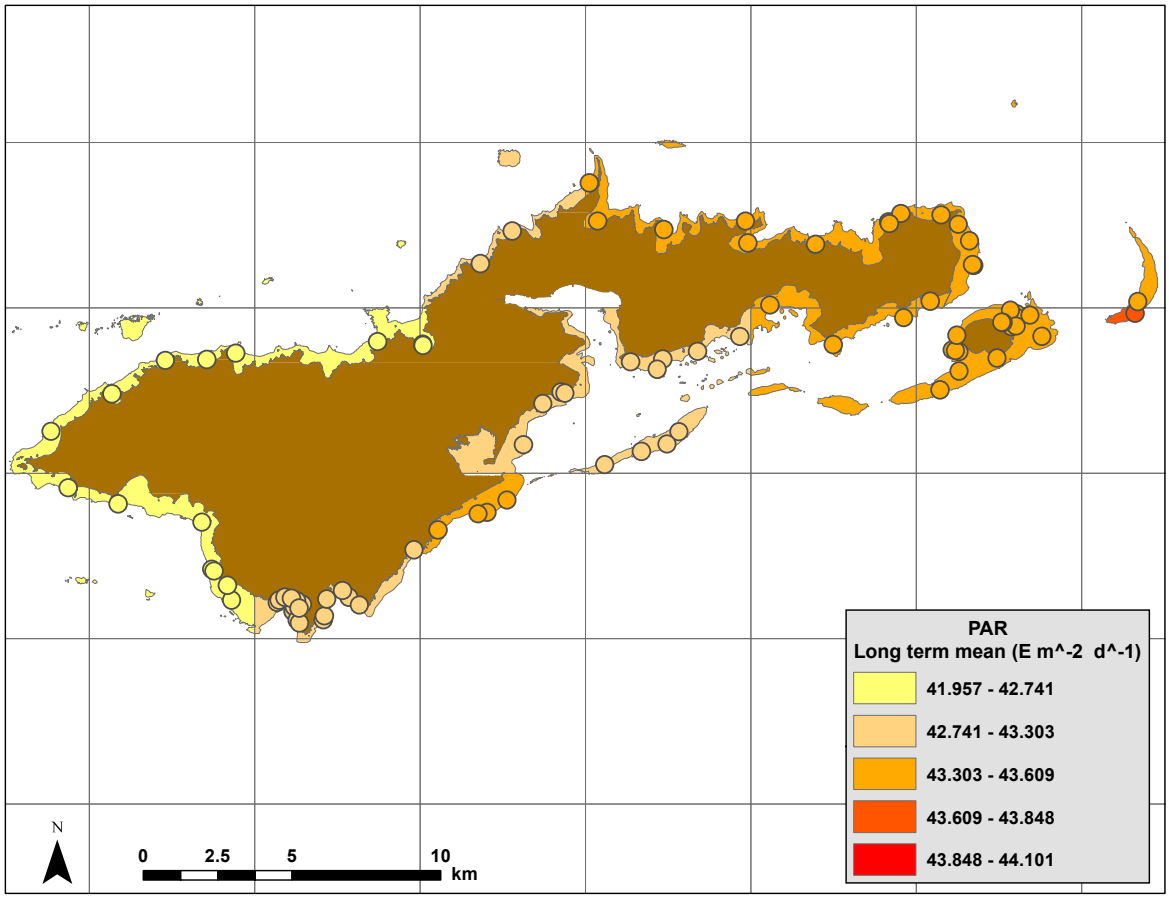

**Figure 9b**: End product showing coral REA sites with spatially joined PAR temporal mean nearest neighbor values. Ofu and Olosega (top) and Tau Island (bottom)

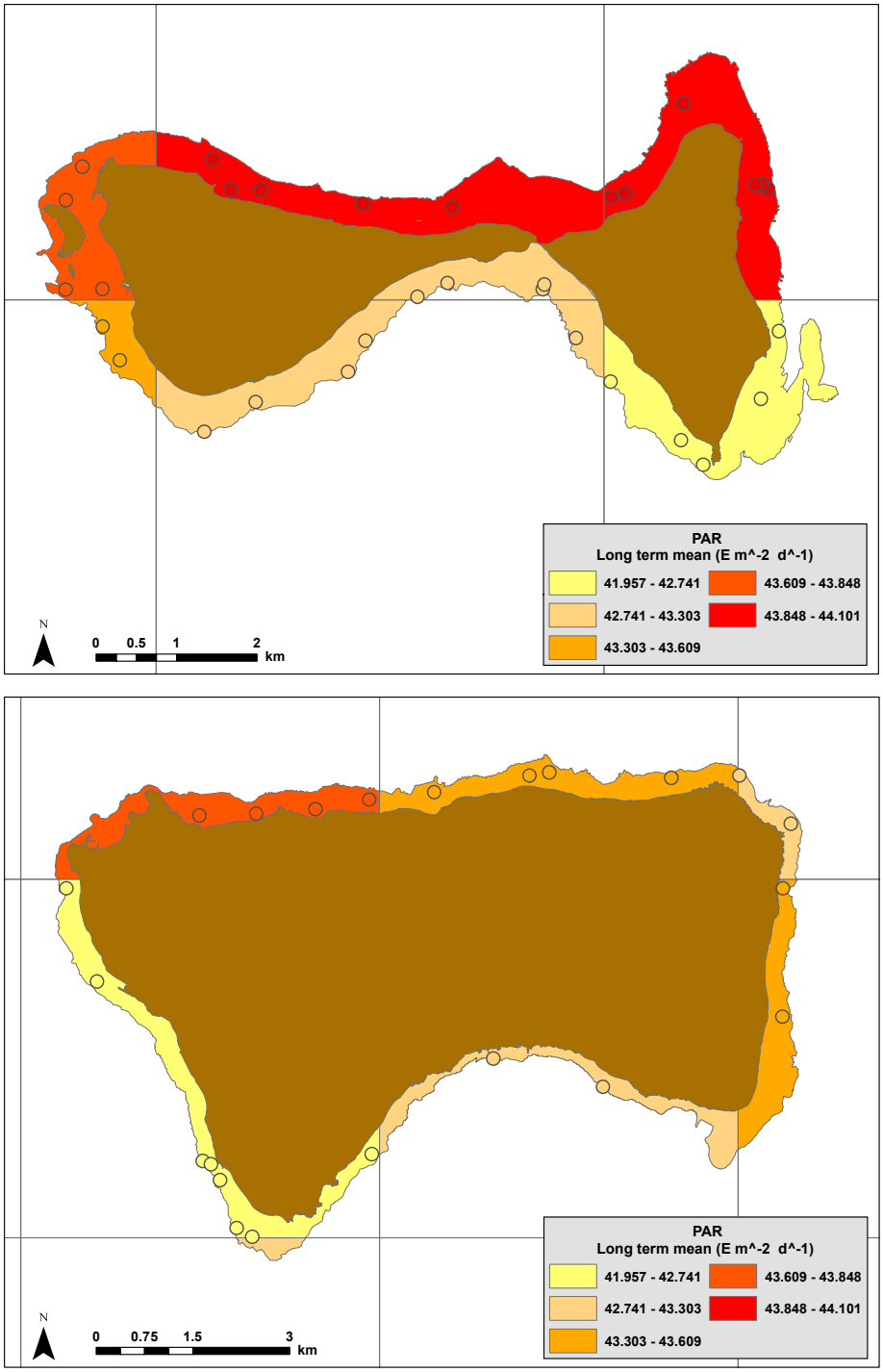

**Figure 9c**: End product showing coral REA sites with spatially joined PAR temporal mean nearest neighbor values. Rose Atoll (top) and Swains Island (bottom)

**Figure 10a**: End product showing coral REA sites with spatially joined SST temporal mean nearest neighbor values for Tutuila.

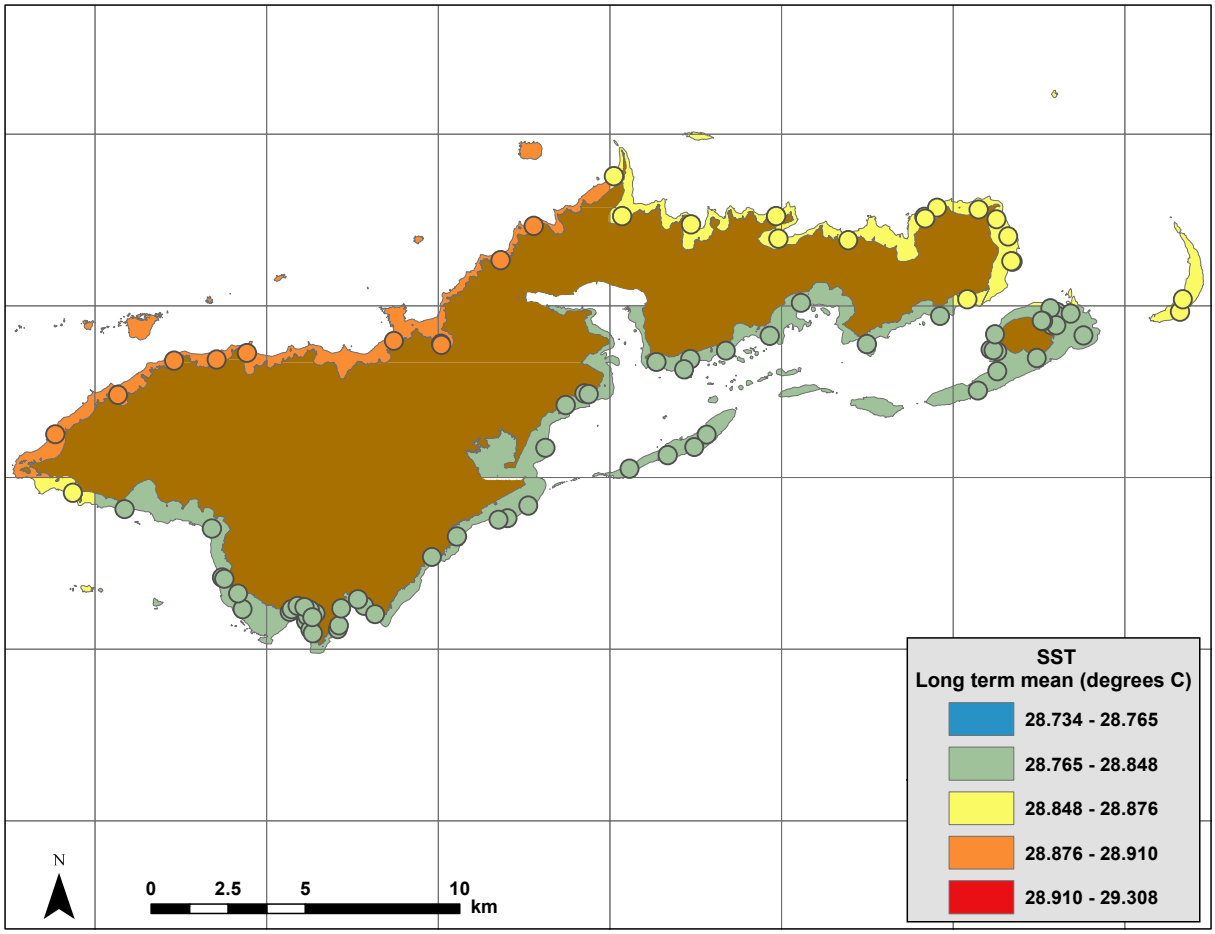

**Figure 10b**: End product showing coral REA sites with spatially joined SST temporal mean nearest neighbor values. Ofu and Olosega (top) and Tau (bottom).

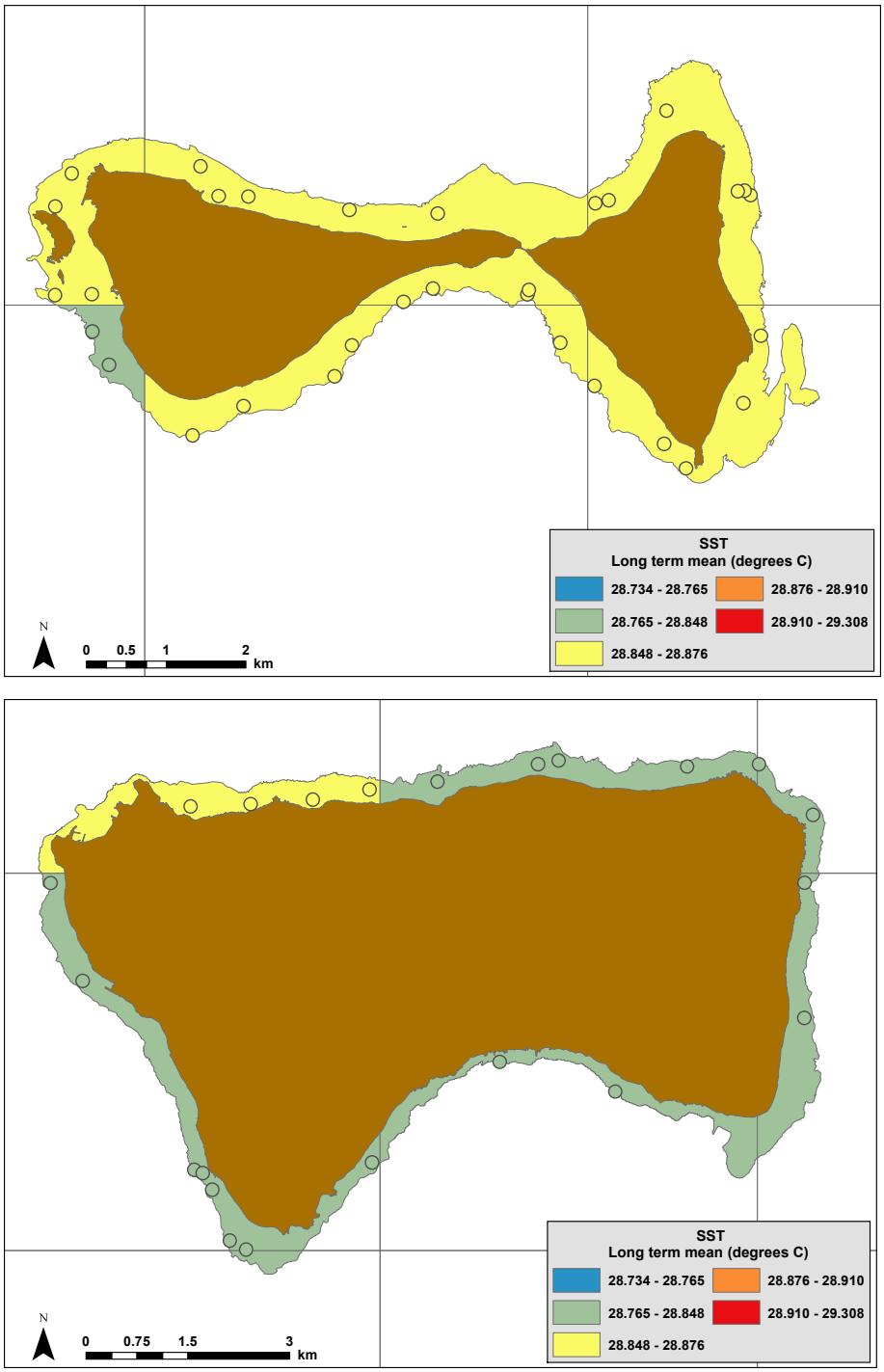

**Figure 10c**: End product showing coral REA sites with spatially joined SST temporal mean nearest neighbor values. Rose Atoll (top) and Swains (bottom).

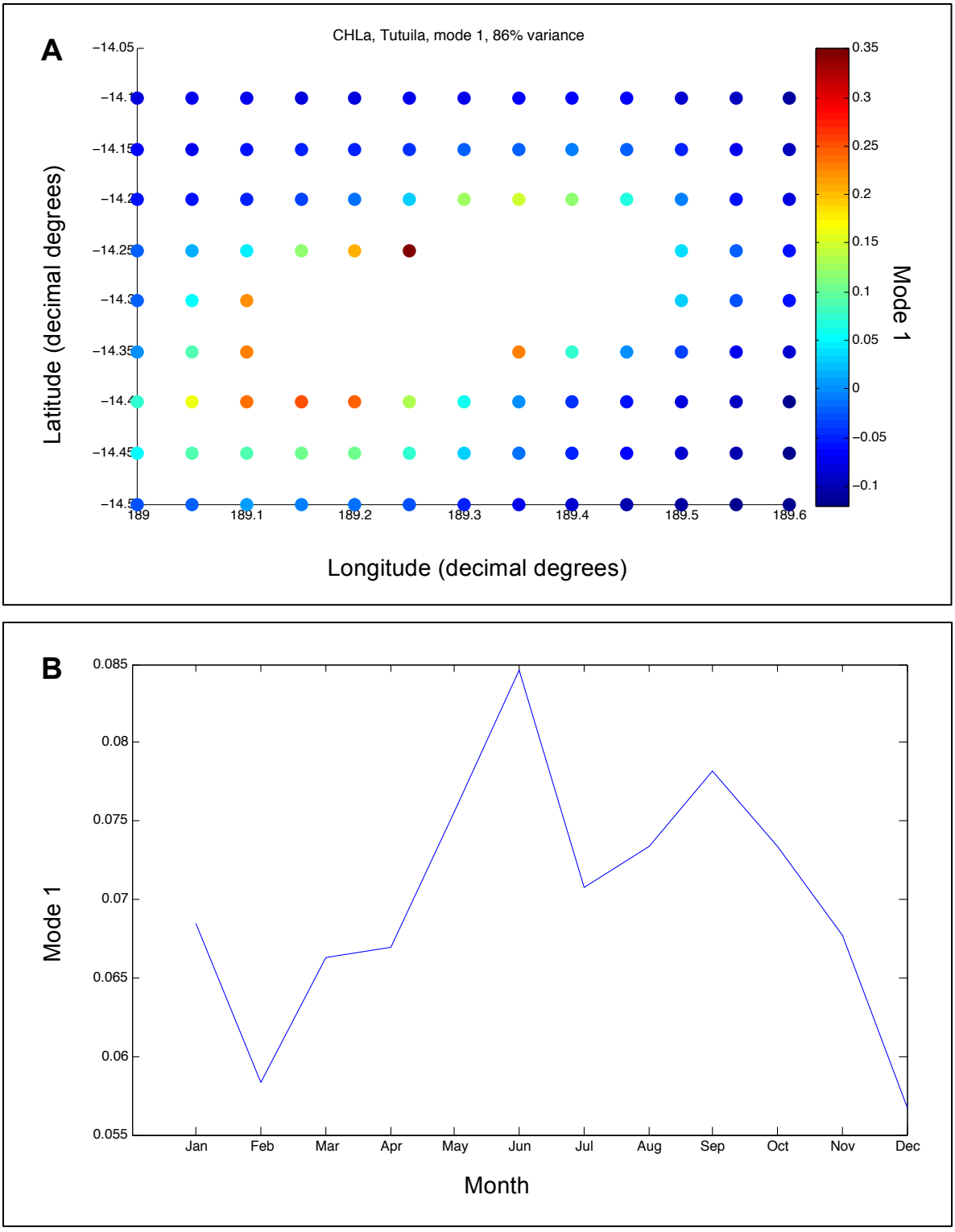


**Figure 11**: EOF analysis on chl-*a* seasonal means for each pixel around Tutuila. Eigenvectors of Mode 1 (variance explained by Mode 1 of original time series = 86%) shows how the amplitude of variations varies **A**) across space and **B**) across time.

**Figure 12a**: End product showing coral REA sites with spatially joined chl-a temporal mean nearest neighbor plus corrected nearshore-offshore gradient predicted values for Tutuila.

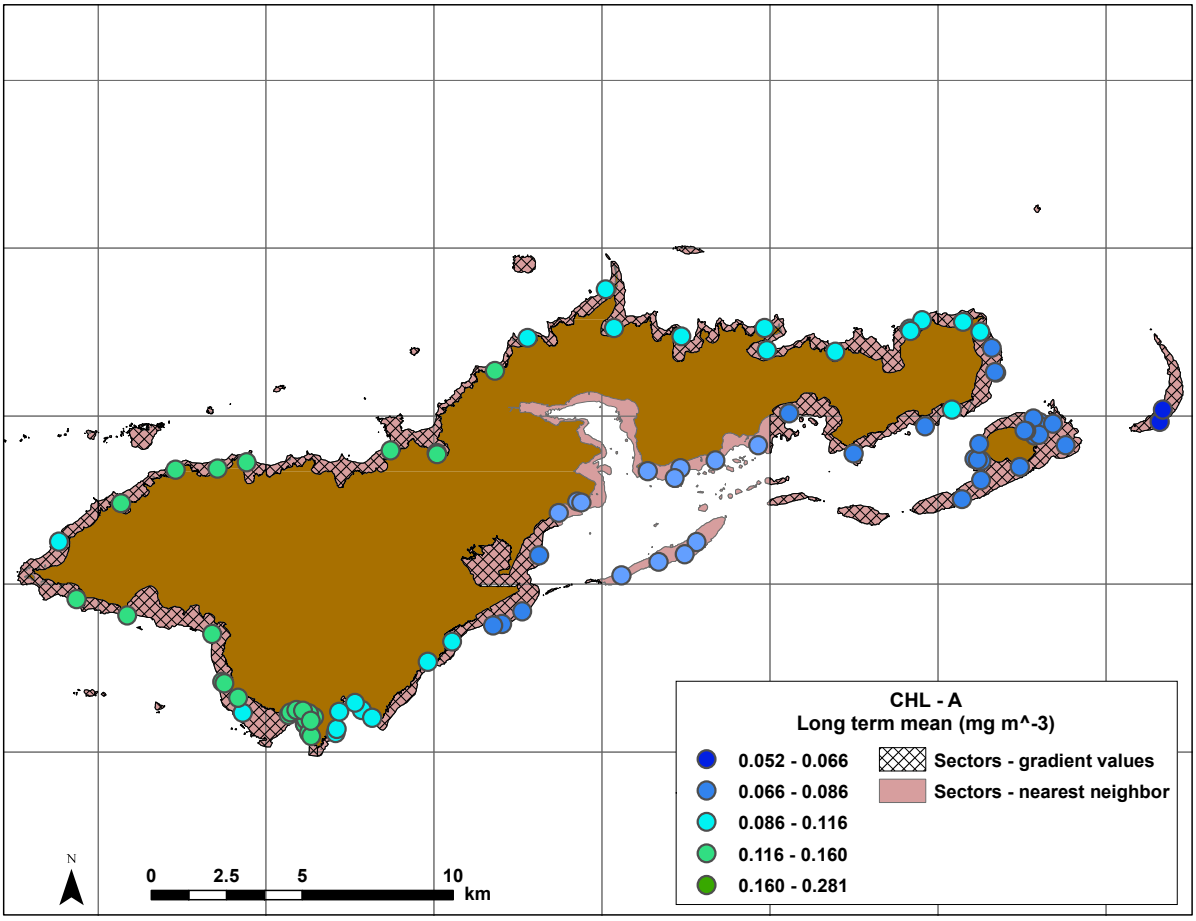

**Figure 12b**: End product showing coral REA sites with spatially joined chl-a temporal mean nearest neighbor plus corrected nearshore-offshore gradient predicted values for Ofu and Olosega (top) and Tau (bottom).

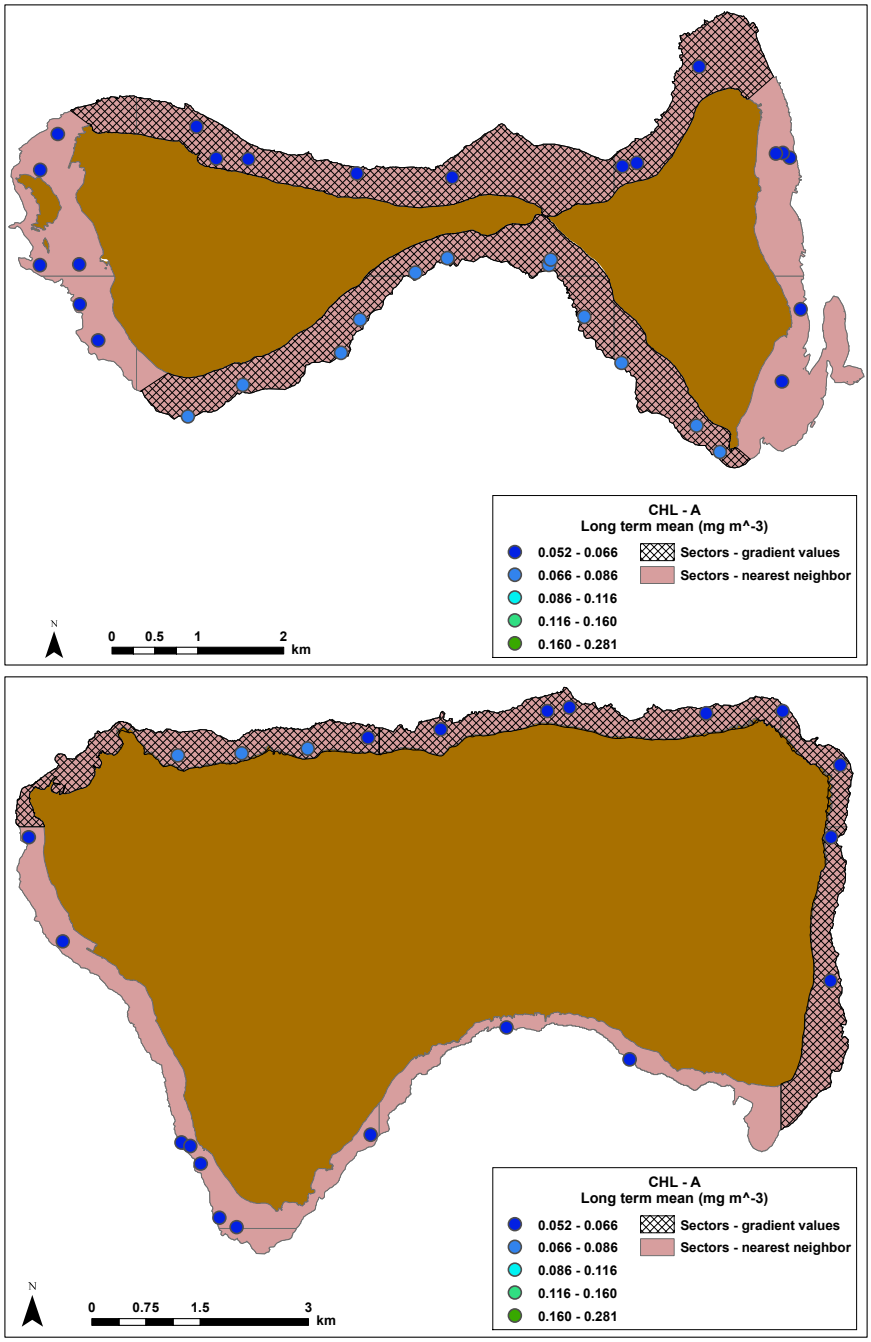

**Figure 12c**: End product showing coral REA sites with spatially joined chl-a temporal mean nearest neighbor plus corrected nearshore-offshore gradient predicted values for Rose Atoll (top) and Swains (bottom).

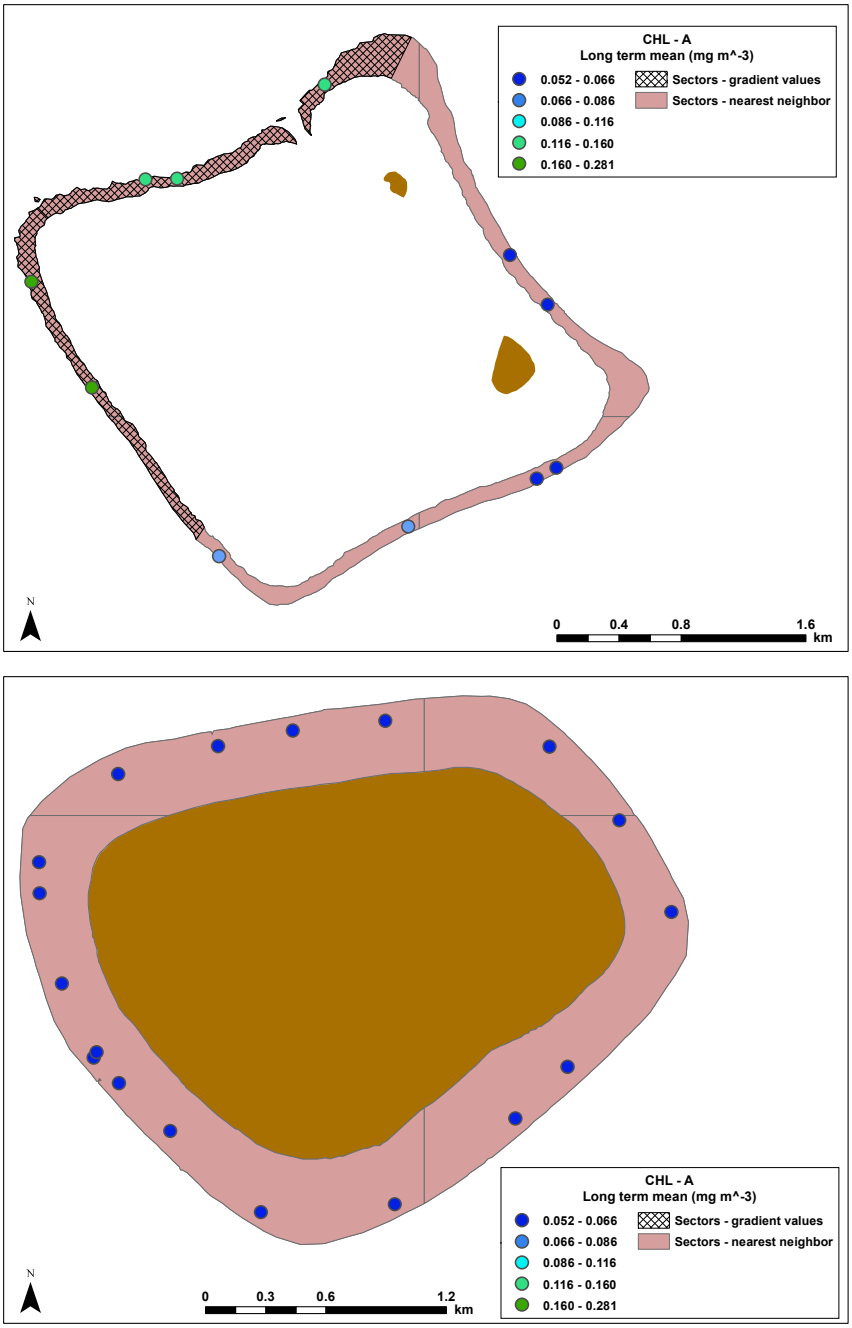

**Figure 13a**: End product showing coral REA sites with spatially joined PAR temporal mean nearest neighbor plus corrected nearshore-offshore gradient predicted values for Tutuila.

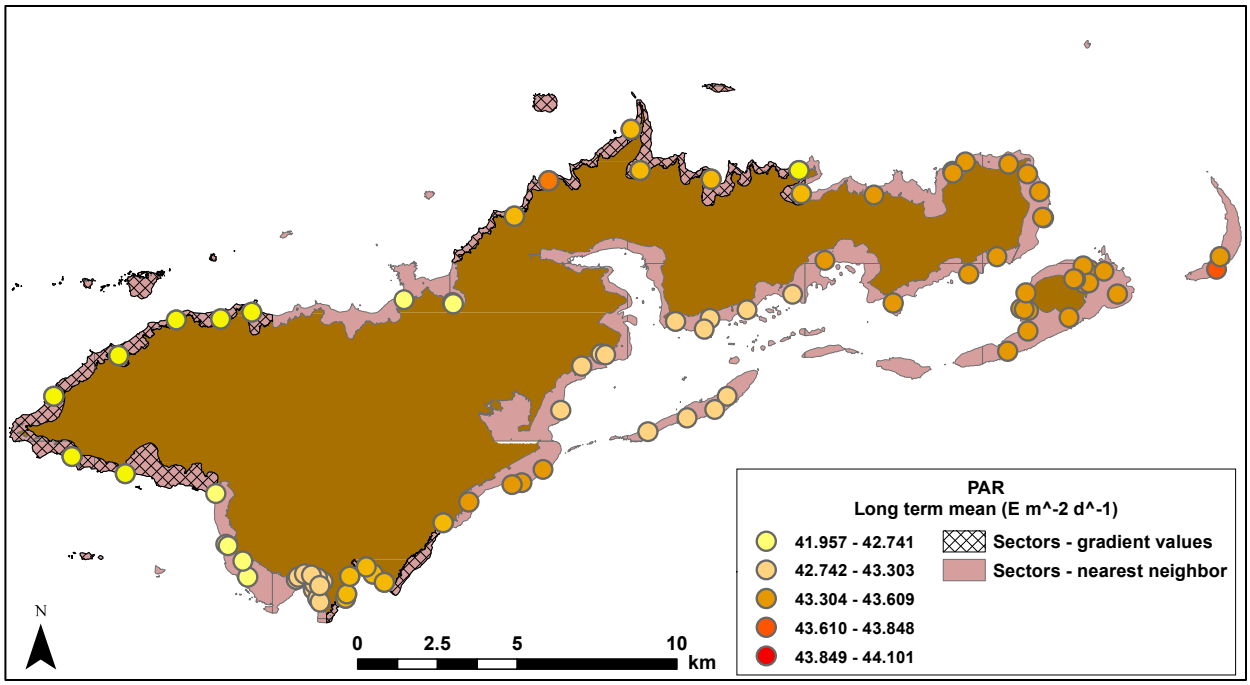

**Figure 13b**: End product showing coral REA sites with spatially joined PAR temporal mean nearest neighbor plus corrected nearshore-offshore gradient predicted values for Ofu and Olosega (top) and Tau (bottom).

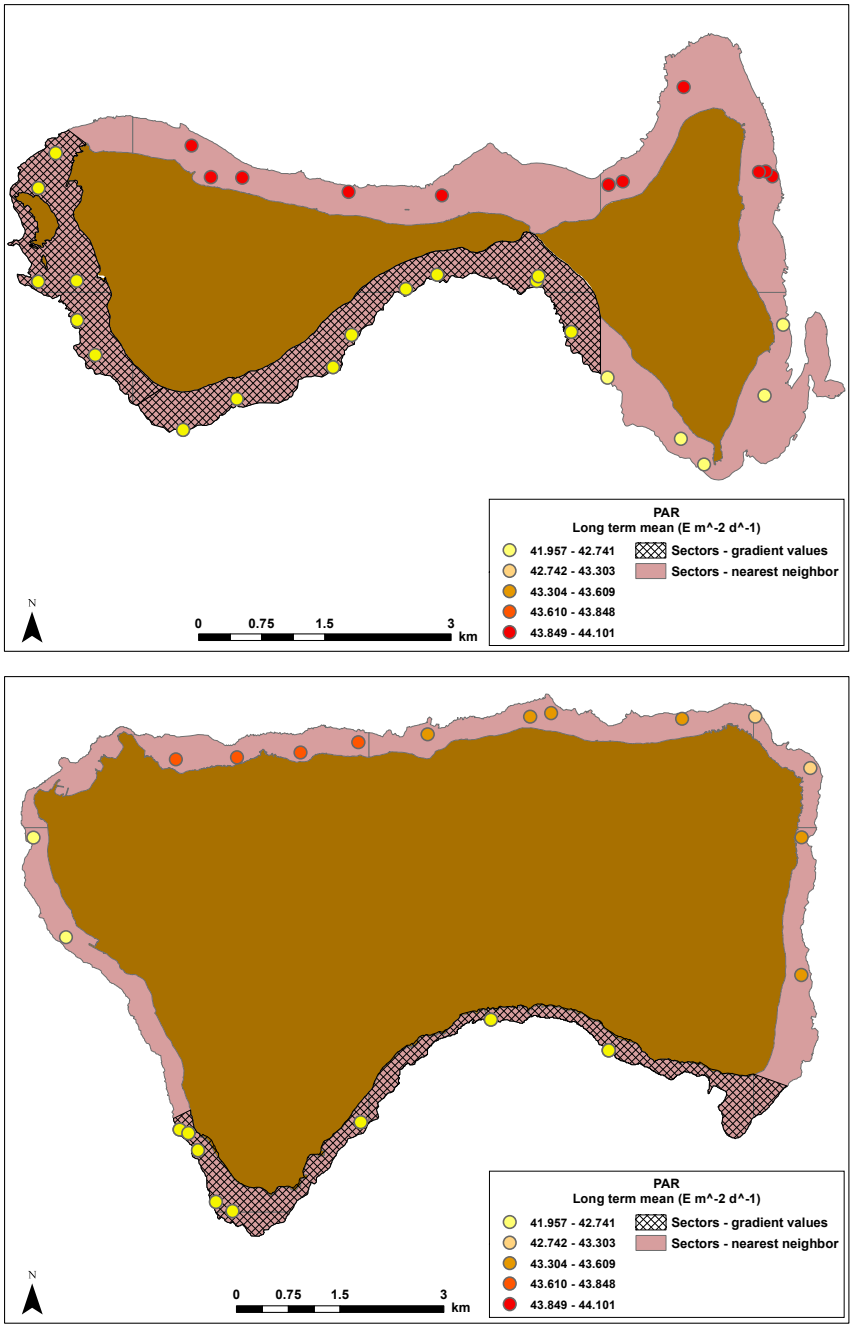

**Figure 13c**: End product showing coral REA sites with spatially joined PAR temporal mean nearest neighbor plus corrected nearshore-offshore gradient predicted values for Rose Atoll (top) and Swains (bottom).

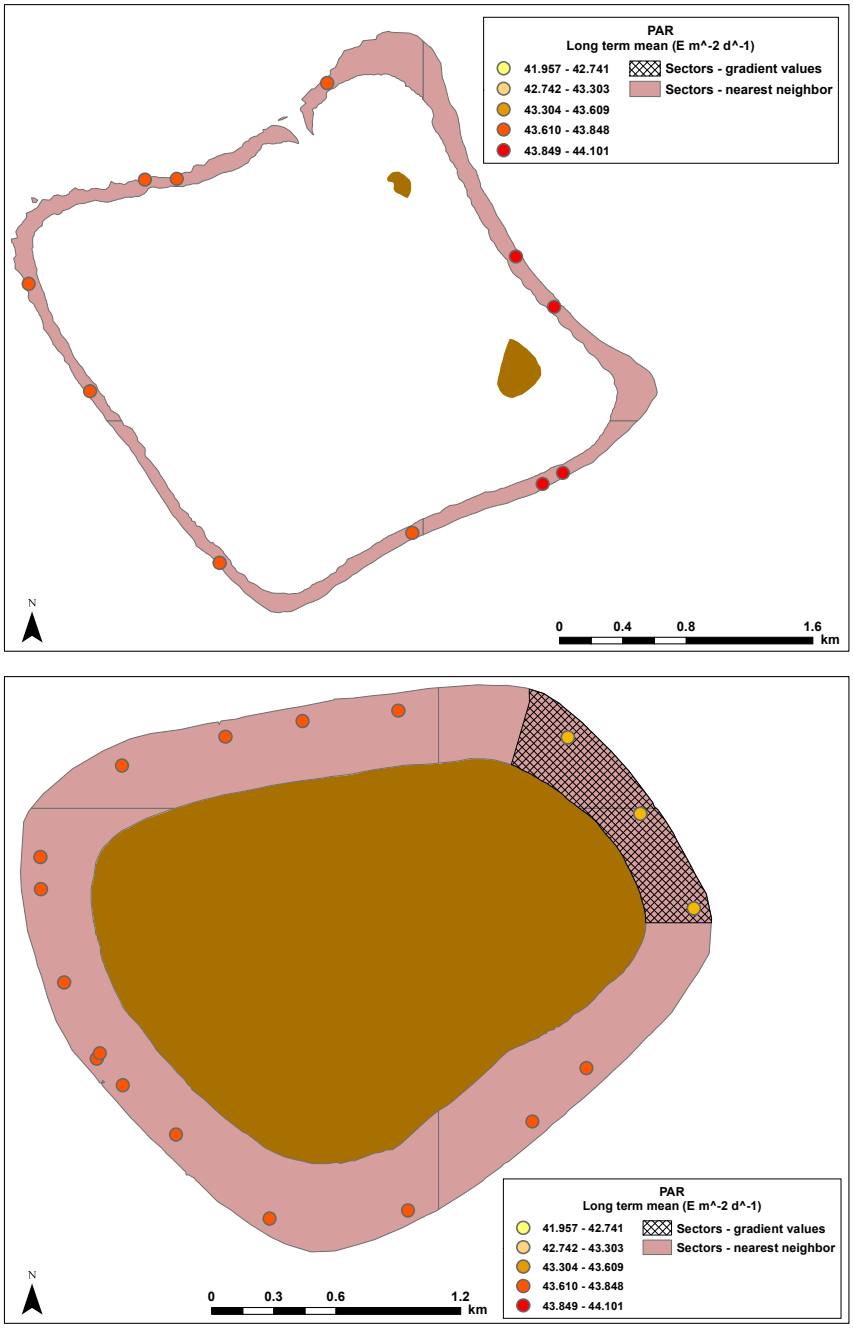

**Figure 14a**: End product showing coral REA sites with spatially joined SST temporal mean nearest neighbor plus corrected nearshore-offshore gradient predicted values for Tutuila.

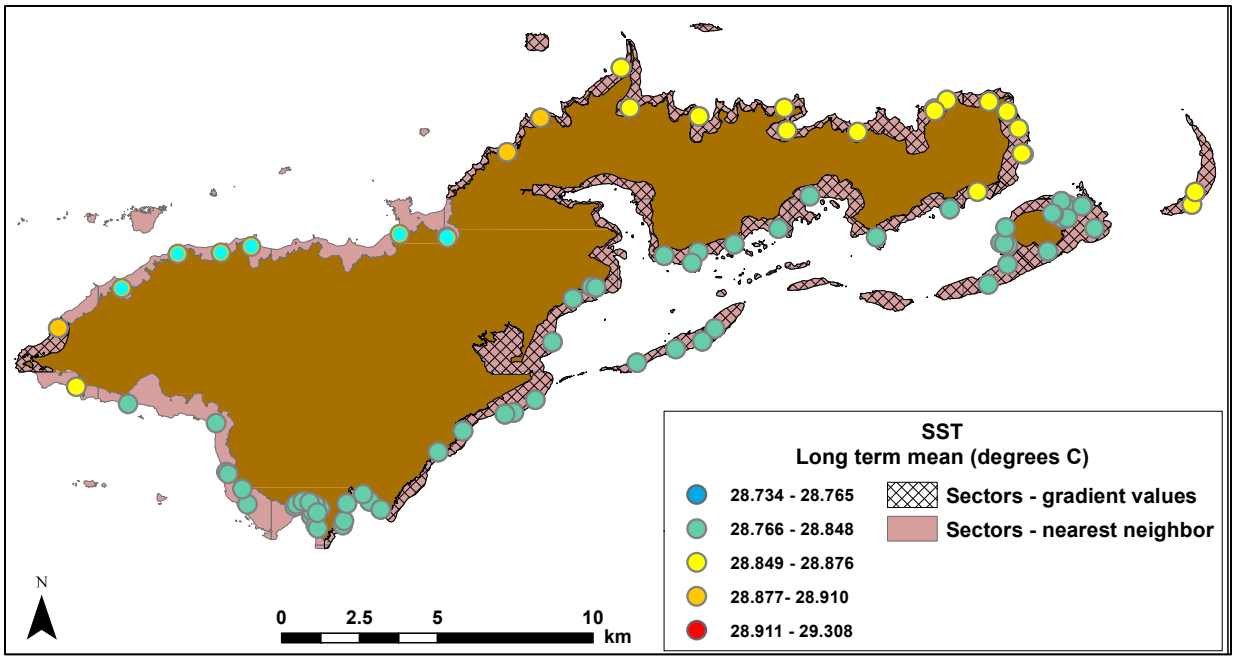

**Figure 14b**: End product showing coral REA sites with spatially joined SST temporal mean nearest neighbor plus corrected nearshore-offshore gradient predicted values for Ofu and Olosega (top) and Tau (bottom).

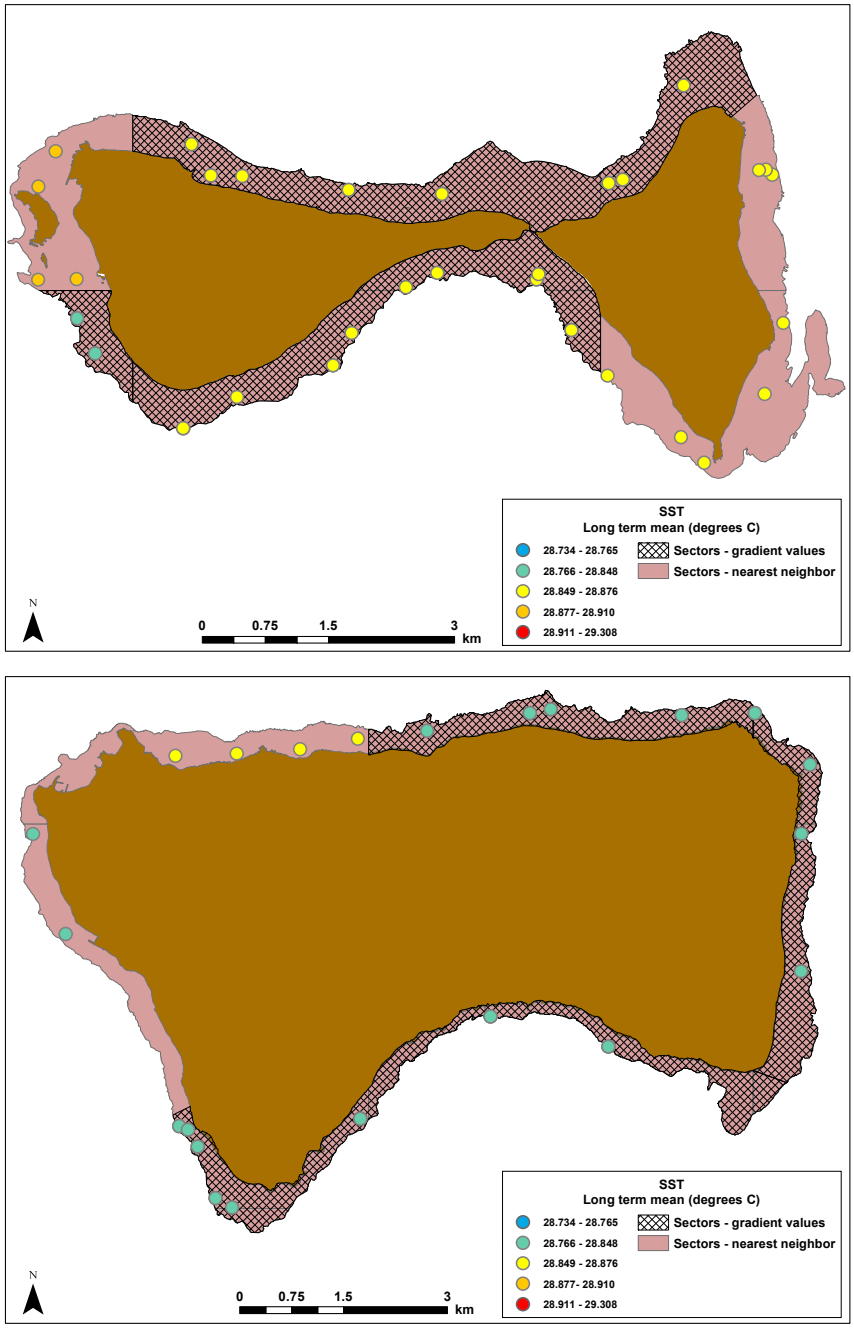

**Figure 14c**: End product showing coral REA sites with spatially joined SST temporal mean nearest neighbor plus corrected nearshore-offshore gradient predicted values for Rose Atoll (top) and Swains (bottom).

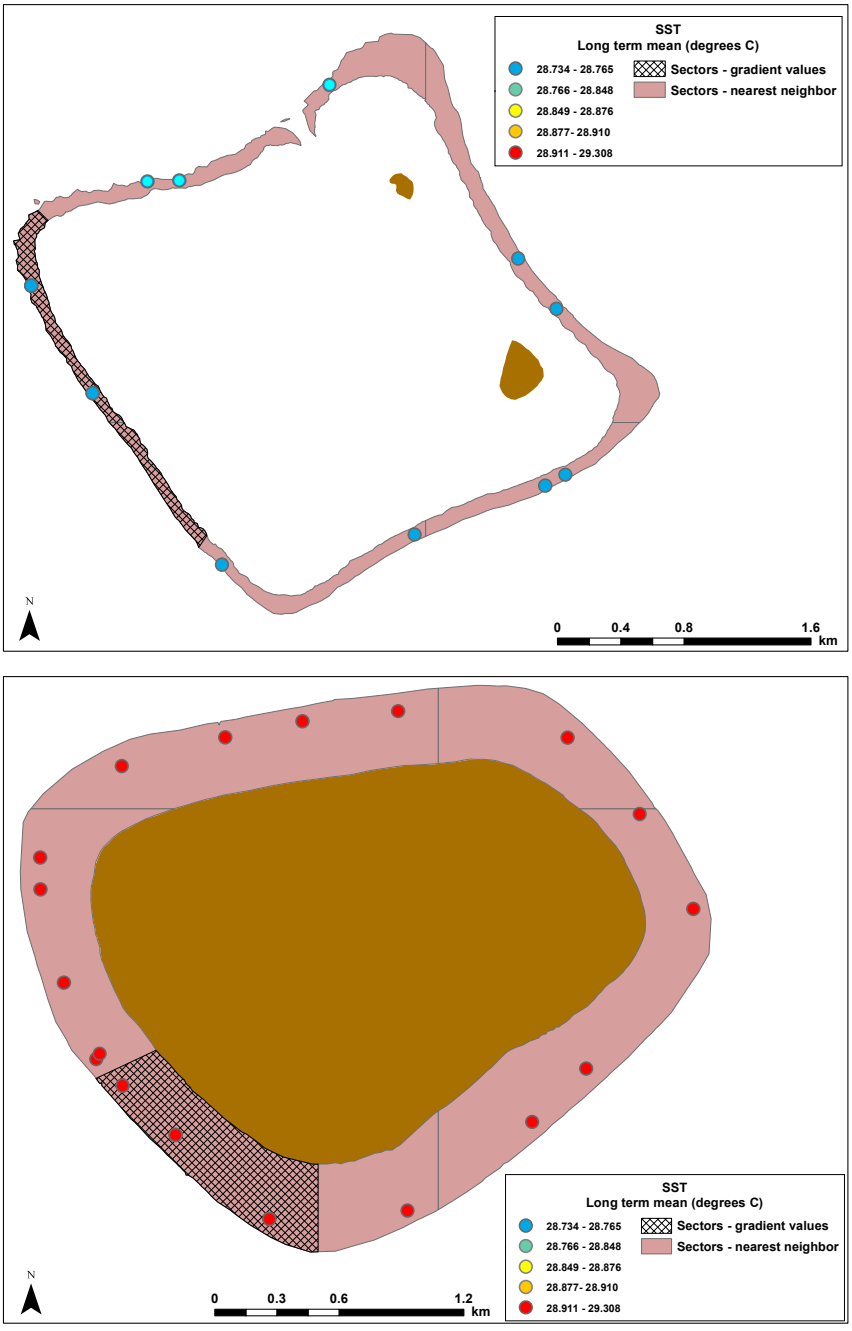

**Figure 15a**: End product showing coral REA sites with spatially joined long-term mean wave energy estimates for Tutuila.

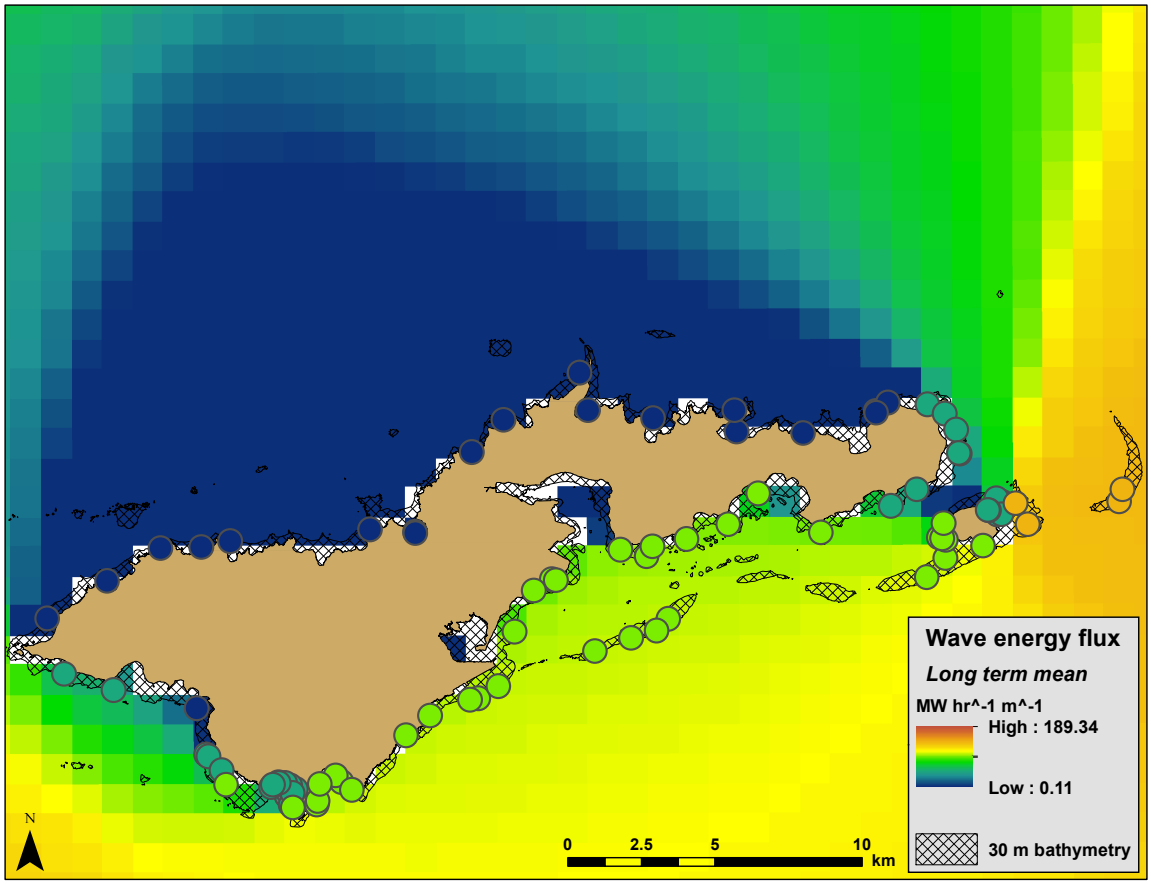

**Figure 15b**: End product showing coral REA sites with spatially joined long-term mean wave energy estimates. Ofu and Olosega (top) and Tau (bottom).

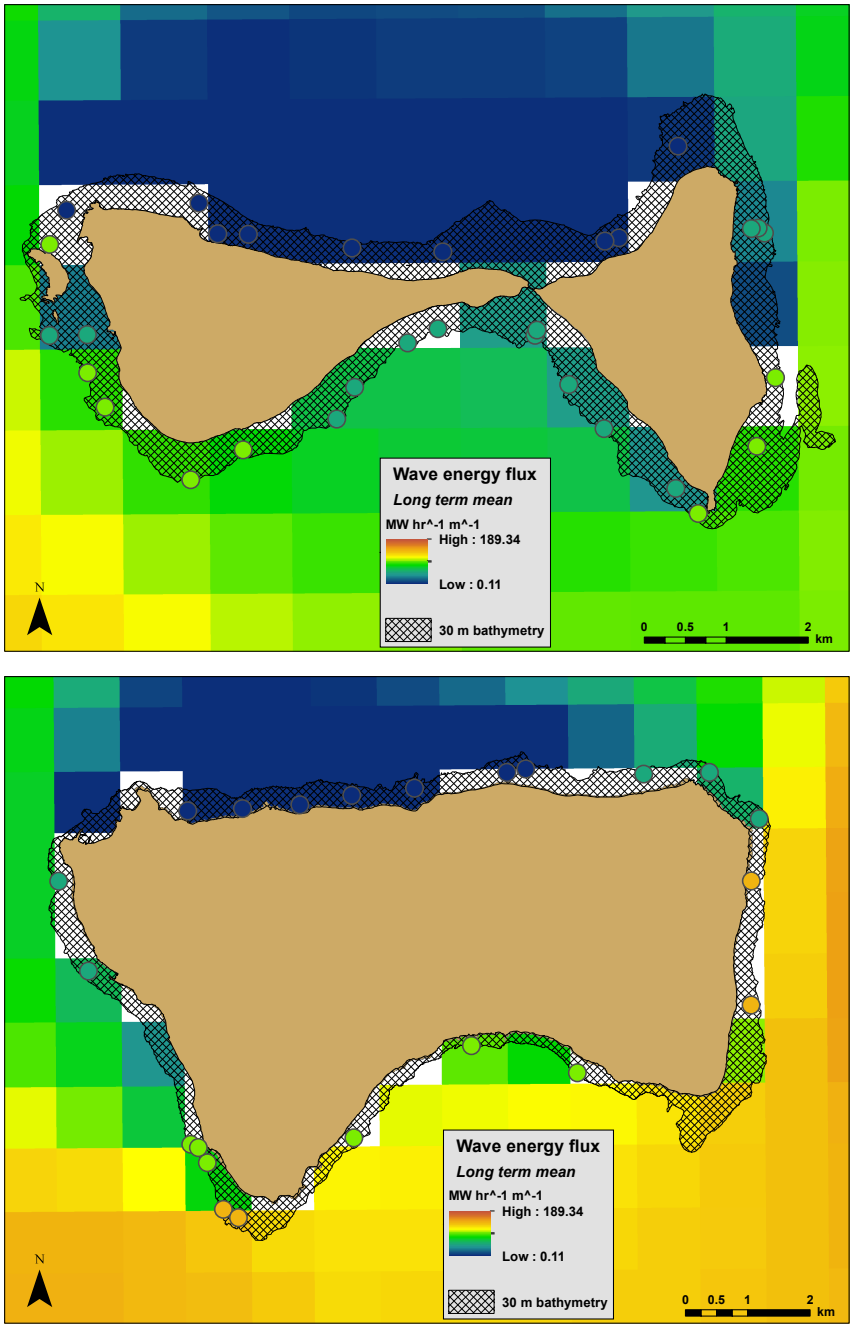

**Figure 15c**: End product showing coral REA sites with spatially joined long-term mean wave energy estimates. Rose Atoll (top) and Swains (bottom).

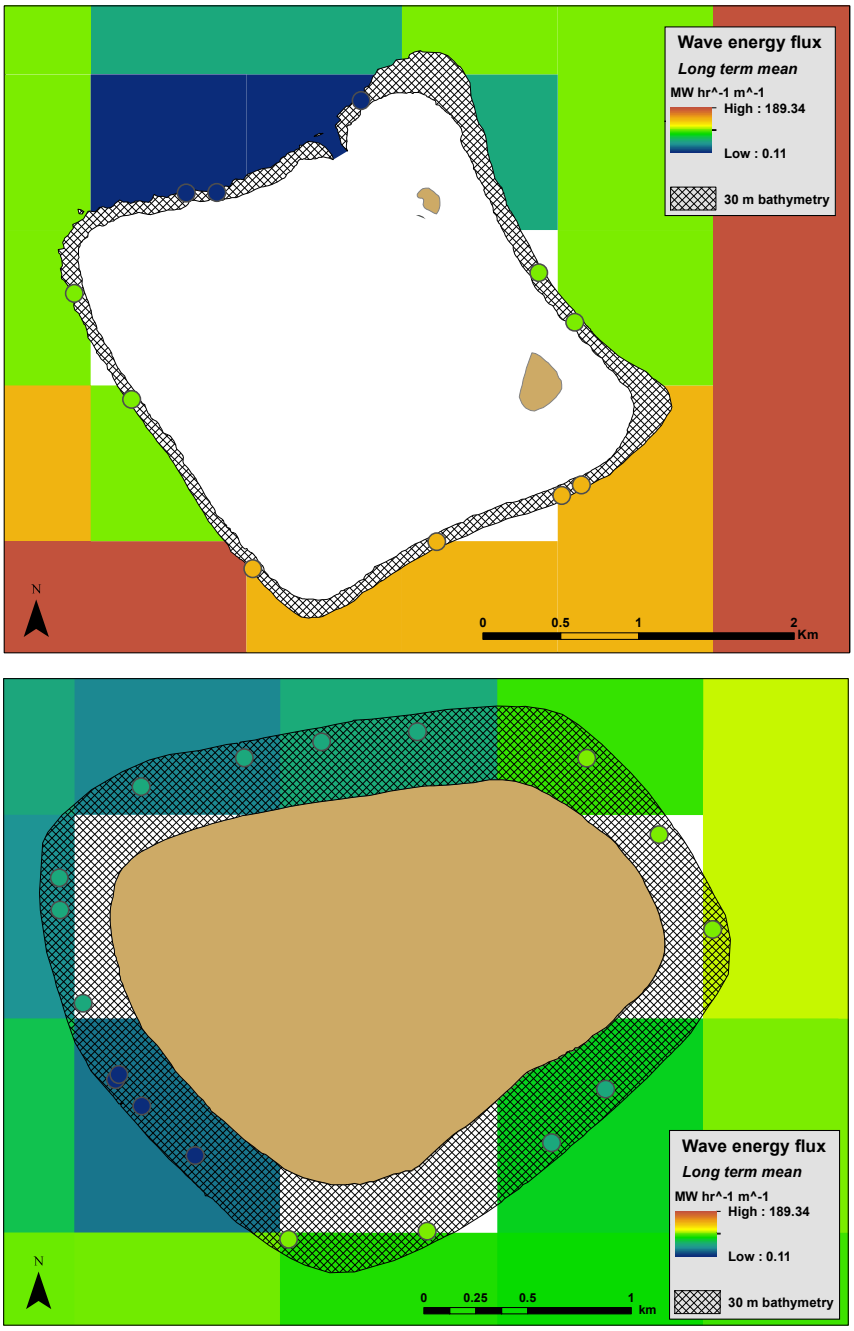

**Figure 16a**: End product showing coral REA sites with spatially joined bathymetric slope (top) and slope variability (bottom) estimates for Tutuila.

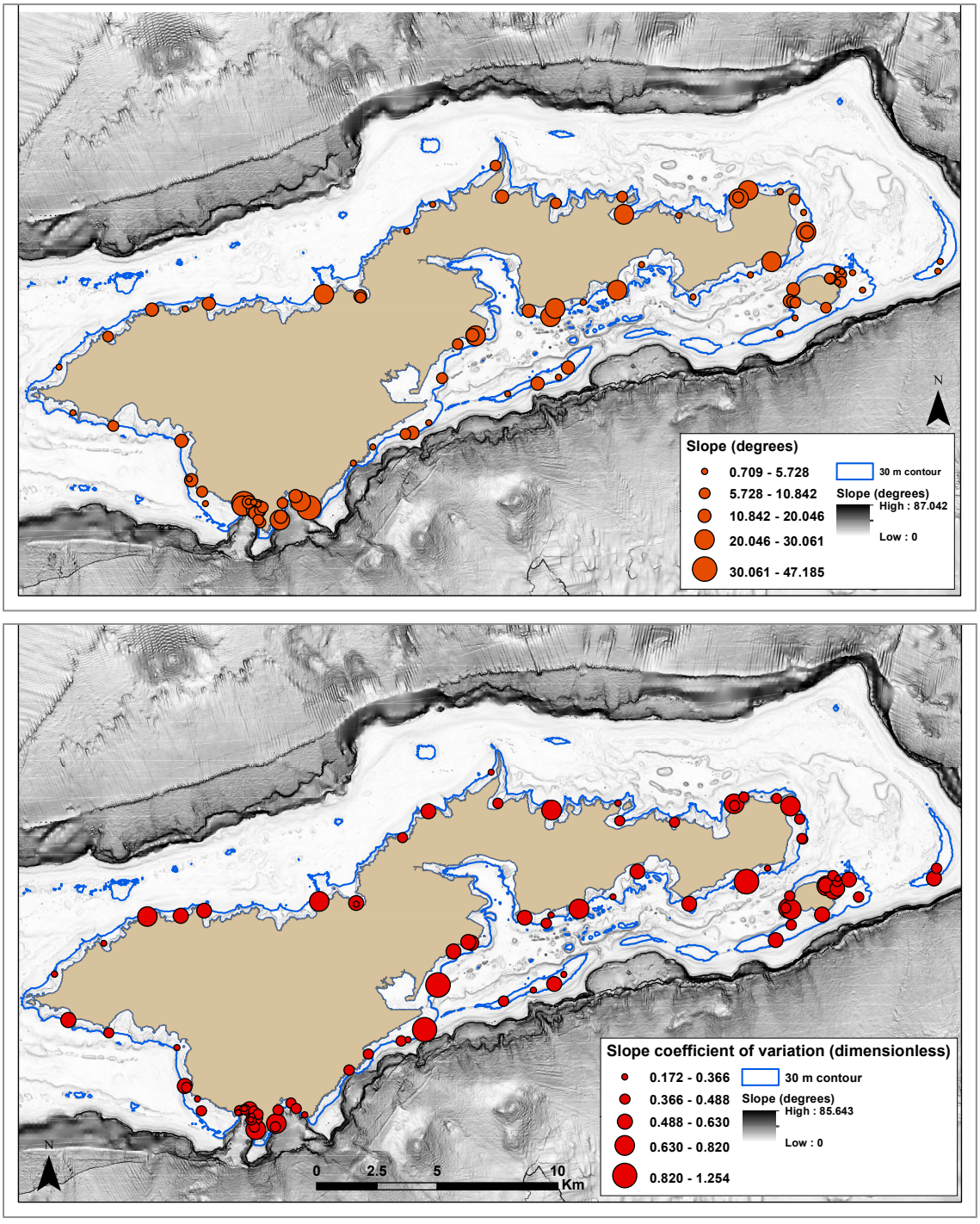

**Figure 16b**: End product showing coral REA sites with spatially joined bathymetric slope (top) and slope variability (bottom) estimates for Ofu and Olosega.

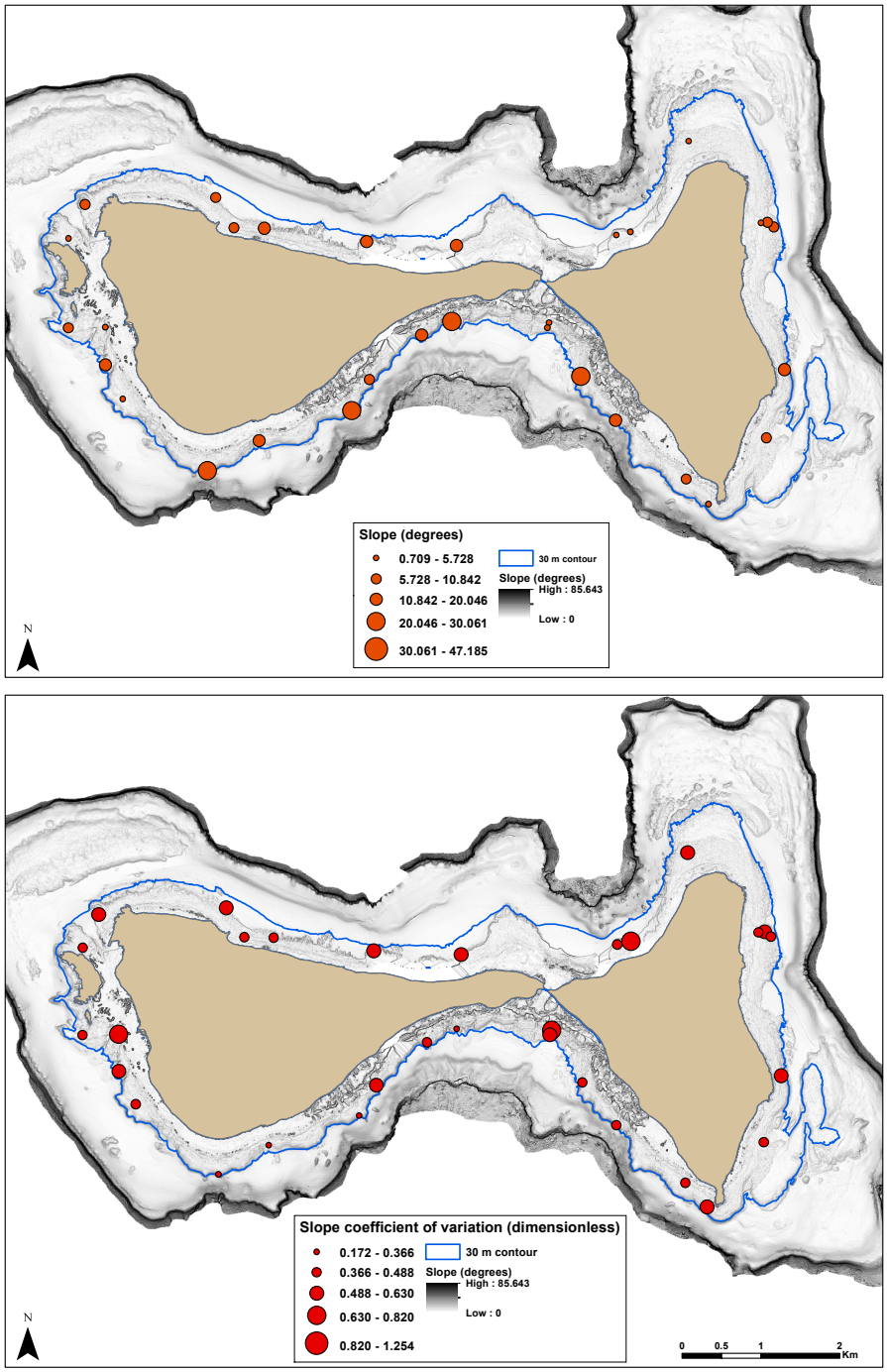

**Figure 16c**: End product showing coral REA sites with spatially joined bathymetric slope (top) and slope variability (bottom) estimates for Tau.

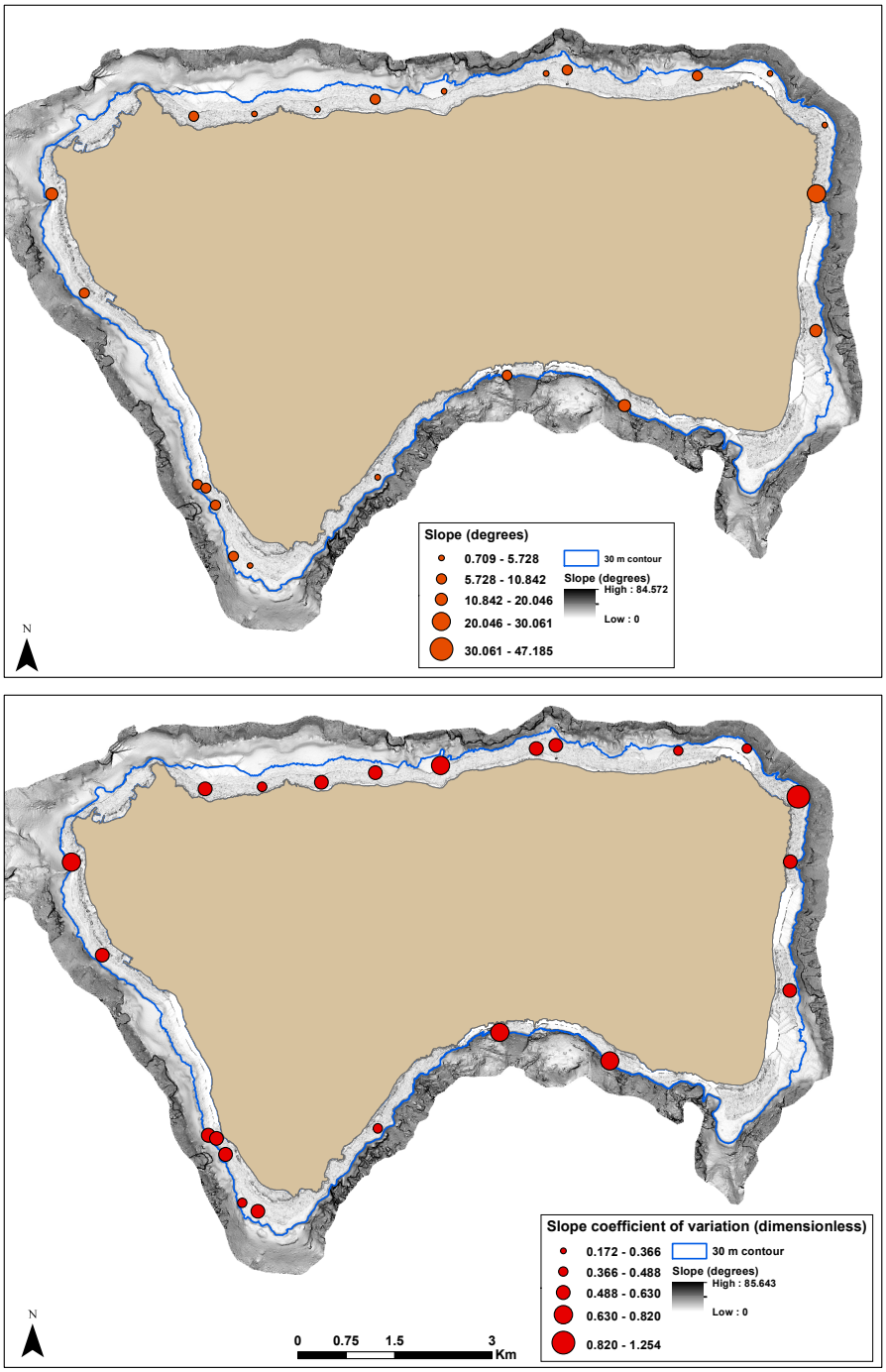

**Figure 17**: Visualization of relationship between size spectrum shape parameters and median coral colony size modeled at resolutions, **(a)** *Isopora spp.* site-level and stratum-level, and **(b)** *Montastrea curta* site-level and stratum-level. The left plot in **(a)** displays shape parameters < 10 and the right plot in **(a)** displays outliers (shape parameter > 10). The left plot in **(b)** displays shape parameters < 13 and the right plot in **(b)** displays outliers (shape parameter > 13). Linear regression lines and confidence intervals (shaded areas) were fit to data with outliers removed.

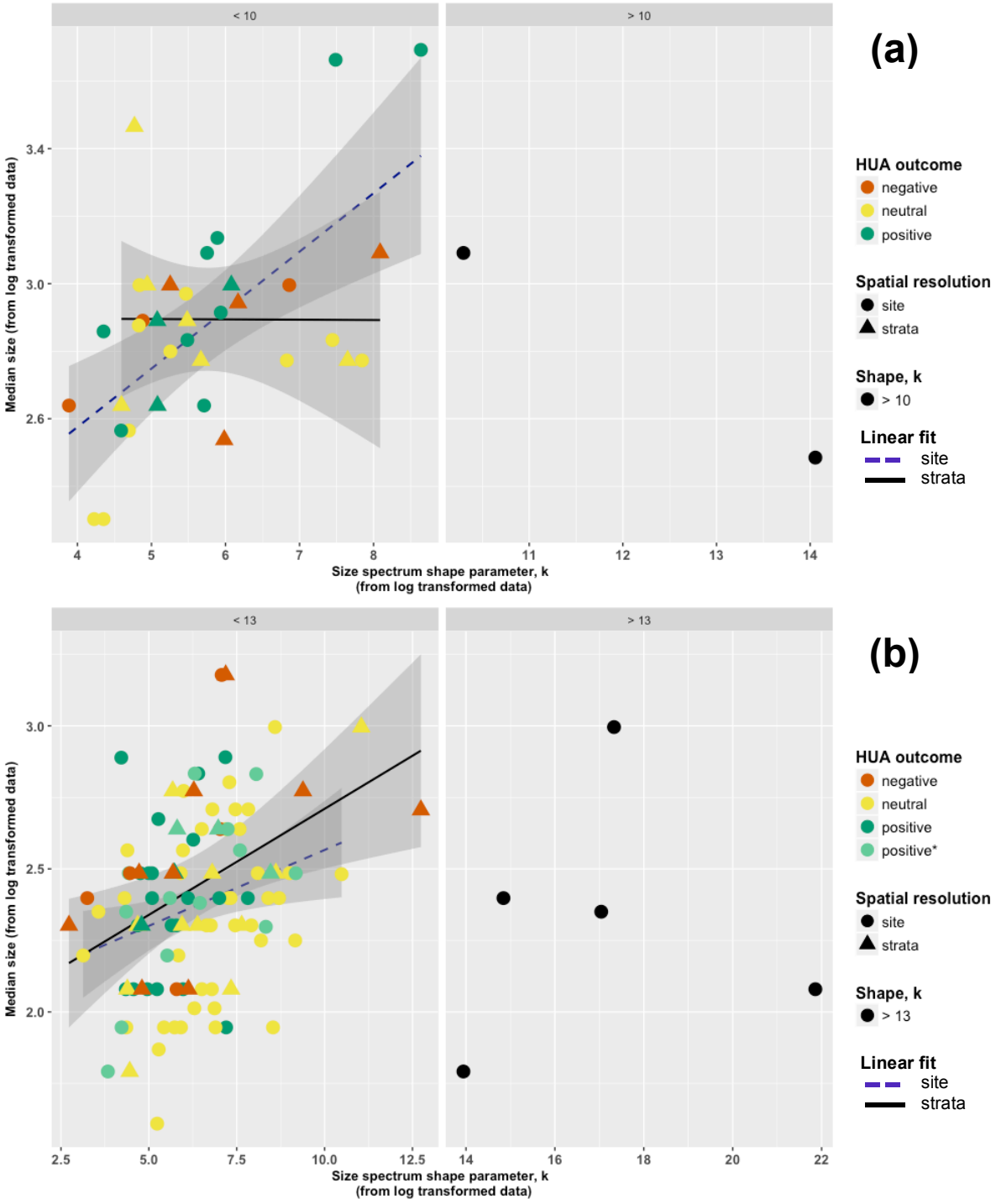

**Figure 18**: Visualization of relationship between size spectrum shape parameters and skewness modeled at resolutions, **(a)** *Isopora spp*. site-level and stratum-level, and **(b)** *Montastrea curta* site-level and stratum-level. The left plot in **(a)** displays shape parameters < 10 and the right plot in **(a)** displays outliers (shape parameter > 10). Linear regression lines and confidence intervals (shaded areas) in **(a)** were fit to data points with outliers removed.

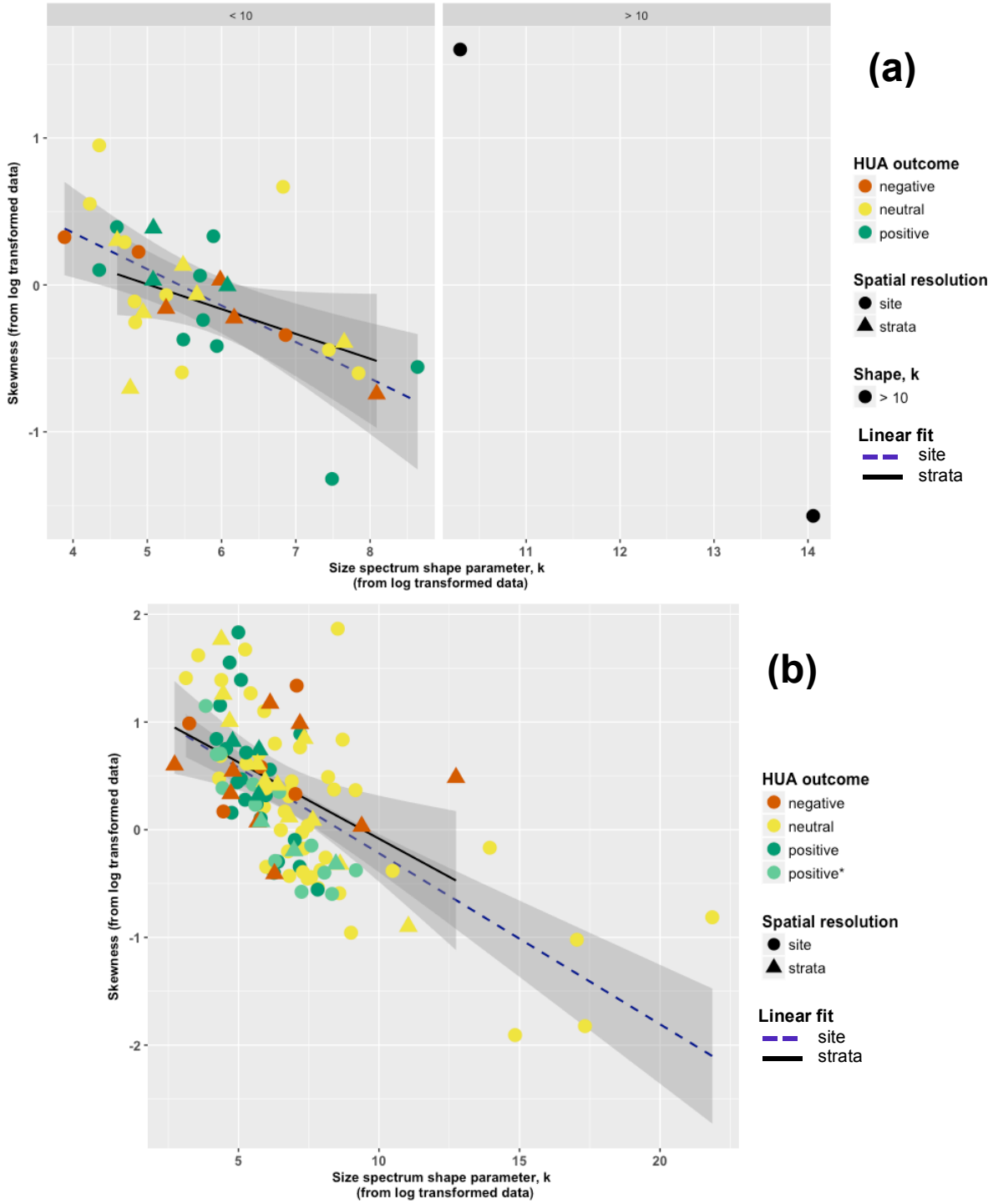

**Figure 19**: Visualization of relationship between median coral colony size and skewness modeled at resolutions, **(a)** *Isopora spp*. site-level and stratum-level, and **(b)** *Montastrea curta* site-level and stratum-level. *Isopora spp*. outliers in **(a)** are identified as shape parameters > 10. Linear regression lines and confidence intervals (shaded areas) in **(a)** were fit to data with outliers removed.

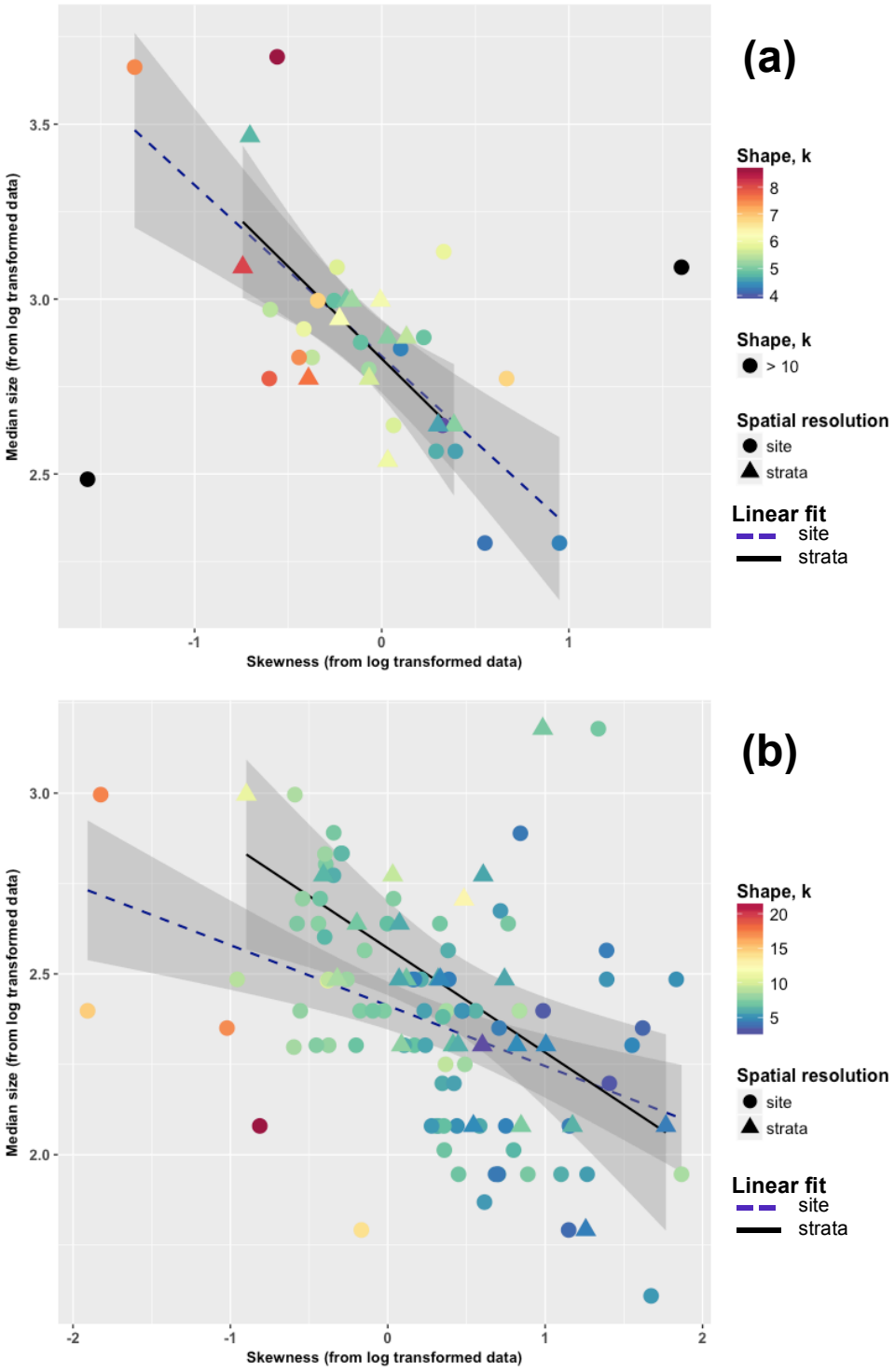

**Figure 20**: Predictor variables in relation to the response variable, shape parameter *k*, for the *Isopora spp*. site-specific best-fit model. Shaded areas show 95% confidence intervals.

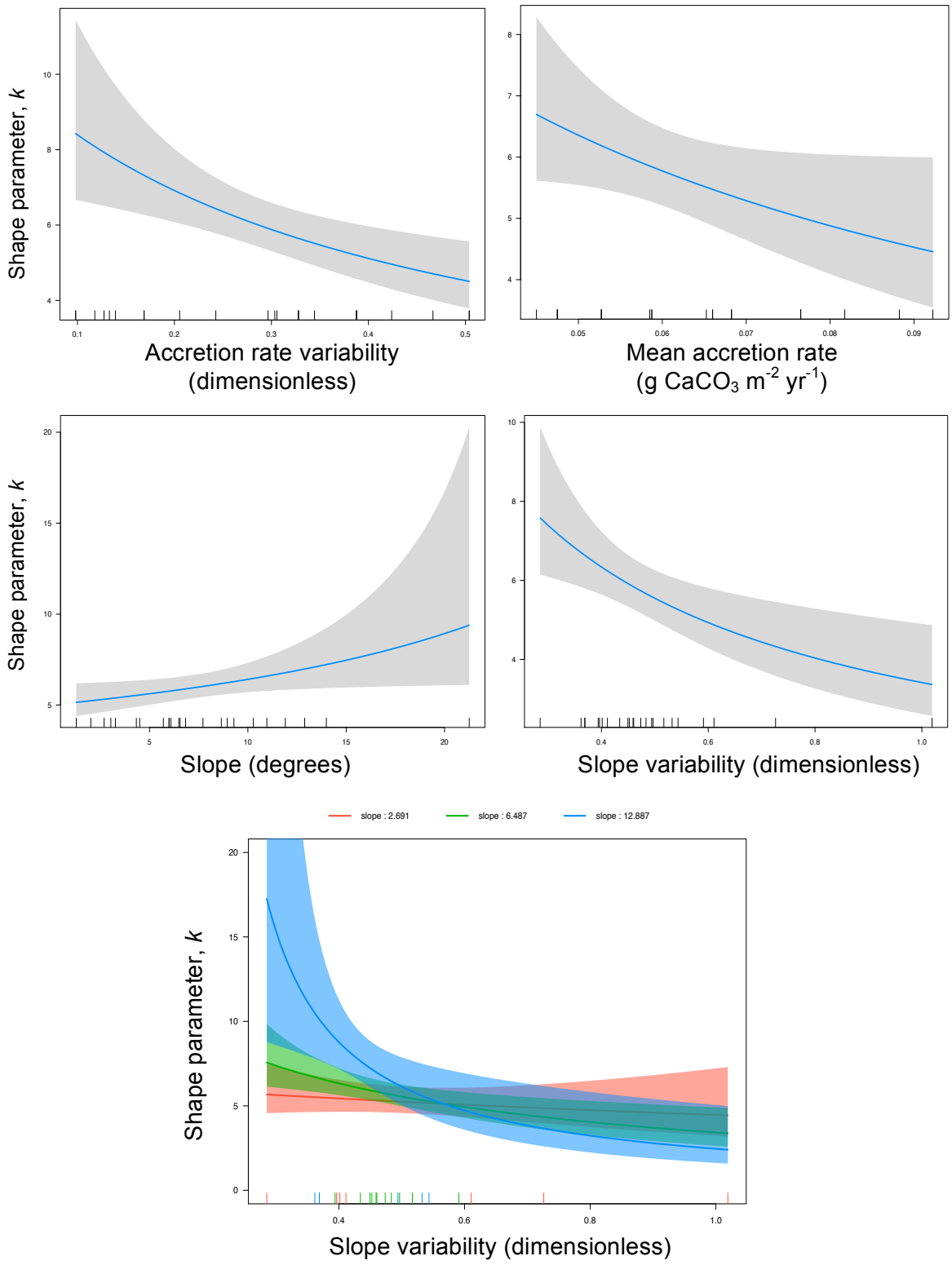

**Figure 21**: Predictor variables in relation to the response variable, shape parameter *k*, for the *Montastrea curta* site-specific best-fit model. Shaded areas show 95% confidence intervals.

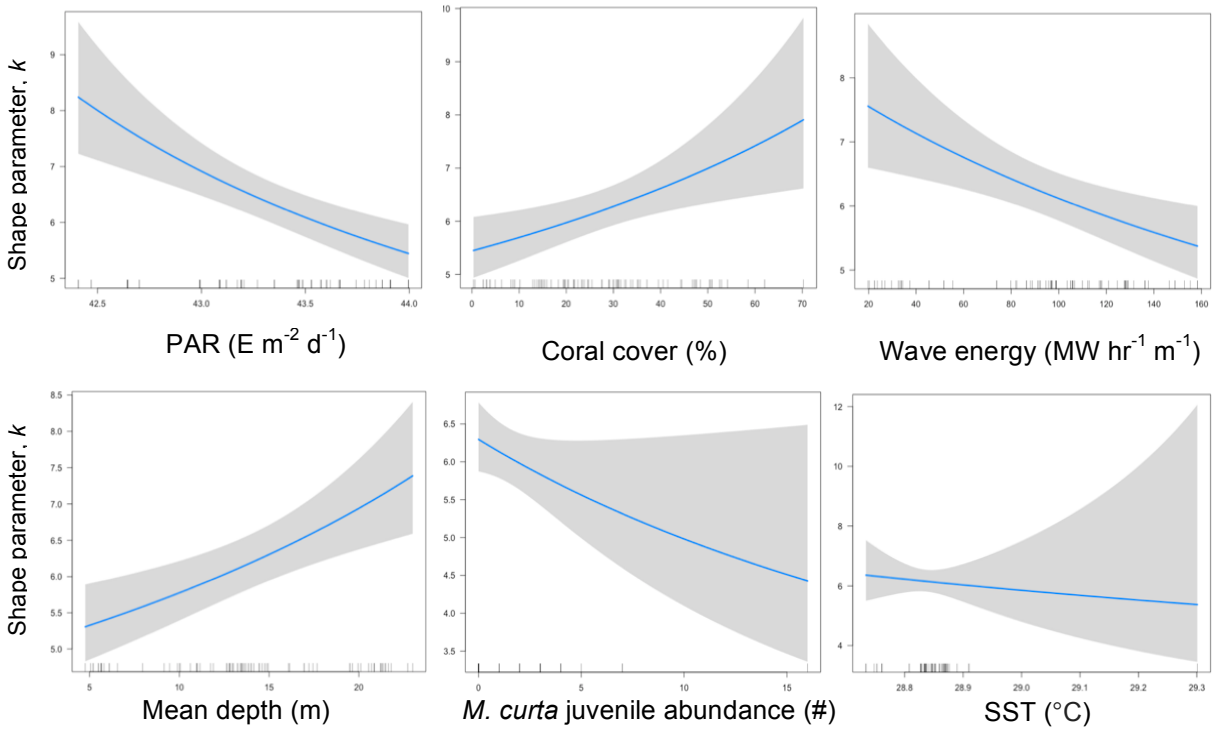


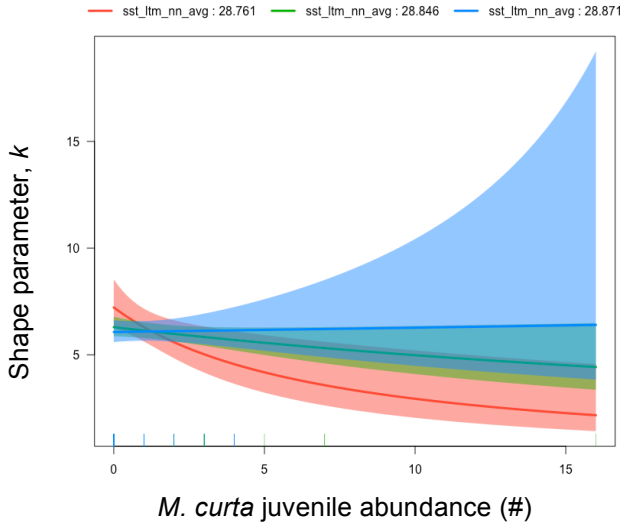

**Figure 22**: Predictor variables in relation to the response variable, shape parameter *k*, for the *Isopora spp*. stratum-level best-fit model. Shaded areas show 95% confidence intervals.

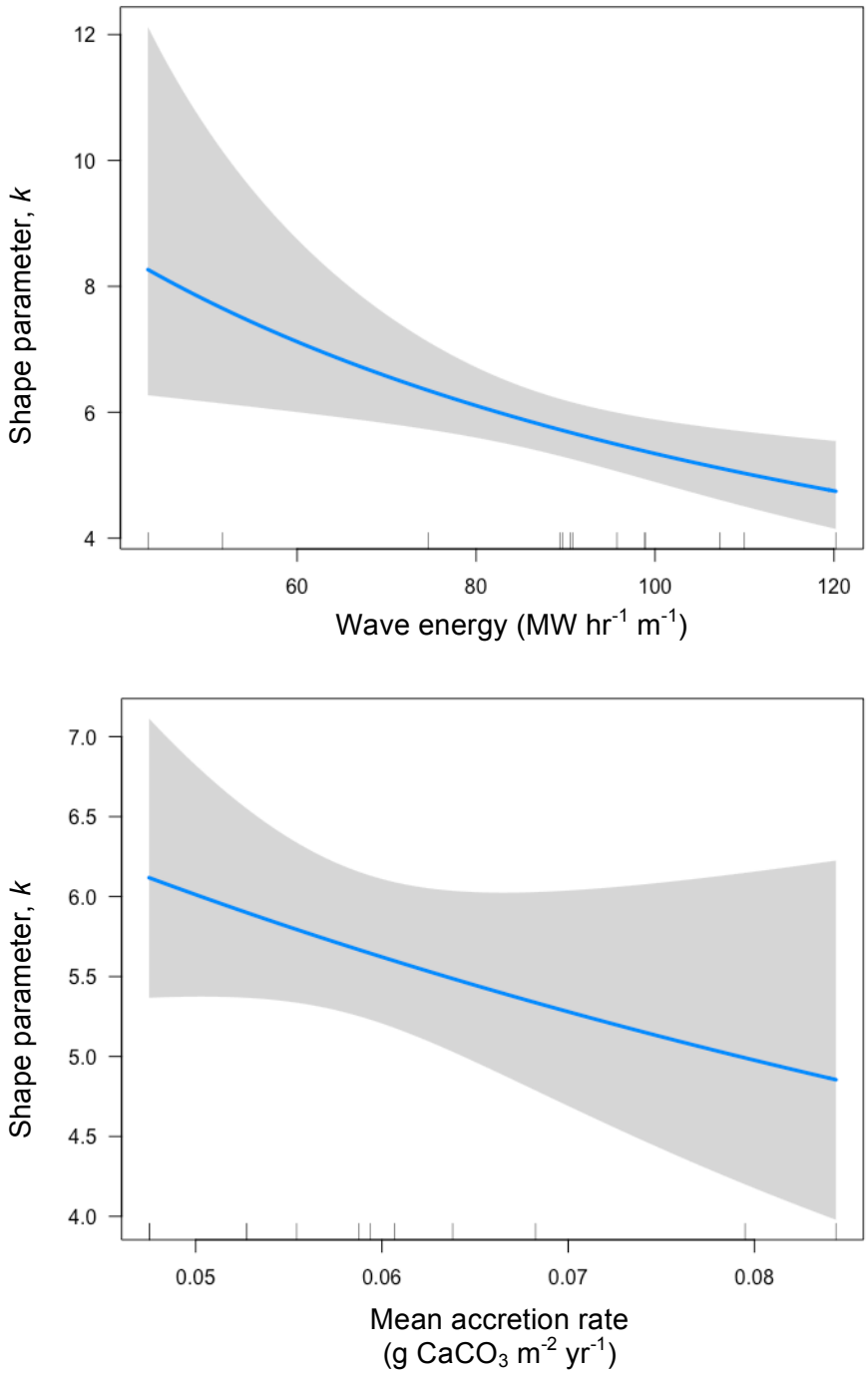

**Figure 23**: Predictor variables in relation to the response variable, shape parameter *k*, for the *Montastrea curta* stratum-level best-fit model. Shaded areas show 95% confidence intervals.

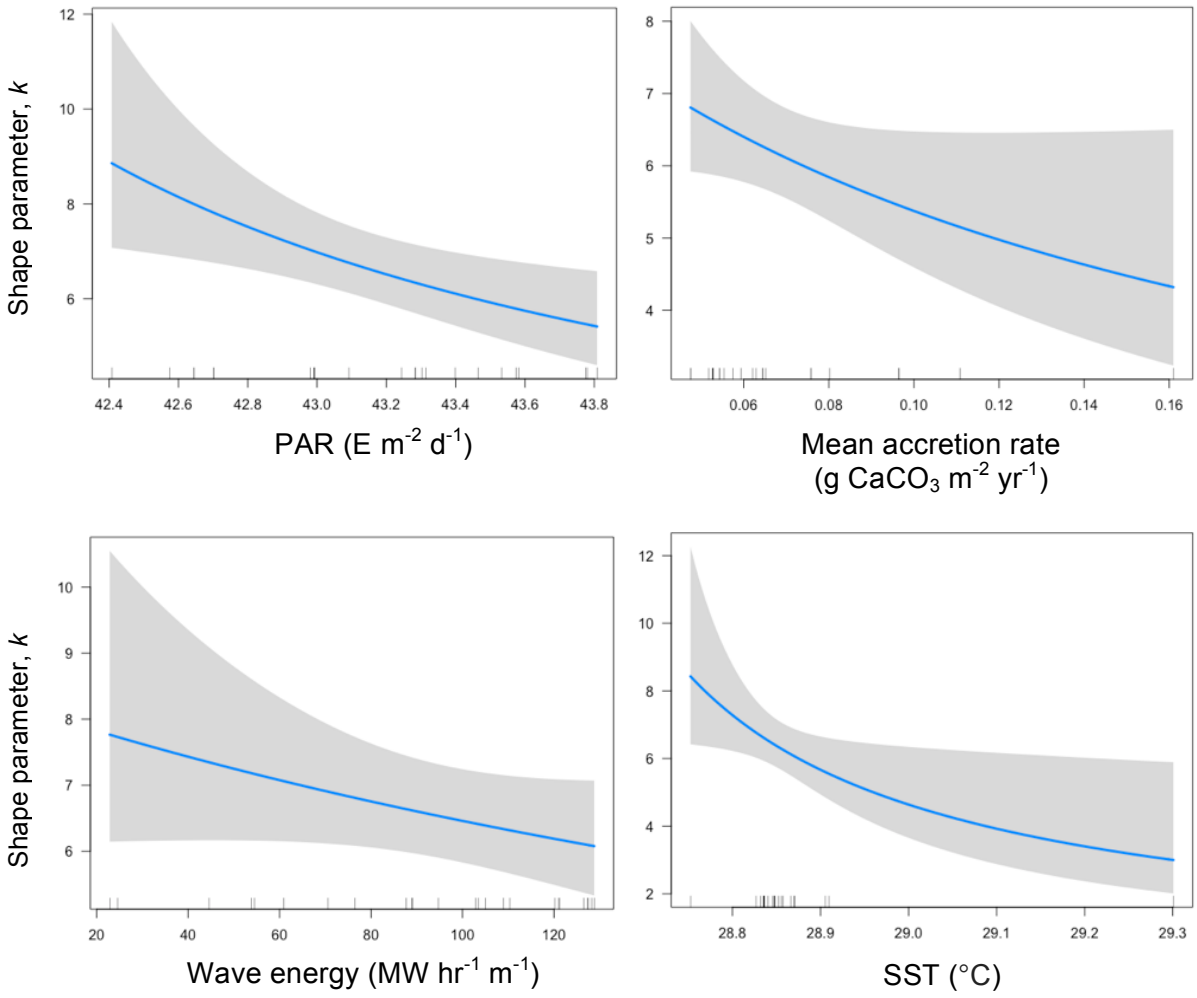

**Figure 24**: Strata outcome results with respective shape parameter estimates for *Isopora spp.* (top) and *M. curta* (bottom). Black dotted lines indicate Domain level shape parameter estimates.

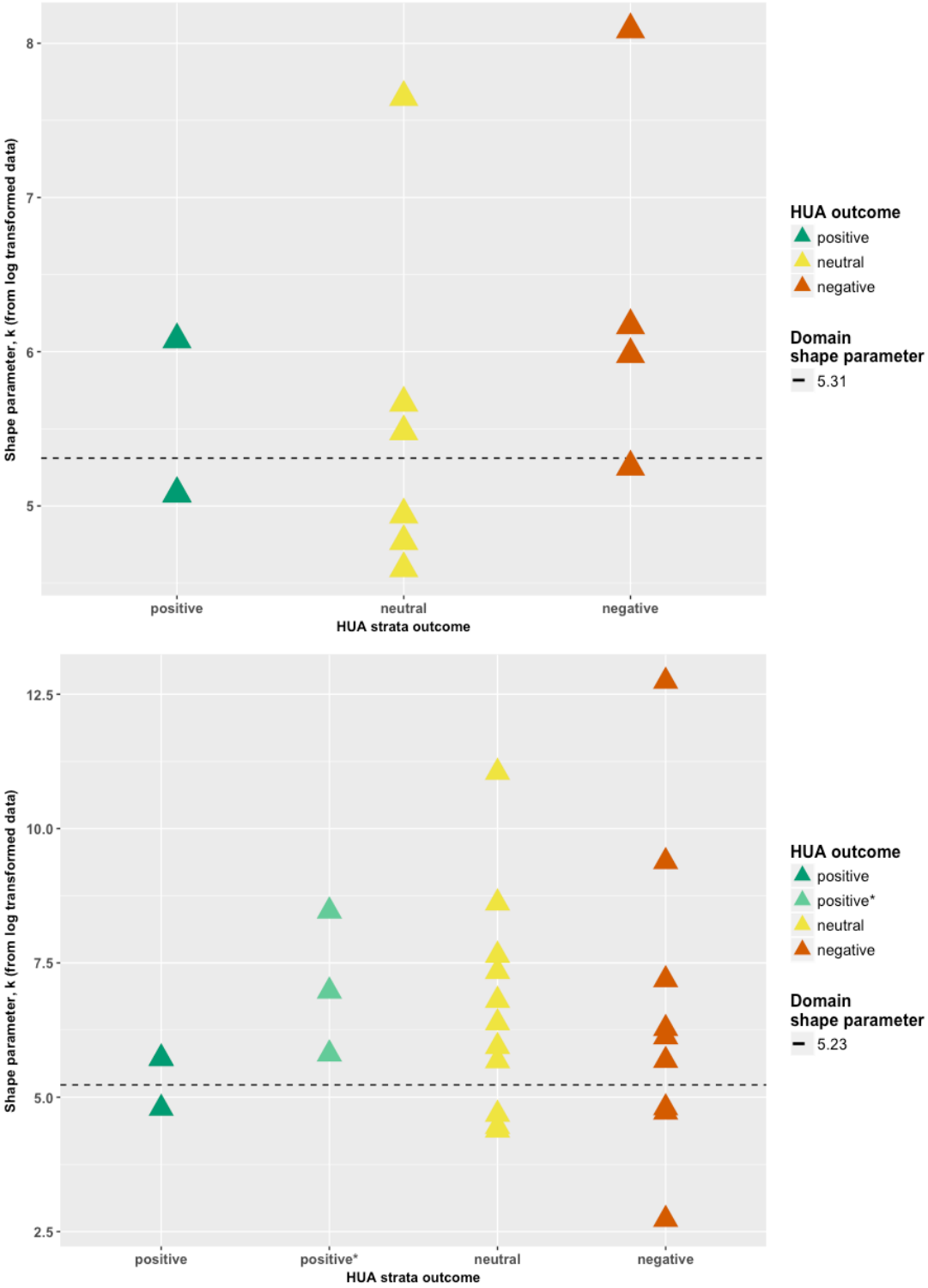

**Figure 25a**: Mean carbonate accretion rate (top) and carbonate accretion variability (bottom) plotted for all benthic REA sites on Tutuila.

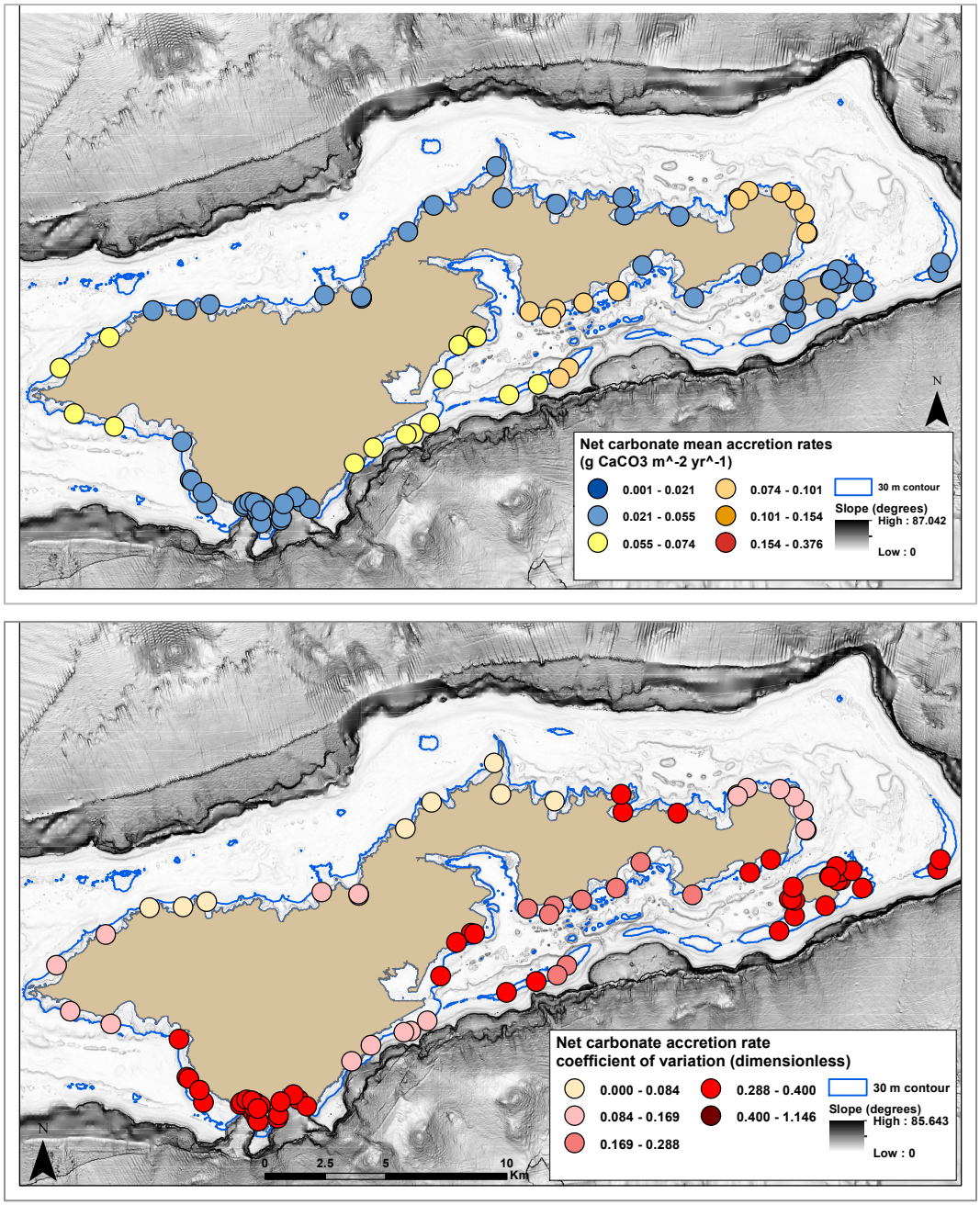

**Figure 25b**: Mean carbonate accretion rate (top) and carbonate accretion variability (bottom) plotted for all benthic REA sites on Ofu and Olosega.

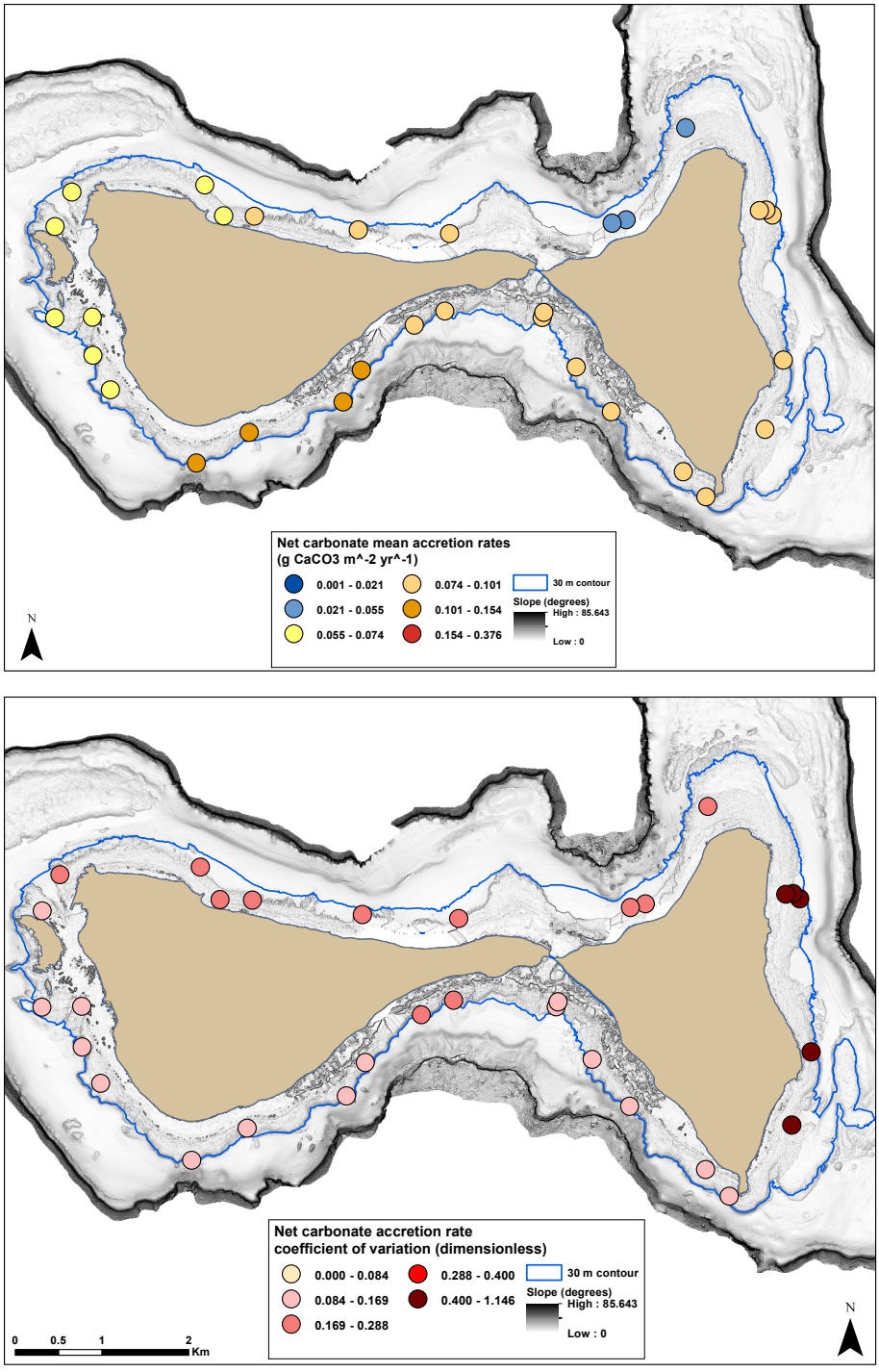

**Figure 25c**: Mean carbonate accretion rate (top) and carbonate accretion variability (bottom) plotted for all benthic REA sites on Tau.

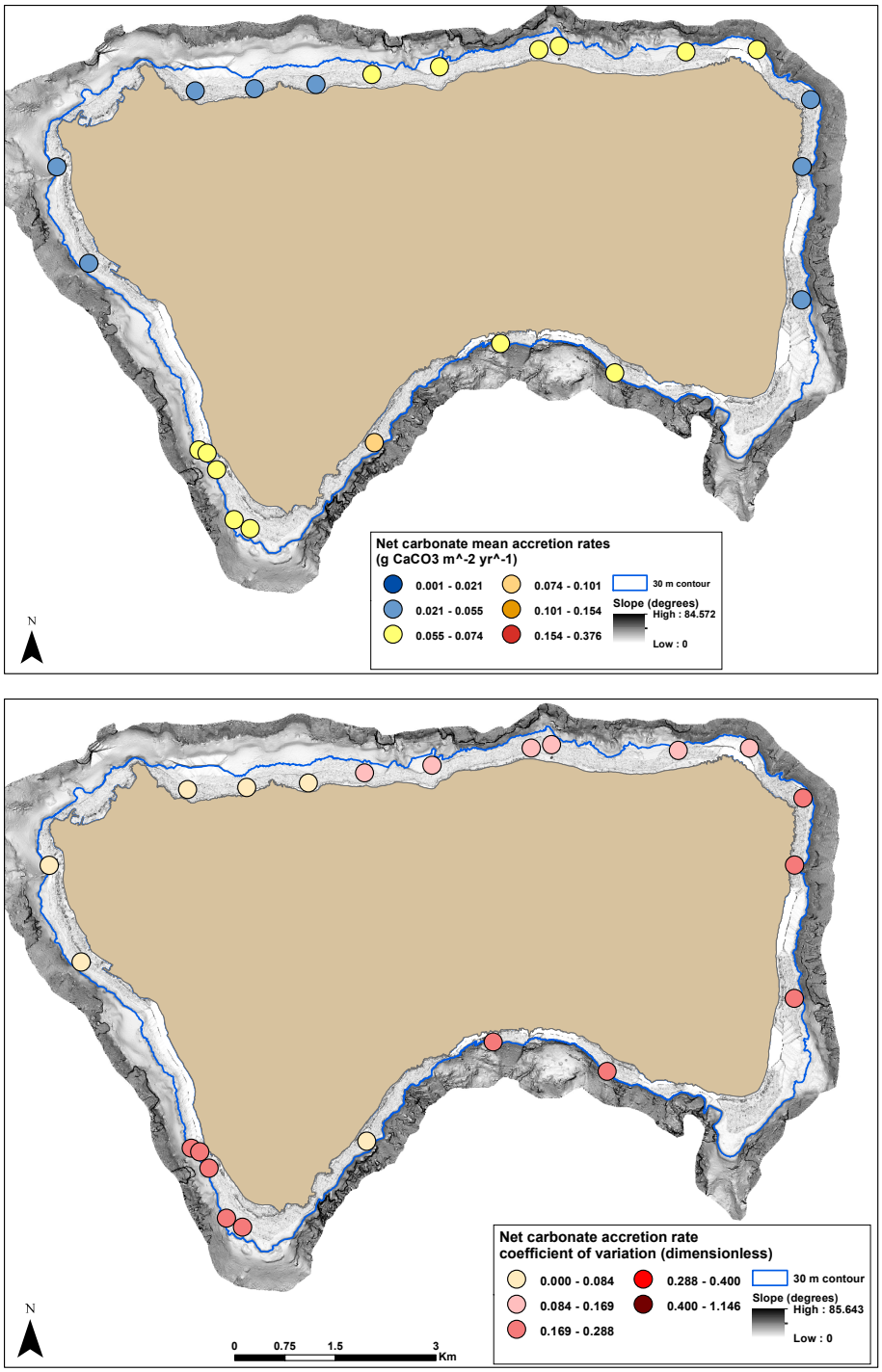

**Figure 25d**: Mean carbonate accretion rate (top) and carbonate accretion variability (bottom) plotted for all benthic REA sites on Rose Atoll.

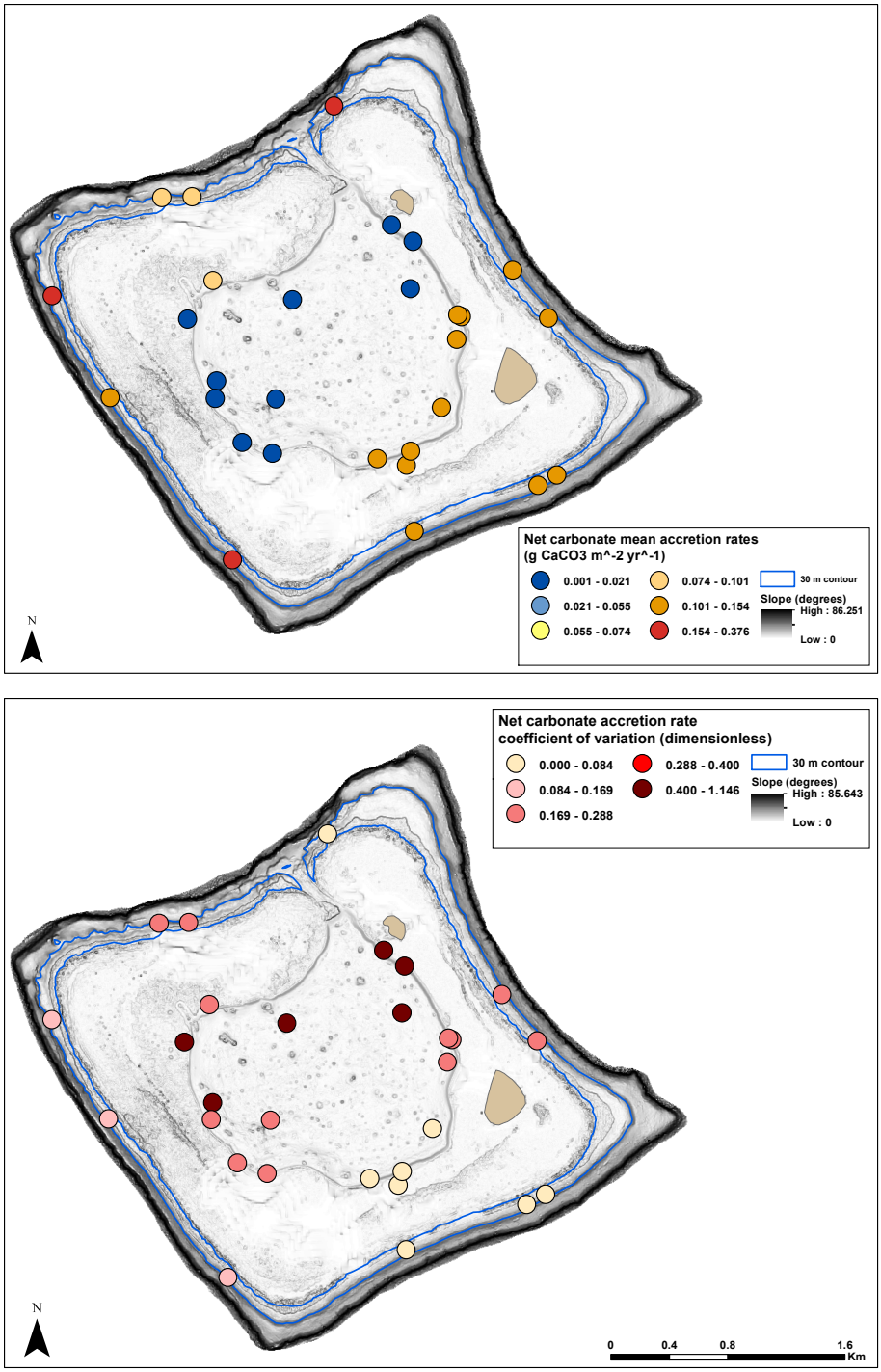

**Figure 25e**: Mean carbonate accretion rate (top) and carbonate accretion variability (bottom) plotted for all benthic REA sites on Swains.

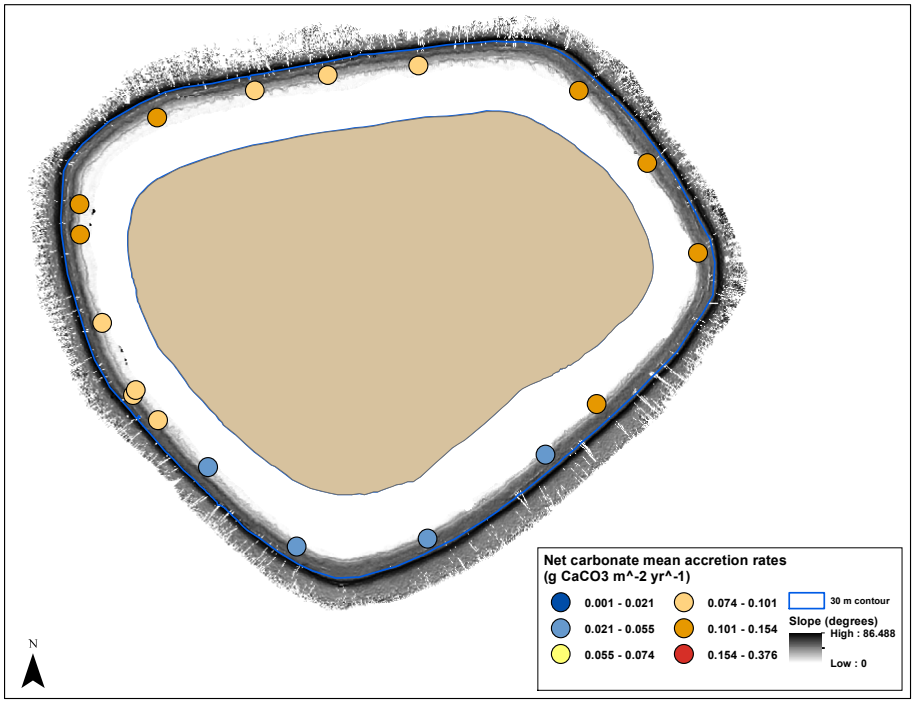


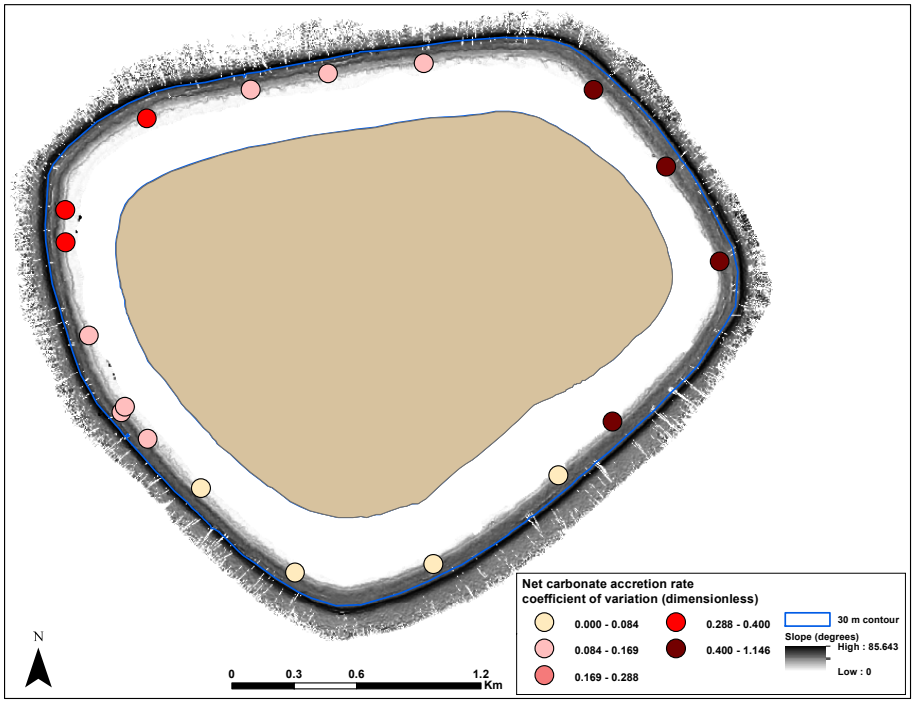

**Figure 26**: *Isopora spp.* site-level size structure histograms displaying logged coral size data (**left plots**) and unlogged coral size data (**right plots**) for **A**) a low shape parameter estimate, **B**) moderate shape parameter estimate, and **C**) high shape parameter estimate. Red lines: Weibull fits.

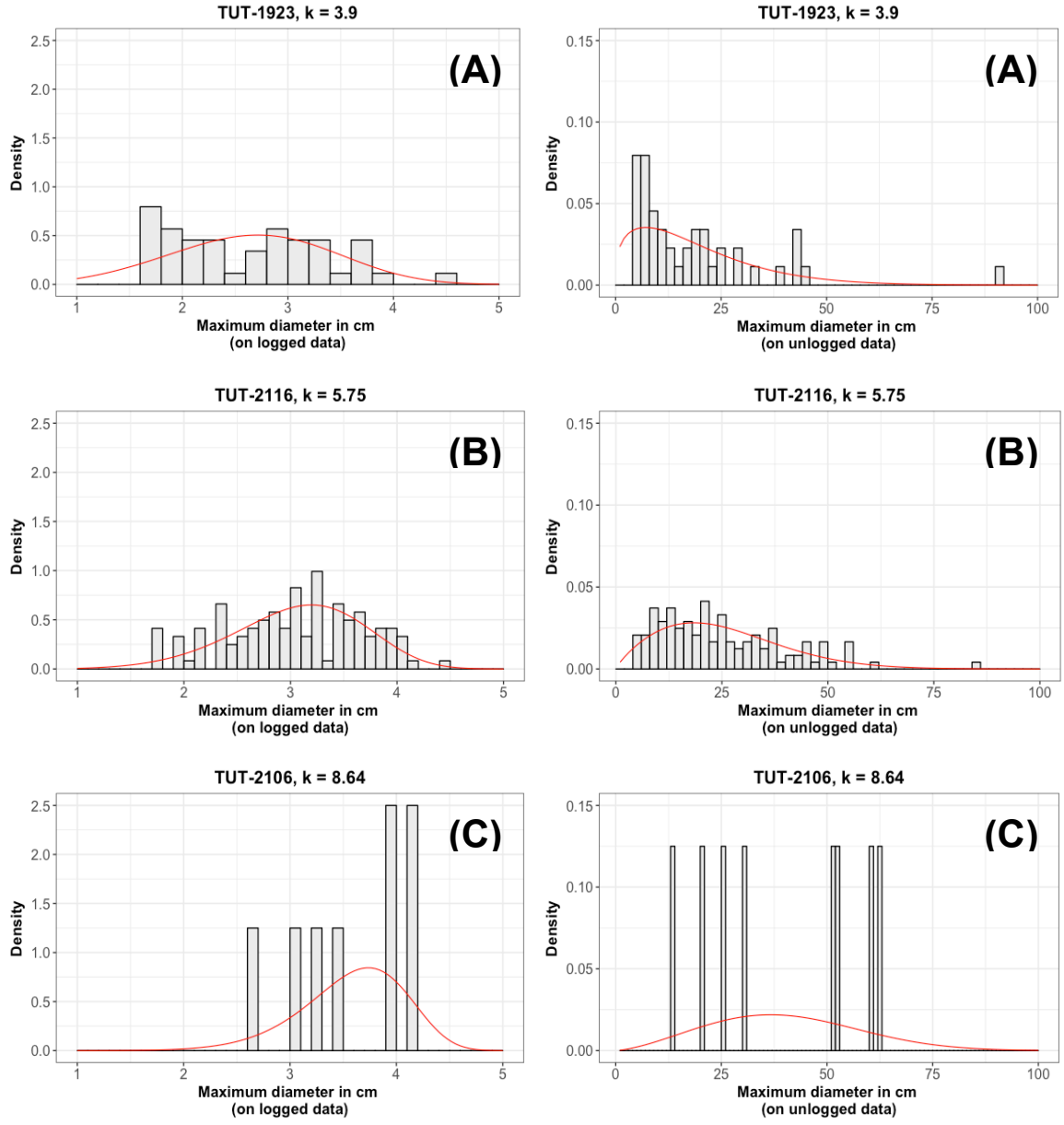

**Figure 27a**: *Isopora spp.* site-level shape parameter estimates across *Isopora spp.* spatial range (Ofu and Olosega, Tau, and Tutuila).

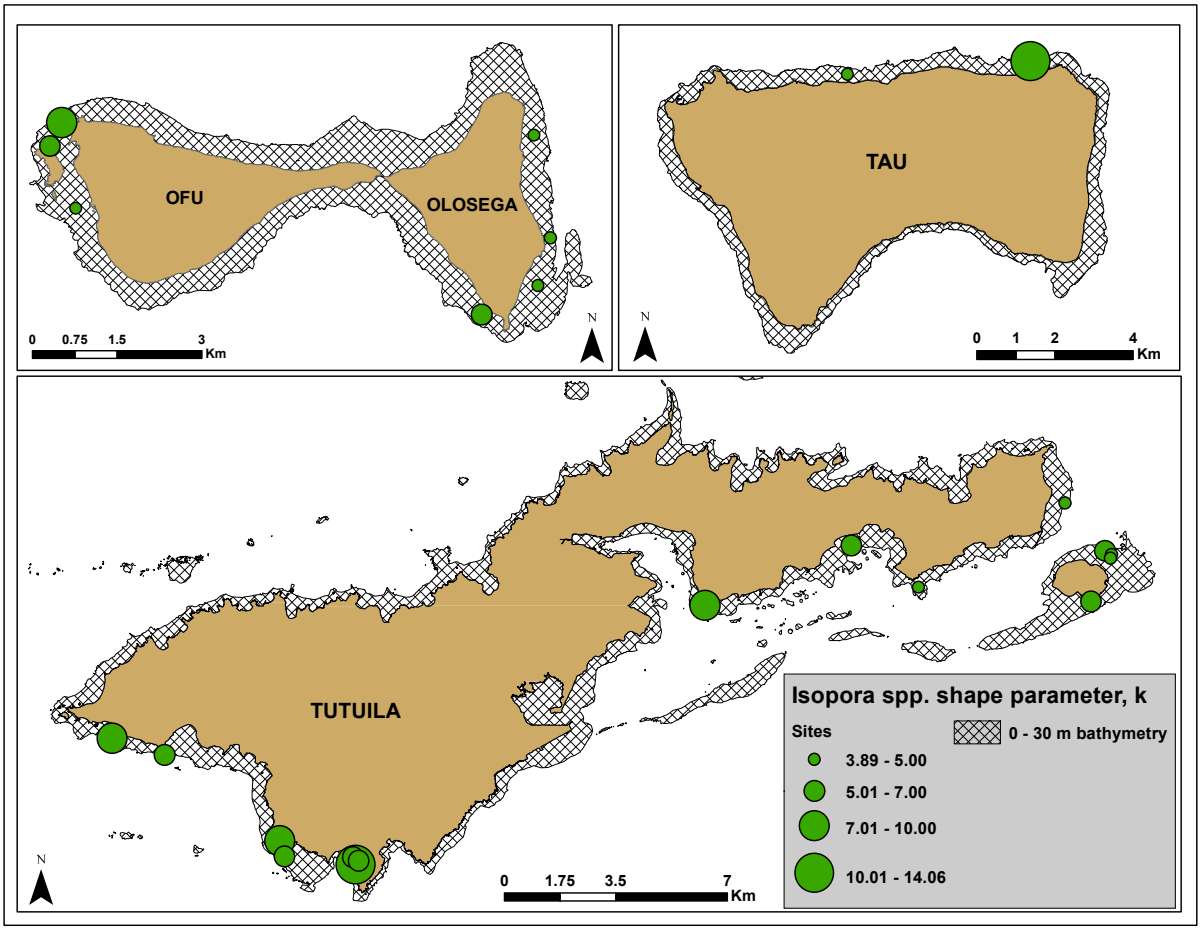

**Figure 27b**: *Isopora spp.* strata-level shape parameter estimates across *Isopora spp.* spatial range (Ofu and Olosega, Tau, and Tutuila).

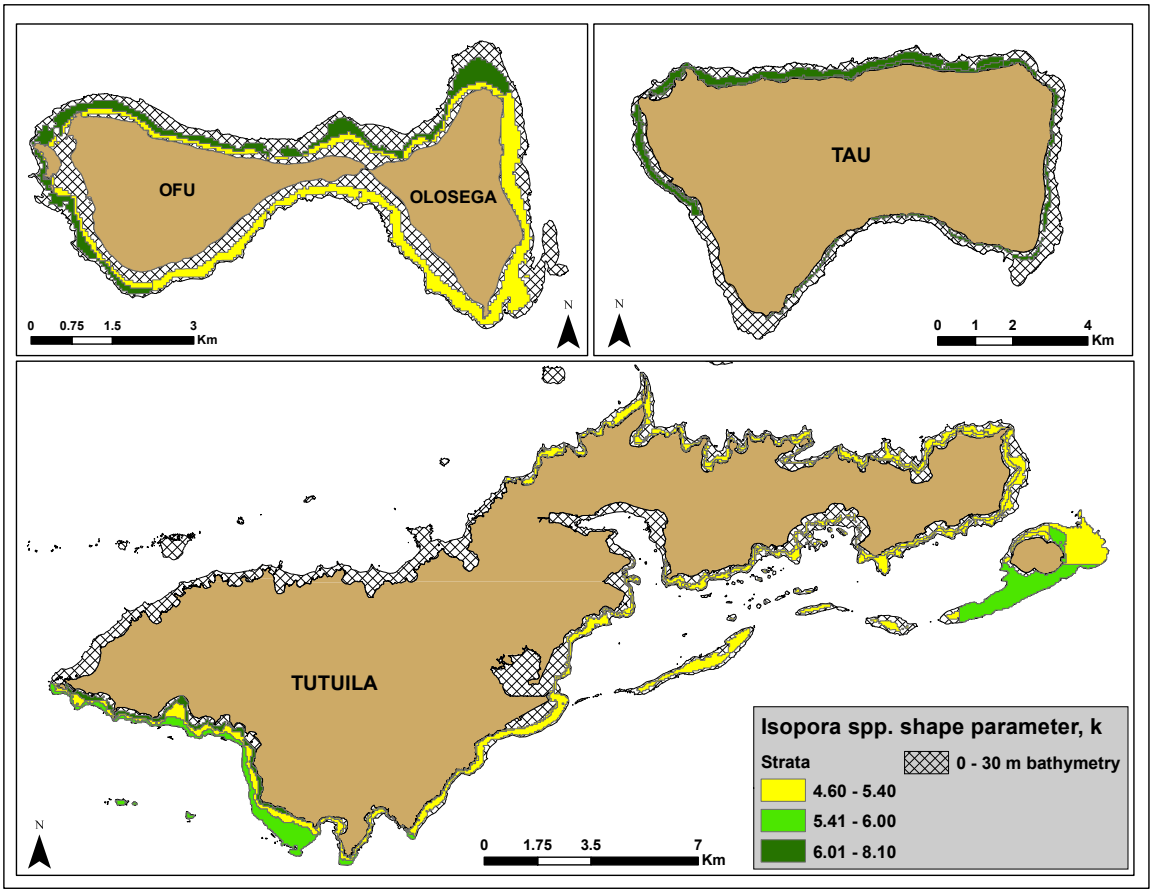

**Figure 28a**: *Montastrea curta* site-level shape parameter estimates across *Montastrea curta* spatial range (Ofu and Olosega, Tau, Rose Atoll, Swains, and Tutuila).

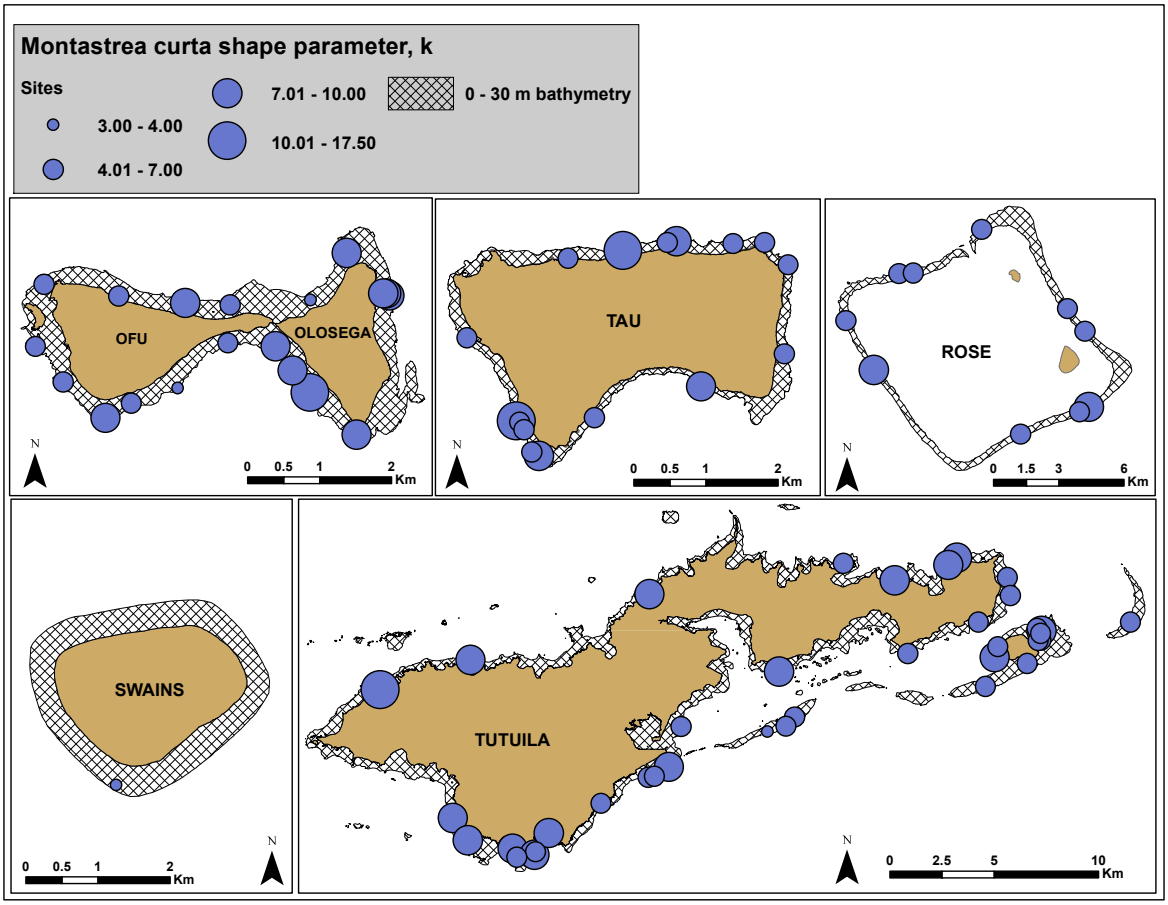

**Figure 28b**: *Montastrea curta* strata-level shape parameter estimates across *Montastrea curta* spatial range (Ofu and Olosega, Tau, Rose Atoll, Swains, and Tutuila).